





# Master Thesis

for the achievement of the academic degree

Diplom-Ingenieur

in the field of study Electrical Engineering at TU Wien

# Optimal Investment and Dispatch of District Heating Technologies with Participation in Electricity Day-Ahead, Intraday, and Balancing Markets

submitted at Institute of Energy Systems and Electrical Drives Supervisor: Associate Prof. Dipl.-Ing. Dr.techn. Johann Auer Assistent: Univ.Ass. Dipl.-Ing. Dr.techn. Sebastian Zwickl-Bernhard

by

Andreas Zimmer 51831086

Vienna, September 2025



# **Abstract**

This thesis studies the cost-optimal operation and expansion of a district heating portfolio under electricity—market uncertainty. A two-stage stochastic optimization model with hourly resolution over the planning horizon 2025–2035 is developed to assess the role of power-to-heat technologies—electric boilers (EB) and heat pumps (HP)—when participating in the day-ahead (DA), intraday (ID), and balancing markets. The technology set comprises HP, EB, combined heat and power (CHP), geothermal (GT), solar thermal (ST), waste-to-energy (WtE), and tank thermal energy storage (TTES).

Market uncertainty is represented by an exogenous-input autoregressive model (AR-X) that generates price scenarios conditional on wind and photovoltaic feed-in. Five discrete levels "trajectories" (low, lower, base, higher, high) are constructed for each market; their Cartesian product yields 25 joint DA/ID price scenarios. First-stage decisions determine investments and capacities; second-stage problems optimize hourly dispatch scenario-wise. To manage downside risk, the objective augments expected cost with a Conditional Value-at-Risk (CVaR) term, enabling a tunable trade-off between mean performance and tail losses.

Key findings are threefold. First, explicit access to ID and reserve provision (mFRR-down capacity reservation only; physical activation is not modeled) enables more opportunistic electrification, shifting HP operation into low-price hours and monetizing EB's flexibility. Second, the optimal portfolio exhibits a robust two-block structure: WtE provides dependable baseload, while HP/EB coordinated by TTES supply the flexible share. Third, in a stylized case study calibrated to an existing physical district heating network in Salzburg, the stochastic approach can reduce total system costs relative to a deterministic baseline by  $\approx 9\%$ , illustrating the value of scenario-based market participation and risk-aware planning.

# Kurzfassung

Diese Arbeit untersucht die kostenoptimale Betriebsführung und den Ausbau eines Fernwärmeportfolios unter Unsicherheit auf den Strommärkten. Hierzu wird ein 2-stage stochastic optimization model mit stündlicher Auflösung für den Zeitraum 2025–2035 entwickelt. Bewertet wird die Rolle von Power-to-Heat-Technologien—Elektrokessel (EB) und Wärmepumpe (HP)—bei Teilnahme am Day-Ahead- (DA), Intraday- (ID) und Regelenergiemarkt. Der betrachtete Technologiesatz umfasst HP, EB, Kraft-Wärme-Kopplung (CHP), Geothermie (GT), Solarthermie (ST), Waste-to-Energy (WtE) sowie Tank-Wärmespeicher (TTES).

Die Marktunsicherheit wird über ein autoregressives Modell mit exogenen Eingängen (AR-X) abgebildet, das Strompreisszenarien in Abhängigkeit von Wind- und PV-Einspeisung generiert. Für DA und ID werden jeweils fünf diskrete Trajektorien (low, lower, base, higher, high) definiert; ihr kartesisches Produkt ergibt 25 gemeinsame Preisszenarien. In der ersten Stufe werden Investitions- und Kapazitätsentscheidungen getroffen, in der zweiten Stufe erfolgt der stündliche Dispatch szenarioweise. Zur Begrenzung von Abwärtsrisiken wird die Erwartungswert-Zielfunktion um einen Conditional Value-at-Risk (CVaR) ergänzt, wodurch ein einstellbarer Trade-off zwischen durchschnittlichen Kosten und Verlusten in den Extremen möglich ist.

Die Ergebnisse lassen sich wie folgt zusammenfassen: (i) Der explizite Zugang zum ID-Markt und die Vorhaltung von mFRR-down-Reserve (capacity reservation only; physische Aktivierung wird nicht modelliert) ermöglichen eine opportunistischere Elektrifizierung. HP-Betrieb wird systematisch in Niedrigpreisstunden verschoben und die Flexibilität des EB monetarisiert. (ii) Das optimale Portfolio zeigt eine robuste Zwei-Blöcke-Struktur: WtE stellt eine verlässliche Grundlast, während HP/EB—koordiniert über TTES—den flexiblen Anteil bereitstellen. (iii) In einer an ein bestehendes physisches Fernwärmenetz in Salzburg kalibrierten Fallstudie kann der stochastische Ansatz die Gesamtsystemkosten gegenüber einem deterministischen Basismodell reduzieren (um ca. 9%), was den Wert szenariobasierter Marktteilnahme und risikobewusster Planungsansätze unterstreicht.

# **Contents**

ΑD	ADSTract				
Κu	ırzfas	sung			
1	1.1 1.2 1.3	duction2Motivation2Research Question3Case Study Region4			
2	2.1 2.2 2.3	ground and Model Inputs  District Heating			
3	<b>Met</b> l 3.1 3.2	nodology         Optimization Problem       25         3.1.1 Mathematical Introduction       25         3.1.2 2-Stage Stochastic Optimization Model       26         3.1.3 Objective Function       29         3.1.4 Conditional Value at Risk (CVaR)       31         3.1.5 Constraints       32         Electricity Price Simulation       47         3.2.1 AR-X Forecasting Model       47         3.2.2 Scenario Generation       48         3.2.3 DA Price Simulation Methodology       49         3.2.4 ID Price Simulation Methodology       52			
4	<b>Scen</b> 4.1 4.2 4.3	Scenario Tree			

## Contents

5	Results					
	5.1	Deterministic Model Results	63			
		5.1.1 Load curve and load duration curve	63			
	5.2	2-Stage Stochastic Model Results	69			
	5.3	Comparison of the 2 Models	72			
6	Conclusion and Outlook					
Bil	bliogr	raphy	77			

## Contents

### **Abbreviations**

DH District Heating

 $\mathbf{D}\mathbf{A}$ Day-ahead

IDIntraday

mFRR Manual Frequency Restoration Reserve

 $\mathbf{EB}$ Electric Boiler

HPHeat Pump

CHPCombined Heat and Power

WtEWaste to Energy

HOP Heat only Plant

TTES Tank Thermal Energy Storage

GTGeothermal

 $\mathbf{ST}$ Solar Thermal

COPCoefficient of Performance

 $\mathbf{TE}$ Thermal Energy

 $\mathbf{PV}$ Photovoltaic

Conditional Value at Risk **CVaR** 

 $\mathbf{AR}$ Auto Regressive

EPF Electricity Price Forecasting

**CAPEX** Capital Expenditures

0&MOperations and Maintenance

**CAGR** Compound annual Growth Rate

€ Euro

kWKilowatt MWMegawatt

 $\mathbf{V}$ Volt

kVKilovolt

# Introduction

### 1.1 Motivation

The ongoing expansion of renewable energy sources (RES) in the European power system is leading to increasingly volatile electricity price dynamics. These are characterized by frequent periods of low or even negative prices, particularly driven by high shares of wind and solar generation. This development creates new economic opportunities for district heating (DH) operators, especially through the flexible operation of power-to-heat technologies such as large-scale heat pumps, electric boilers, and thermal energy storage systems.

At the same time, DH is expected to play a major role in future heat supply, potentially covering up to 50% of total heating demand in urban areas [1]. Decarbonizing these systems requires not only the integration of renewable heat sources but also a shift toward electricity-based heat generation. Flexibility and optimized operational strategies are therefore key to ensuring cost-efficient and sustainable system transformation.

While the Day-Ahead (DA) electricity market is already considered in optimization models, the Intraday (ID) and balancing market is often neglected. However, due to its higher temporal resolution and short-term responsiveness, the ID market offers additional flexibility potential. It allows for better integration of volatile RES generation and for minimizing electricity procurement costs through real-time adjustments. Furthermore, balancing markets—such as the market for manual Frequency Restoration Reserve (mFRR)—provide additional economic value streams, especially through down-regulation offers (mFRR-down), which reward the temporary reduction of electricity consumption.

This thesis aims to develop a stochastic DH optimization model that integrates multiple electricity markets: the DA market, the ID market, and the balancing market (mFRRdown). The goal is to analyze how optimal dispatch strategies, investment decisions, and overall system costs are affected by participation in these markets. The resulting insights are intended to support strategic planning for DH operators aiming to enhance flexibility and cost-efficiency in a renewables-dominated energy landscape.

#### 1 Introduction

## 1.2 Research Question

This thesis investigates how the participation of DH systems in various electricity markets affects optimal investment and dispatch decisions. In particular, it compares two model variants:

- a deterministic base model without electricity market scenarios, considering only average DA prices, and
- a stochastic two-stage model that integrates DA and ID price scenarios, as well as the balancing market (mFRR down).

The stochastic price scenarios are generated using an adapted AR-X regression model, which incorporates forecast bandwidths of photovoltaic and wind generation based on current literature. This enables a more realistic representation of market uncertainty and short-term price fluctuations.

The following research questions are addressed:

- 1. How can different electricity markets, especially the Intraday and balancing electricity markets, be integrated into typical district energy optimization models?
- 2. To what extent do the optimal generation portfolio and dispatch decisions of district heating systems change when market uncertainties, Intraday prices, and balancing market revenues are considered compared to a conventional deterministic model?

The first question focuses on the necessary model extensions, including the development of a scenario-based stochastic optimization framework, the temporal integration of ID market dispatch, and the modeling of mFRR reserve provision (balancing) by flexible power-toheat technologies. It addresses how price uncertainty, short-term market responsiveness, and balancing capacity provision can be adequately represented in techno-economic energy system models.

The second question quantifies the practical implications of these model extensions. It evaluates changes in investment strategies, operational schedules, and total system costs when transitioning from a simplified, deterministic approach to a comprehensive model that reflects real-world market dynamics and uncertainty.

# 1.3 Case Study Region

The regional analysis for this thesis focuses on the Oberpinzgau region in the province of Salzburg, Austria. This alpine area comprises nine municipalities and lies within the district of Zell am See, bordering Tyrol and located near the borders of Carinthia and South Tyrol (Italy). The region is characterized by a mix of mountainous terrain, a low share of permanently settled land (only around 10% of the area), and a strong dependency on tourism and agriculture. The main transportation corridors, including the B165/B168 federal roads and the Pinzgauer Lokalbahn railway, run through the valley along the river Salzach. The population density within the permanent settlement areas is approximately 283 inhabitants/km<sup>2</sup>. Moreover, there is no natural gas grid available in the region, which further increases the relevance of alternative heat supply strategies [2].

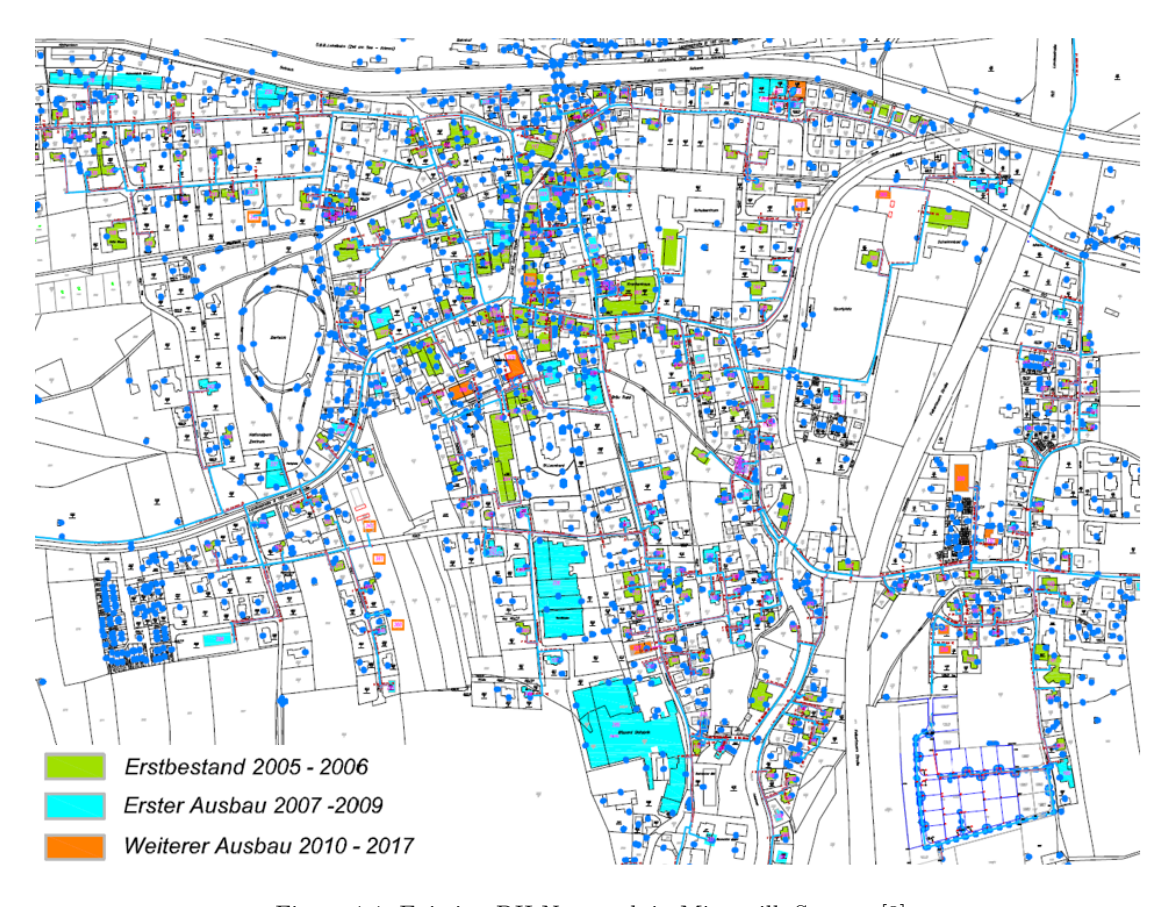


Figure 1.1: Existing DH Netzwork in Mittersill; Source: [3]

As part of the national climate and energy strategy, the Oberpinzgau region has been identified as a "Klima- und Energiemodellregion" (KEM) [2] due to its significant

#### 1 Introduction

potential for the use of renewable energy. 6 DH systems already exist in the area, all based on biomass. However, according to the Austrian Forest Inventory ("OWI"), only a remaining expansion potential of about 10% of the currently used biomass can be considered sustainable. This indicates that future developments of new DH networks in the region will likely require alternative renewable or electricity-based heat sources. Furthermore, according to the KEM Oberpinzgau report, approximately 79% of buildings in municipalities without access to DH are still heated with fuel oil, which is counterproductive to national climate targets.

For the purposes of this thesis, one of the existing biomass-based DH networks has been selected as a reference system. The chosen network is located in the municipality of Mittersill and supplies around 20 GWh of thermal energy per year. The design characteristics of this system, such as thermal demand and spatial extent, are used as the foundation for developing a representative case study.

The goal is not to replicate the existing network, but to explore how a similar DH system could be newly designed using cost-optimal technology combinations that account for electricity market participation. This approach assumes that similar heating networks could be developed in other nearby municipalities (e.g., Bramberg, Hollersbach, or Niedernsill), where there is no biomass-based DH in place. The analysis explicitly considers the integration of electricity market dynamics by allowing cost-optimal dispatch and investment decisions across three market levels: the DA, ID and balancing energy (mFRRdown) markets.

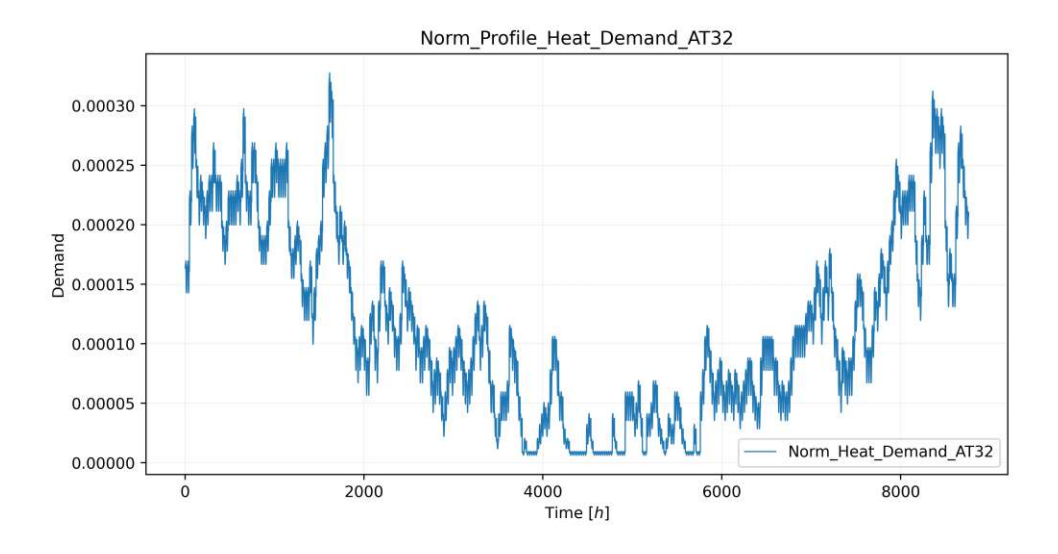


Figure 1.2: Hotmaps Demand Norm Profile AT32 (Salzburg)



### 1 Introduction

To characterize the heat demand for the case study, standard hourly load profiles from the Hotmaps [4] database were used. These were scaled to match the annual energy demand of the Mittersill reference network. In addition, monthly data for February to May 2025 from the actual network operator were made available. A comparison of the measured values with the Hotmaps profiles for the state of Salzburg shows a very good agreement, validating the use of Hotmaps profiles for the full-year simulation.

The case study region offers an ideal test environment to analyze the economic and operational effects of flexible, electricity-based DH in alpine rural areas. The modeling results can thus be interpreted as representative not only for Mittersill, but also for similar medium-scale municipalities in the region that aim to decarbonize their heating sector while facing biomass supply limitations.



# 2.1 District Heating

Heating accounts for approximately half of the EU's total energy demand, yet the sector has made far less progress in decarbonisation compared to electricity. Residential heating is still dominated by individual gas boilers, reflecting a strong reliance on imported fossil fuels and exposing the EU to geopolitical risks. While previous efforts focused mainly on energy efficiency through building retrofits, there is now a growing emphasis on transforming the heat supply itself.

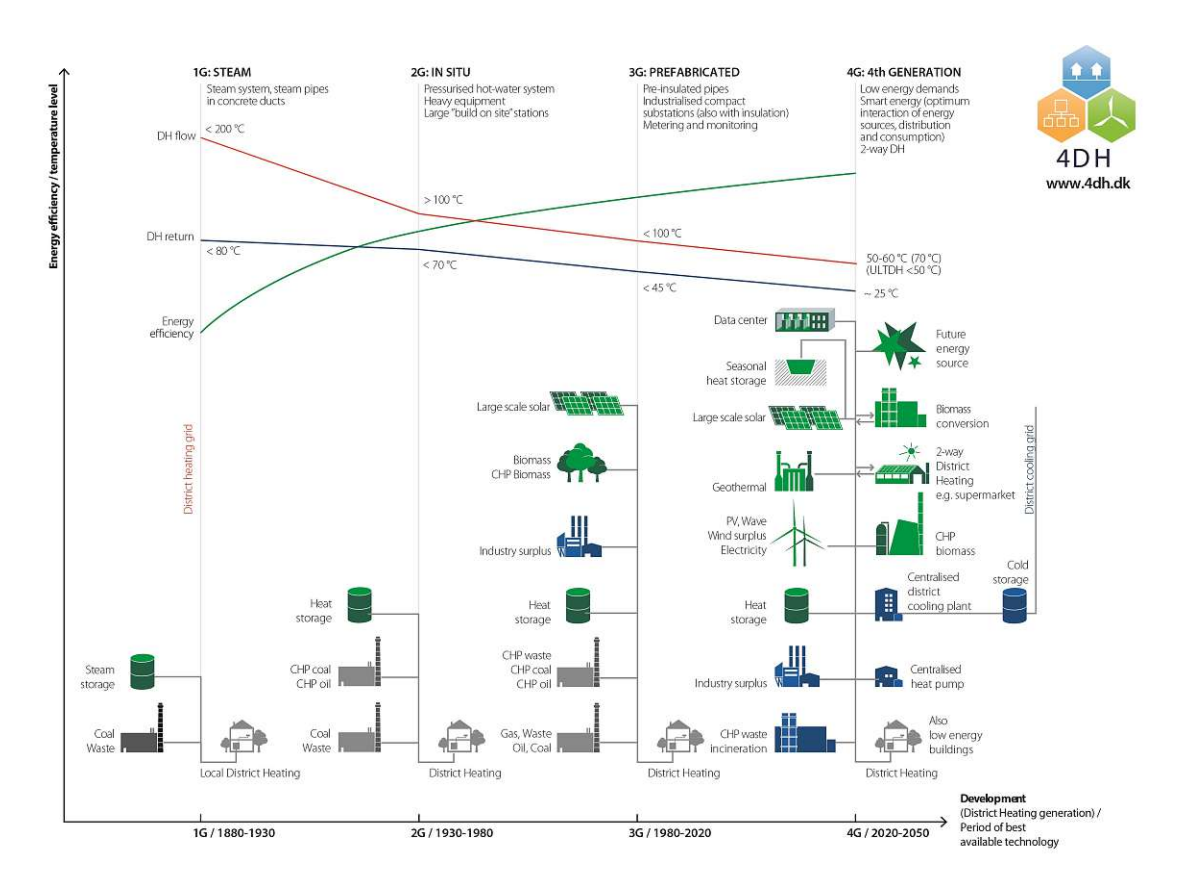


Figure 2.1: Evolution of DH systems to 4G; Source: [5]

DH offers a strategic solution by enabling the use of local, renewable, and otherwise wasted heat sources—such as surplus industrial heat (IEH), geothermal energy (GT), and solar thermal systems (ST). Urban DH networks are particularly well suited for integrating combined heat and power (CHP), waste-to-energy (WtE), and a broad mix of renewable sources. Studies indicate that surplus heat in Europe could theoretically cover nearly the entire heating demand. DH systems are also evolving toward a fourth generation [6], marked by lower distribution temperatures and closer integration with the power sector. This new generation increasingly utilizes technologies like large-scale heat pumps (HP), or electric boilers (EB), positioning DH as a key pillar in Europe's transition to a low-carbon, resilient energy system.

## 2.2 District Heating in Austria

In 2015, DH accounted for approximately 22% of Austria's total heat demand. According to the Heat Roadmap Europe 4, this share should increase to at least 40% by 2050 to support a cost-effective and low-carbon energy transition. Technically and economically, an expansion up to 65% would be feasible without significantly raising overall system costs [7].

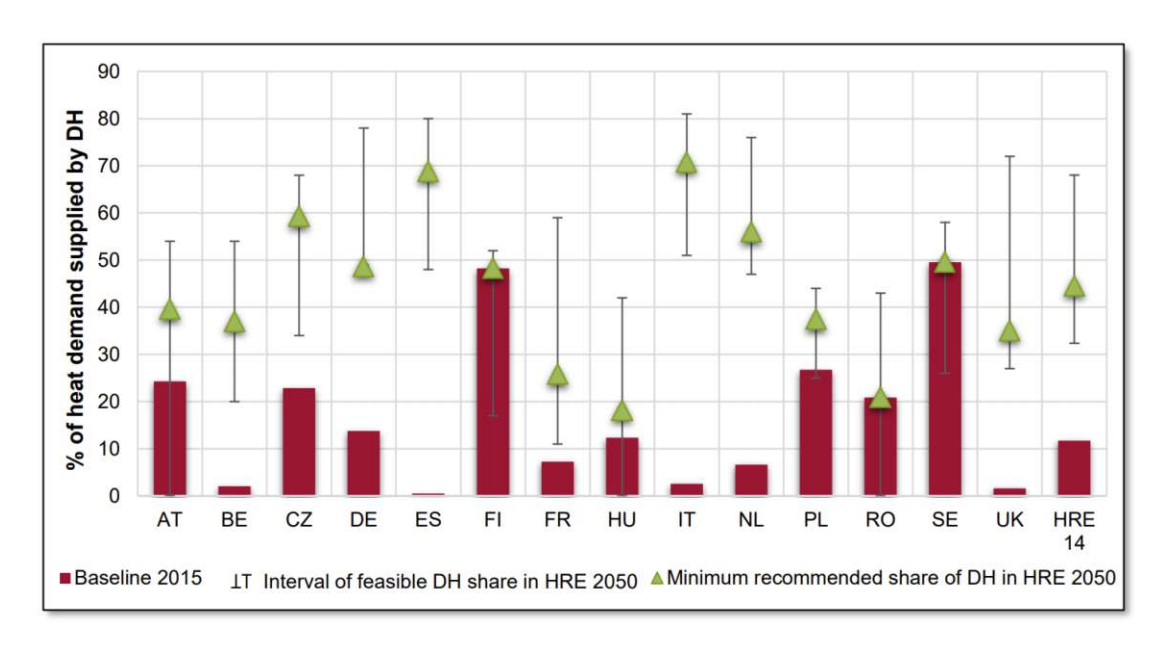


Figure 2.2: Baseline share of DH in 2015 and the minimum recommended level of DH share in HRE4; Source: [7]

### 2.2.1 Technology Parameters

#### CO<sub>2</sub> Emissions

According to Austria's electricity disclosure data (approximate share), 84.72% of the electricity mix is attributed to renewable energy sources [8]. The Guarantees of Origin (HKN) used throughout Austria for electricity disclosure resulted in average CO<sub>2</sub> emissions of 61.68g/kWh. This value refers exclusively to the energy sources covered by the guarantees of origin.

As of May 2025, the average price of EU Emission Allowances (EUAs) under the European Union Emissions Trading System (EU ETS) is approximately 65 € per tonne of CO<sub>2</sub>, reflecting current market conditions. This price represents the cost for companies to emit one tonne of CO<sub>2</sub> within the EU ETS framework, which applies uniformly across all participating member states, including Austria. The EU ETS serves as a central instrument in the EU's climate strategy by setting a cap on total emissions and allowing trading of emission allowances.

This average price is based on market observations and short-term forecasts, considering the dynamic nature of carbon pricing within the EU ETS. For the most up-to-date and detailed information on EUA prices, the European Energy Exchange (EEX) provides real-time data on its Market Data Hub: [9].

In line with long-term climate targets, several institutions, including the European Commission and the International Energy Agency, project a significant rise in CO<sub>2</sub> prices under the EU ETS. Based on official scenario modelling [10], average EUA prices are expected to reach between  $82 \in$  and  $160 \in$  per tonne of  $CO_2$  by 2030. Depending on the policy trajectory and emission reduction commitments, these projections reflect the anticipated tightening of emissions caps and the increasing cost of carbon-intensive energy use.

Therefore, for long-term modeling purposes, a forward-looking CO<sub>2</sub> price trajectory within this range is considered scientifically justified and consistent with current EU climate policy frameworks. In this context, a value of  $100 \in$  per tonne of CO<sub>2</sub> is selected for use in the optimization model as a representative and policy-aligned estimate for the year 2030.

Assuming a linear increase in  $CO_2$  prices between 2025 and 2030, starting at  $65 \in$  per tonne in 2025 and reaching  $100 \in$  per tonne in 2030, the annual growth rate is calculated as:

Annual increase = 
$$\frac{100 \in -65 \in}{2030 - 2025} = \frac{35 \in}{5} = 7 \in /year$$
 (2.1)

Extrapolating this trend linearly to the year 2035 yields the following estimate:

2 Background and Model Inputs

$$Price_{2035} = 100 \in +(5 \cdot 7 \in) = 135 \in /t CO_2$$
 (2.2)

#### **COP Calculation**

To determine the hourly COP of the large-scale HP, a temperature-dependent approach based on the Lorenz efficiency model is applied, as described in [11]. This method considers the logarithmic mean temperatures of both the heat source and the heat sink to determine a theoretical COP value. To reflect real-world conditions, this value is then multiplied by a technology-specific efficiency factor. This method accounts for thermodynamic losses by incorporating logarithmic mean temperatures of both the heat source and the heat sink.

Hourly outdoor air temperature values  $T_t$  [°C] are used as the inlet temperature of the heat source  $(T_{\text{source,in},t})$ , while the outlet temperature is assumed to be 5 K lower  $(T_{\text{source,out},t} = T_t - 5)$ . On the sink side, fixed values of 75 °C for supply and 40 °C for return temperature are used, as these reflect the conditions of the case study presented in this thesis and are based on data from a real-world DH system [12]. All temperatures are converted to Kelvin before calculation.

The logarithmic mean temperatures for the heat source and sink are calculated as follows:

$$T_{\text{lm,source},t} = \frac{T_{\text{source,in},t} - T_{\text{source,out},t}}{\ln\left(\frac{T_{\text{source,in},t}}{T_{\text{source,out},t}}\right)}$$
(2.3)

$$T_{\rm lm,sink} = \frac{T_{\rm sink,out} - T_{\rm sink,in}}{\ln\left(\frac{T_{\rm sink,out}}{T_{\rm sink,in}}\right)}$$
(2.4)

Using these, the theoretical COP according to the Lorenz model is determined as:

$$COP_{\text{Lorenz},t} = \frac{T_{\text{lm,sink}}}{T_{\text{lm,sink}} - T_{\text{lm,source},t}}$$
 (2.5)

To reflect technical and practical inefficiencies, the realistic COP is obtained by multiplying the Lorenz COP with a technology-specific efficiency factor  $\eta_{\text{Lorenz}}$ . For large-scale HPs in



the 10 MW range, a value of 0.60 is applied, based on data from existing installations and current projects that typically operate 7,000–8,000 hours per year and have an expected lifetime of 15–25 years [11]:

$$COP_{\text{real},t} = \eta_{\text{Lorenz}} \cdot COP_{\text{Lorenz},t}$$
 (2.6)

This method enables the calculation of realistic, time-resolved COP values for an entire year based on hourly ambient air temperatures and fixed network temperature assumptions.

#### **Electricity Network Tariffs**

For the case study region Oberpinzgau in Salzburg, electricity network tariffs are based on the tariff structure of Salzburg Netz GmbH for Netzebene 3. Both the capacity-based Leistungspreis [50,640  $\in$  /MW/year] and the energy-based Arbeitspreis [7.2  $\in$  /MWh] are considered in the modelling of electricity-based heat generation technologies.

In addition, for the provision of balancing reserves (mFRR down) in the Salzburg AG area an energy-based network fee of  $Arbeitspreis = 0.85 \in MWh$  applies; the corresponding capacity component of about 1,000 €/MW/year is omitted because its contribution is negligible in the context of this study.

To simplify the analysis, certain cost components have been excluded: network loss charges (Netzverlustentgelte) are not taken into account, potential subsidies or tariff reductions are disregarded, and any further network usage charges related to balancing services beyond the stated items are neglected so that the focus remains on the primary cost drivers relevant for the optimisation model.

#### 2.2.2 Investment Costs, Fixed and Variable O&M Costs

In this thesis, data for investment costs (CAPEX) is mainly derived form the Danish Energy Agency (DEA)[11]. Accurate data for specific countries such as Austria, or even for subnational regions is rarely available. Therefore, implemented and planned projects are additionally used as sources for estimating specific investment costs.

In addition to CAPEX, fixed and variable operating expenditures (OPEX) are considered.



#### HP Investment Costs, Fixed and Variable O&M Costs

For example, the planned project "ThermaFLEX Wien Spittelau High Temperature Heat Pump" has a budget of approximately 40 million € for a capacity of 16MW, as stated in [13]. This corresponds to specific investment costs of 2.5 million  $\in$ /MW.

According to the Danish Energy Agency [11], specific investment costs for air-source compression HPs in the 3MW range are estimated at 0.95 million €/MW in 2025 and 0.86 million €/MW by 2030. In addition, the study by Billerbeck et al. [14] assumes specific investment costs of 0.76 million €/MW for large-scale air-source HPs used in DH systems. This estimate aligns with the general trend towards cost-efficient electrification of heating and supports the assumed cost trajectories in this thesis.

While large-scale compression HPs are largely derived from established industrial refrigeration technologies, they often require customized components capable of handling higher pressure levels due to elevated temperature demands in DH. These specific requirements, along with relatively low production volumes—especially for units exceeding 10MW—restrict economies of scale and contribute to higher unit costs. In contrast, HPs in the 1-10MW range offer promising potential for standardization and modular design, which could significantly reduce specific investment costs through larger production series and simplified project execution [15]. It is assumed that the investment costs of HPs will decrease over time, at an estimated rate of 1.97% per year

In addition to investment costs, fixed and variable operating expenditures must be considered. According to the Danish Technology Catalogue [11], fixed O&M costs for largescale HPs in the 3 MW range are estimated at  $2,000 \in MW$  and year, which corresponds to approximately 0.21% of the specific investment cost. Furthermore, variable O&M costs are reported as 2.2 €/MWh of thermal output. These low O&M values reflect the relatively simple mechanical structure and low maintenance requirements of industrial-scale HP systems.

#### Investment Costs EB, Fixed and Variable O&M Costs

In the case of electric boilers integrated into DH systems, the PtH feasibility study for biomass heating plants in Salzburg estimates that a 1.5MW installation entails investment costs of approximately 0.26 million €/MW, while a 3MW system may reach around 0.22 million €/MW [16].

According to the study, installations exceeding 1MW in size can offer a robust business case with payback periods of less than 10 years, assuming good integration into electricity markets and stable revenues from negative secondary control reserve capacity.

In contrast, smaller systems below 1,MW are found to be significantly less cost-effective due to higher specific investment costs and limited economic potential in the balancing

market.

On the other hand, according to the Danish Energy Agency [11], the specific investment costs for EB in the 1–5MW range are estimated at approximately 0.15 million €/MW for 400/690V systems in 2020, decreasing slightly to 0.14 million €/MW by 2030. For systems operating at 10–15kV, the costs are significantly lower, around 0.07 million  $\in$ /MW. In this thesis, EB are assumed to operate at 400/690V. It is assumed that the investment costs of EB will decrease slightly over time, at an estimated rate of 1.37% per year, mainly due to market expansion and increased sales volumes, rather than through significant technological improvements.

In addition to investment costs, fixed and variable operating expenditures must be considered. According to the Danish Technology Catalogue [11], fixed O&M costs for largescale EB are estimated at 1,070 €/MW and year, which corresponds to approximately 0.71% of the specific investment cost. Variable O&M costs are reported as 0.9€/MWh of thermal output. These relatively low O&M values reflect the simple design and high technical availability of EB systems.

Electric boilers are modelled as direct electricity-to-heat units with an efficiency of 99%, supplying either directly to the DH network or to TTES.

#### Investment Costs CHP, Fixed and Variable O&M Costs

CHP plants based on biomass combustion with steam turbines, as reported in [17], show specific investment costs of approximately 3.1 million €/MW<sub>el</sub>. This value is based on a biomass-fired CHP plant with a thermal output of around  $17MW_{th}$  and a net electrical output of  $5MW_{el}$ .

In the Technology Data Catalogue of the Danish Energy Agency, similar values for CHP plants based on biomass woodchip combustion are reported, with specific investment costs of approximately 3.5 million  $\in$ /MW<sub>el</sub>. At a typical total efficiency of  $\eta_{\text{total}} = 0.85$ , the specific investment costs of biomass CHP plants are:

Investment per 
$$MW_{th} = 3.5 \cdot \left(\frac{5MW_{el}}{17MW_{th}}\right) \approx 1.03 \text{ million} \in /MW_{th}$$
 (2.7)

In biomass-fuelled CHP plants (e.g. using wood chips), no CO<sub>2</sub> price is typically applied, as emissions are considered climate-neutral under sustainable forest management and are not accounted for in the EU ETS [18].

Gas-fired combined cycle plants with backpressure steam turbines in the 10–100MW range show significantly lower specific investment costs of approximately 1.30 million €/MW<sub>el</sub>



in 2020 and 1.20 million €/MW<sub>el</sub> in 2030 according to the Danish Energy Agency. In this thesis, due to the case study's location where no natural gas connection is available. the investment cost assumptions of  $3.3 \in /MW_{el}$  for CHP are based on a medium-scale biomass CHP plant. According to data provided by the Danish Energy Agency, a typical biomass CHP plant (wood chips) is assumed to operate with an electrical efficiency of:

$$\eta_{\rm el} = 0.29$$
 (2.8)

and a total efficiency of:

$$\eta_{\text{total}} = 0.85 \tag{2.9}$$

From this, the thermal efficiency can be derived as:

$$\eta_{\rm th} = \eta_{\rm total} - \eta_{\rm el} = 0.56 \tag{2.10}$$

The power-to-heat ratio s, also referred to as the specific electricity yield, is calculated as the ratio of electrical to thermal efficiency:

$$s = \frac{\eta_{\rm el}}{\eta_{\rm th}} = \frac{0.29}{0.56} \approx 0.518 \tag{2.11}$$

This implies that for every 1MWh of thermal energy extracted, approximately 0.518MWh of electricity is also generated. Both values refer to the useful energy outputs extracted from the CHP process. Furthermore, It is assumed that the investment costs of biomass CHP will decrease slightly over time, at an estimated rate of 1.59% per year.

In addition to investment costs, fixed and variable operating expenditures must be considered. According to the Danish Technology Catalogue [11], fixed O&M costs for CHP systems are estimated at 4.3% of the specific investment cost. Variable O&M costs are reported as 4.5 €/MWh of thermal output. These values reflect the more complex mechanical structure and the higher maintenance and operational requirements of CHP units compared to purely electric heating technologies.

#### Investment Costs WtE, Fixed and Variable O&M Costs

In the case of waste-to-energy heat-only plants (WtE HOP), the Whitebook Waste-to-Energy in Austria reports that specific treatment costs of below  $100 \in$  per ton of residual waste can be achieved for small-scale facilities (with annual capacities of approximately 80,000 to 100,000 tons), provided that existing infrastructure and year-round heat

utilization are available. Capital expenditures represent the largest cost component, accounting for 37–53% of total treatment costs depending on project-specific parameters such as site characteristics, available infrastructure, and plant scale [19].

2 Background and Model Inputs

According to the Danish Energy Agency, specific investment costs for waste-to-energy heat-only plants (HOP) with flue gas condensation are estimated at approximately 580€ per annual tonne of waste input in 2020, corresponding to about 1.74 million €/MW of heat output and 1.71 million €/MW of heat output by 2030 [11]. Therefore it is assumed that the investment costs of WtE HOP will decrease marginally over time, at an estimated rate of 0.17% per year.

In Austria, the average generation of municipal solid waste amounts to approximately  $521 \,\mathrm{kg}$  per capita per year, according to [20]. Assuming that around 60-70% of this waste is suitable for thermal utilization, a significant portion of the waste stream could be used as input for WtE plants, particularly for the provision of DH services. In line with typical values from waste incineration plants documented by the Danish Energy Agency, the lower heating value (LHV) of municipal solid waste is assumed to be

$$H_{\text{waste}} = 2.7 \,\text{MWh/ton}$$
 (2.12)

The net operational cost of the plant considers both direct operation and maintenance costs as well as revenues from gate fees. Specifically, the operational expenditure is set to

$$c_{\rm op} = 22.9 \in /\text{ton}$$
 and  $c_{\rm waste} = -50 \in /\text{ton}$ . (2.13)

Furthermore, the average fossil CO<sub>2</sub> emissions per ton of waste are estimated based on a typical emission factor of 37 kg/GJ. With the given heating value, this corresponds to

$$e_{\rm CO_2} = 0.36 \, \rm tCO_2/ton$$
 (2.14)

These values are used consistently in the variable cost calculation of the model. According to Directive (EU) 2023/959 [21], the inclusion of municipal waste incineration in the EU ETS is being considered from 2028 onward, with a potential obligation starting in 2030; therefore, CO<sub>2</sub> pricing is only incorporated into the optimization model from 2030 onwards.

For waste-to-energy heat-only plants without flue gas condensation, a lower heating value (LHV)-based thermal efficiency of

$$\eta_{\rm th, LHV} = 0.876$$
(2.15)

is assumed in the model. This value is based on typical gross efficiencies of 76% reported on a higher heating value (HHV) basis for WtE plants at DH return temperatures around 40°C [11]). To ensure consistency with the fuel input data, the efficiency is converted to



an LHV basis using a typical HHV/LHV ratio of 1.15 for municipal solid waste (average values: 12.2 MJ/kg HHV and 10.6 MJ/kg LHV).

According to the Danish Technology Catalogue [11], fixed O&M costs for waste-to-energy (WtE) plants are estimated at 4.5% of the specific investment cost. Variable O&M costs are reported as 7.4 €/MWh of thermal output. These relatively high values reflect the need for continuous flue gas cleaning, residue handling, and the complex operational processes involved in municipal waste incineration.

#### Investment Costs GT, Fixed and Variable O&M Costs

Deep, medium-depth, and shallow GT energy systems exhibit some of the highest specific investment costs among heat source technologies for DH. According to a joint analysis by Agora Energiewende and Fraunhofer IEG, these costs typically range from 2.2-3.6 million €/MW th, with 60–80% of the total capital expenditure attributed to the development of the GT heat source itself [15]. At favorable locations with low geological risk, drilling costs alone can drop to around 1.8–2.2 million €/MW, depending on borehole depth and success probability. For shallow GT energy systems including the HP unit, specific investment costs are reported to be approximately 2.50 million €/MW.

More granular data from the Danish Energy Agency's Technology Catalogue estimates total investment costs for GT heat-only plants with compression HPs at approximately 2.65 million €/MW in 2025, decreasing to 2.50 million €/MW by 2030 for systems with 1,200m depth and DH temperatures of 80/40°C [11]. The share of the HP unit itself amounts to approximately 0.67 million €/MW. For deep GT configurations, specific investment costs are reported to be approximately 6\% higher. Furthermore, it is assumed that the investment costs for this technology decrease slightly over time, at an estimated annual rate of 1.16%.

In this thesis, a GT heat source is assumed at a depth of approximately 800 m, with a constant reservoir temperature of 35°C. This value is based on a typical GT temperature gradient of 3.5 °C per 100 m depth, as reported for Austrian conditions by the Energieinstitut an der Johannes Kepler Universität Linz [22]. The simplified assumption of a constant source temperature allows for the use of a time-invariant COP for the associated compression HP.

The COP is calculated using the temperature-based approach presented in Equations (2.3) to (2.6) of this thesis, which accounts for the logarithmic mean temperatures on the source and sink sides. A Lorenz efficiency factor of  $\eta_{\text{Lorenz}} = 0.50$  is applied to reflect practical system limitations. Based on the assumed source temperature of 35°C and sink temperatures of 75°C (supply) and 40°C (return), the resulting COP used in the model is  $COP_{GT} = 6.69$ .

In addition to the electricity required for the HP itself—which is implicitly captured in the COP—geothermal systems typically require further electrical energy to operate auxiliary components such as submersible pumps and reinjection systems. These elements ensure continuous fluid circulation between the production and injection wells. According to the Danish Energy Agency, this auxiliary electricity consumption is not included in the COP definition and typically ranges between 2% and 10% of the extracted thermal energy, depending on site-specific depth and flow conditions. In this thesis, a representative value of 5% is applied to account for these non-COP-related electricity demands.

In addition to investment costs, fixed and variable operating expenditures must be considered. According to the Danish Technology Catalogue [11], fixed O&M costs for GT heat-only plants are estimated at approximately 0.83% of the specific investment cost. Variable O&M costs are reported at 5.7€/MWh of thermal output. These O&M values reflect the higher maintenance demands and auxiliary systems required for GT operation, including submersible pumps, reinjection, and water treatment systems.

#### Investment Costs ST, Fixed and Variable O&M Costs

For example, the DH project in Grenaa, Denmark, is listed in [23] with specific investment costs of approximately 0.33 million €/MW of thermal capacity, based on a collector area of 20,673m<sup>2</sup> and a total capacity of 14.5MW. Systems in the capacity range between 3 and 5MW show specific investment costs of approximately 0.55 million €/MW.

According to the Danish Energy Agency, the specific investment costs for a solar DH system with a collector area of 10.000m<sup>2</sup> are reported at approximately 429€/MWh of annual heat output [11]. Based on a typical annual solar yield of 450kWh/m<sup>2</sup>, this corresponds to a total annual heat generation of about 4.5GWh. Assuming that 1MW of installed thermal capacity requires roughly 1,350m<sup>2</sup> of collector area, the resulting full load hours are estimated at approximately 600h/year. This allows the conversion of the given value into specific investment costs of roughly 0.26 million €/MW of installed thermal capacity. In contrast, [14] reports specific investment costs of 0.31 million €/MW of installed thermal capacity for ST systems. A comparatively low annual cost decrease of 0.86% is applied, reflecting the limited cost-reduction potential expected for this mature technology.

In this thesis, a maximum collector area of 10,000m<sup>2</sup> is assumed for the ST installation. The system is designed with flat plate collectors (FPC), which are the most commonly used collector type in European solar DH applications [23]. These systems typically achieve output temperatures of up to 70°C depending on weather conditions, orientation, and flow rate. For modeling purposes, a constant output temperature of 65°C is assumed throughout the year, reflecting an average operational value under central European conditions.



Since the DH supply temperature exceeds the solar field output, an auxiliary heat upgrading device is integrated. However, due to the relatively small temperature lift (from 65°C to 75°C), electrically driven compression HPs would operate inefficiently or may not be technically feasible. Therefore, an absorption heat pump (AHP) is used instead, which is thermally driven and more suitable for this application. AHPs can achieve supply temperatures up to 85–87°C and exhibit typical COP of up to 1,7 [11].

The ST system is modeled with an annual conversion efficiency of 45% in 2020, increasing to 48% by 2030, which corresponds to typical yield levels of around 450/kWh/m<sup>2</sup>/a [11].

The AHP required for temperature elevation is assigned specific investment costs of 0.56 million €/MW of thermal output, based on data reported by the Danish Energy Agency [11]. These costs reflect the additional infrastructure needed to match the thermal output of the solar field to the DH network requirements. Similar to other technologies, cost reductions over time are expected; for AHPs, an annual decrease of 0.93% is assumed, reflecting limited potential for economies of scale and innovation in this mature technology segment.

In addition to investment costs, fixed and variable operating expenditures must be considered. According to the Danish Technology Catalogue [11], fixed O&M costs for the ST collector field are estimated at approximately 0.03% of the specific investment cost, while variable O&M costs amount to 0.30 €/MWh of thermal output. Additionally, land lease costs are assumed at 0.10 €/MWh, resulting in total variable O&M costs of  $0.40 \in MWh$ . For the thermally driven AHP used to upgrade the solar output temperature, fixed O&M costs are assumed to be 0.4% of the specific investment cost, and variable O&M costs are estimated at 1.00 €/MWh. These values reflect the low maintenance requirements of passive collector fields as well as the additional operational costs associated with the thermal driving cycle and auxiliary components of the AHP.

#### Investment Costs TTES, Fixed and Variable O&M Costs

For the case study presented in this thesis with an annual heat generation of 20GWh and a 24-hour storage duration, assuming a uniform daily load, the required storage capacity is approximately 55MWh. Given typical energy densities of water-based TTES systems in the range of 60–80kWh/m<sup>3</sup> [24], this corresponds to a required volume of roughly  $1.000 \text{ to } 1.500 \text{m}^3.$ 

According to Jörg Worlitschek, specific investment costs TTES systems range between 180 € and 220 €/m³ [25]. Assuming a representative design volume of 1,200m³, the resulting total investment amounts to approximately 0.22–0.26 million €. Based on an assumed energy density of 70 kWh/m<sup>3</sup>, this corresponds to specific investment costs of approximately 2,600–3,100 €/MWh of daily storage capacity.

Comparable values are also reported in [26], where a TTES installation with a storage volume of 3,000m<sup>3</sup> is associated with specific investment costs of around 2,900 €/MWh of daily storage capacity.

From a techno-economic perspective, TTES is more favorable for smaller-scale applications or urban areas with limited space (<10,000m<sup>3</sup>), while PTES becomes increasingly attractive at larger scales due to lower unit costs. The economic trade-offs between TTES and PTES highlight the importance of site-specific conditions and system sizing when selecting suitable storage technologies for DH systems [26].

The following calculation is based on an assumed storage volume of 1,200 m<sup>3</sup> and an energy density of 70 kWh/m<sup>3</sup> for TTES:

$$E_{\text{daily}} = V \cdot e = 1,200 \,\text{m}^3 \cdot 70 \,\frac{\text{kWh}}{\text{m}^3} = 84,000 \,\text{kWh} = 84 \,\text{MWh}$$
 (2.16)

Assuming specific investment costs of 3,000 €/MWh of daily storage capacity, the total investment is calculated as:

$$I_{\text{total}} = 84 \,\text{MWh} \cdot 3,000 \,\frac{\text{e}}{\text{MWh}} = 252,000 \text{e}$$
 (2.17)

With a storage duration of 24 hours, this corresponds to a thermal power output of:

$$P_{\rm th} = \frac{E_{\rm daily}}{24 \, \rm h} = \frac{84 \, \rm MWh}{24 \, \rm h} = 3.5 \, \rm MW$$
 (2.18)

Finally, the specific investment cost per MW of thermal output is:

Specific cost = 
$$\frac{I_{\text{total}}}{P_{\text{th}}} = \frac{252,000 \in 72000 = 72,000 = 720000 = 720000 = 720000 = 720000 = 720000 = 720000 = 720000 = 720000 = 720000 = 720000 = 720000 = 7200000$$

In [27], a maximum hourly charging and discharging capacity of 40MW is assumed for a TTES system with a volume of 3,000m<sup>3</sup>. Based on this reference, and considering that the TTES unit in this case study is dimensioned at approximately 1,200m<sup>3</sup>—about one third of the reference size—a scaled technical limit of 13.3MW is applied to define the upper boundary for charging and discharging. This value serves as a technical constraint in the model and does not necessarily reflect the actual operational load profile.



In the literature, TTES systems are reported with varying assumptions depending on the temperature level, insulation quality, and storage duration. For example, a detailed modeling study on high-temperature TTES assumes hourly heat losses of 0.04%, representing relatively conservative conditions for large-scale system simulations [28].

In contrast, empirical data from IRENA indicate that well-insulated seasonal storage tanks operating at around 90°C can retain heat with less than 10% energy loss over six months [29].

In this thesis, a total thermal loss of 20% over a six-month period is assumed for TTES operation. This corresponds to an hourly storage retention factor of approximately 0.99962, equating to 0.038% heat loss per hour. In addition, a charging and discharging efficiency of 0.95 is applied to account for thermal losses during input and extraction processes.

In addition to investment costs, fixed and variable operating expenditures must be considered. According to typical values used in techno-economic assessments of thermal storage systems, fixed O&M costs for TTES are estimated at approximately 1.0% of the specific investment cost. Variable O&M costs are generally very low due to the passive nature of TTES and are assumed to be  $0.10 \in MWh$  of thermal energy charged or discharged. These O&M values reflect the minimal maintenance requirements and the absence of active mechanical components, apart from standard instrumentation and control. Additionally, a charge/discharge cost of 5.5€/MWh is assumed to reflect auxiliary electricity use and operational cycling effects.

To simplify the optimization framework, dynamic constraints such as ramp-up times, minimum up/down times, or startup delays of the thermal generation units are not considered. All technologies are modeled as fully dispatchable within each timestep, assuming instantaneous availability of their installed capacity.

Technology	Specific Investment Costs	Fixed O&M	Var O&M
	[€/MW]	$[\in/\mathrm{MW}]$	$[{\in}/\mathrm{MWh}]$
Heating Technology			
HP	850,000	1,785	2.2
EB	200,000	1,420	0.9
CHP	3,300,000	141,900	4.5
WtE	1,900,000	78,000	7.4
GT	2,200,000	18,260	5.7
ST / HP (AHP)	300,000 / 600,000	90 / 2,400	0,4 / 1,0
Storage Technology			
TTES	72,000	720	0.1

Table 2.1: Technology-specific CAPEX and O&M cost assumptions

# 2.3 Electricity Market

According to [30], european electricity prices have shifted to exchange-based trading since market liberalization, with hourly prices set in DA and ID auctions. These prices inherit clear deterministic structure from demand: weekday/weekend patterns and seasonal shifts in daily load (midday vs. evening peaks).

Beyond those regularities, electricity's limited storability and the need to balance supply and demand every single hour produce hallmark features: high volatility, mean reversion, and occasional jumps/spikes.

In this thesis, three price series are used: (i) the ENTSO-E DA hourly price for Austria (AT), (ii) the EPEX intraday ID3 index for 2019 (the only intraday year available), and (iii) mFRR-down prices. The mFRR-down series is fed into the optimization model as a daily average applied uniformly to all 24 hours of the respective day.

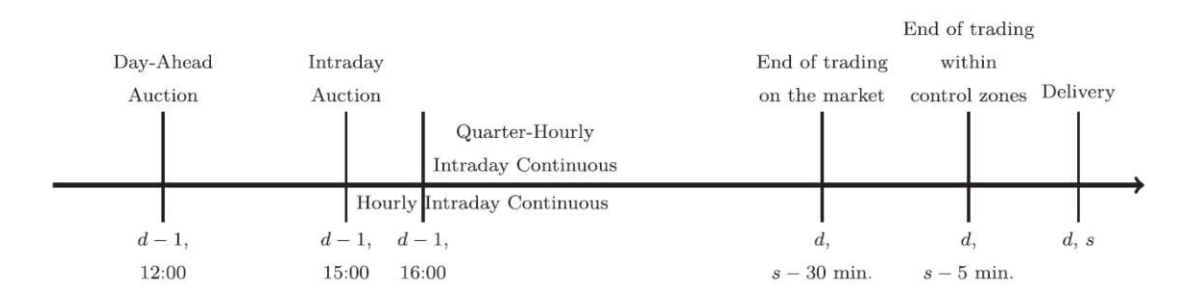


Figure 2.3: Routine of Electricity Market; Source: [31]

For intraday electricity price forecasting (EPF), this thesis follows the literature for example [31] and work with the EPEX ID3 index. Conceptually, ID3 is the volumeweighted average of transaction prices in the last three hours before delivery, ignoring trades in the final 30 minutes within control zones. Let b(d, s) denote the delivery start of product s on day d and define the half-open window

$$\mathbb{T}_3^{d,s} = \left[ b(d,s) - 3, \ b(d,s) - 0.5 \right). \tag{2.20}$$

With  $V_k^{d,s}$  and  $P_k^{d,s}$  the traded volume and price at timestamp k in that window, and  $\mathcal{W}^{d,s}$  the set of relevant transactions (domestic and cross-border; excluding cross-trades), the EPEX definition is

$$ID3^{d,s} = \frac{\sum_{k \in \mathbb{T}_3^{d,s} \cap \mathcal{W}^{d,s}} V_k^{d,s} P_k^{d,s}}{\sum_{k \in \mathbb{T}_3^{d,s} \cap \mathcal{W}^{d,s}} V_k^{d,s}}.$$
 (2.21)

If there are no trades in  $\mathbb{T}_3^{d,s}$ , EPEX extends the averaging window; if no trades at all occur, the respective DA (hourly) or intraday auction (quarter-hourly) price is used. The index is economically relevant—it underlies intraday cap/floor futures—and is empirically justified since most continuous intraday volume concentrates in the ID3 window.

### 2.3.1 Electricity Price Forecasting

EPF has matured into a broad field spanning statistical time-series models, machine learning, and hybrids. Yet, as highlighted by a recent comprehensive review, comparisons have often lacked rigor due to non-public datasets, short test periods, and weak baselines. [32] address these shortcomings by publishing multi-year benchmark datasets, standardized evaluation practices (including proper significance testing), and open-source baselines. They also identify two families that consistently provide strong reference performance across markets: (i) parameter-rich econometric regressions estimated with LASSO/elasticnet (the "Lasso Estimated AutoRegressive," LEAR, i.e., fARX-type with regularization),



and (ii) comparatively simple deep neural networks (DNN), both implemented in the EPFtoolbox.

From a methods perspective, modern "statistical" EPF typically uses linear models with many calendar, autoregressive, and exogenous features and applies implicit feature selection via LASSO/elastic-net. This regularization both shrinks and selects coefficients, yielding robust parameter-rich models that often outperform more parsimonious  $AR(\cdot)$ or ARIMA baselines; variance-stabilizing transformations and careful treatment of seasonality further improve accuracy. The best-practice recommendations in [32]—year-long rolling backtests, strong baselines (LEAR/DNN), appropriate error metrics with significance testing—are followed here insofar as they align with the scenario-generation objective.

#### **Positioning**

This thesis does not aim at minimizing point forecast errors (e.g., MAE) for operational trading; instead, it repurposes the open and reproducible EPF setup of [32] into an X-model (AR-X without the AR part) to generate diverse DA and ID price scenario paths. The intention is to capture a broad dispersion of structurally different conditions—accepting a deliberately higher MAE—so that the stochastic optimization can exploit market-driven flexibility. Methodological details of the X-model and the rolling design are given in Subsection 3.2.1.

### Negative Prices and ARMA (AutoRegressive-Moving Average) Models

Negative prices are a structural feature of European markets (allowed at EEX since 2008). A common and effective approach is to separate deterministic components (trend; daily/weekly/annual patterns) from a stochastic residual, which can be modeled with mean-reversion and ARMA/ARIMA processes; regime switching and an explicit treatment of negative prices markedly improve fit. In evaluations on EEX data, mean-reversion and ARMA delivered the lowest RMSE (and lower MAE than GARCH), while ARMA/ARIMA better preserved daily shapes. These insights motivate variance-stabilizing transformations and robust residual handling compatible with negative values.

#### Modeling choices and summary

Guided by [32], this thesis employs strong, transparent baselines and rigorous rolling evaluation; however, the objective is scenario diversity rather than minimal MAE. ID modeling and evaluation rely on ID3; the X-model with exogenous drivers is used to generate DA/ID price paths for the two-stage stochastic optimization (Subsection 3.2.1).



In this chapter, the methodological framework for solving the district heating optimization problem using two-stage stochastic programming is presented. The objective of this thesis is to enable district heating operators to participate in the DA and especially in the ID and balancing electricity market with flexible electricity-powered district heating technologies. These technologies include heat pumps, electric boilers and heat storage. The first part of this chapter describes the optimization problem with a brief mathematical introduction and the second part the electricity price simulation.

Figure 3.1 depicts the flowchart of the applied methodology.

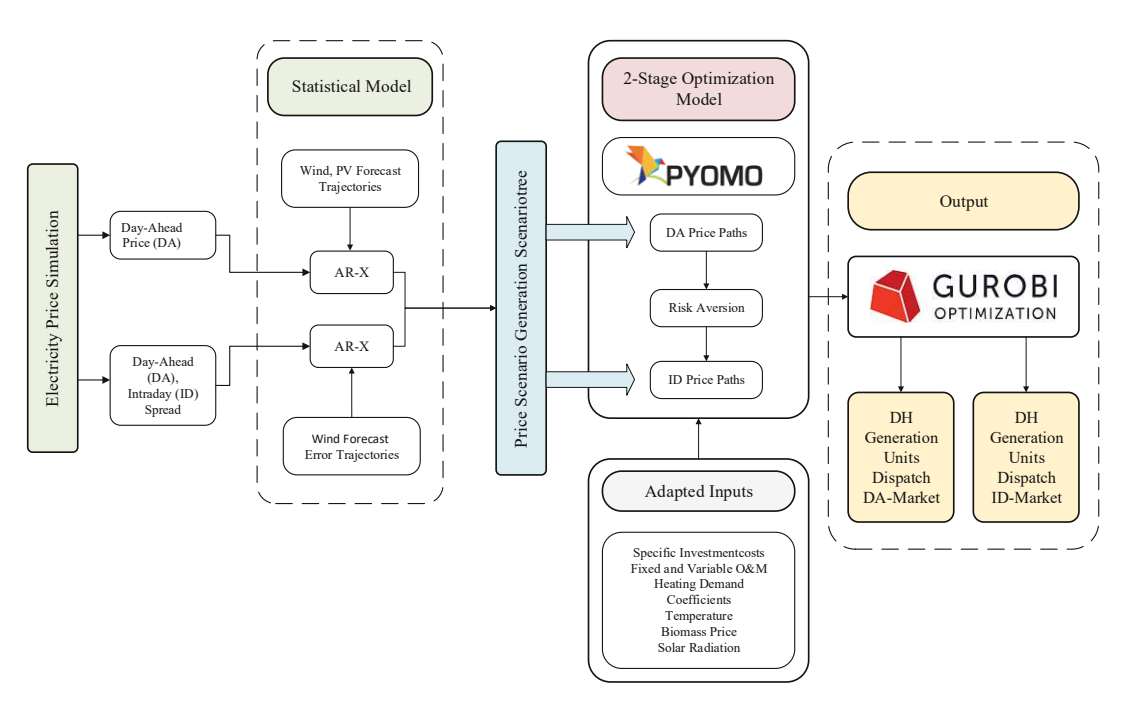


Figure 3.1: Flowchart of the applied methodology

The primary objective of the DH model is to ensure continuous thermal energy supply to all consumers based on their hourly heating demand profiles. To meet this demand, the model can choose from a variety of technologies. For the heating system, 6 different

generation technologies are available which are described in 3.1. Additionally the network includes a thermal storage technology, which accommodate the volatile nature of electricity prices and provides flexibility in meeting the demand profiles.

The primary objective of this work is the integration of DA, ID and balancing electricity market mechanisms into an existing energy optimization model, in order to systematically account for the exploitable flexibility these markets offer. The underlying model focuses solely on the energy supply side, aiming to meet the thermal demand of consumers without considering the physical distribution network [33]. Consequently, infrastructure components such as pipelines, pumps, and associated hydraulic flow dynamics are not included in the scope of this work. As a result, network-related losses and pressure-driven constraints are not reflected in the optimization outcomes.

The two-stage stochastic optimization model presented in 3.1.2 generates a cost-effective configuration of the mentioned DH technologies, based on the defined input parameters and constraints. This enables district heating operators to operate their systems according to economically optimal dispatch schedules.

## 3.1 Optimization Problem

Optimization problems are mathematical models used to find the best possible solution from a set of feasible alternatives. These problems play a crucial role in various fields, including engineering, economics, logistics. The goal of an optimization problem is to either maximize or minimize an objective function while satisfying a set of constraints resulting in a better decision-making, cost reduction, and improved efficiency.

#### 3.1.1 Mathematical Introduction

In general, an optimization problem is characterized by an objective function [34]:

$$\max / \min_{x_1, x_2, \dots} f(x_1, x_2, \dots)$$
 (3.1)

subject to

$$g_i(x_1, x_2, \dots) \le b_i, \quad i = 1, \dots, p$$
  
 $h_j(x_1, x_2, \dots) = 0, \quad i = 1, \dots, q$ 

$$(3.2)$$

with variables

max(min) Maximization (Minimization) problem

 $x_1, x_2, \dots$  Decision variables

$$f(x_1, x_2, \dots)$$
 Objective function (3.3)

 $g_i(x_1, x_2, \dots)$  p Inequality constraints

 $h_i(x_1, x_2, \dots)$  q Equality constraints.



This thesis builds upon an existing linear programming (LP) optimization model, which is described in Section 3.1.2, to develop a two-stage stochastic programming model. Compared to deterministic optimization models with fixed parameters, stochastic programming models involve uncertainty in the data. Uncertainties in the data can be expressed through probability distributions. Another approach is the scenario-based method. This means that the probability distribution is discretized into a set of possible realizations, referred to as "scenarios", each assigned a specific probability.

With a finite set of scenarios  $\Omega = \{\omega_1, \dots, \omega_S\} \subseteq \mathbb{R}^r$  and probabilities  $P(\omega_s) = p_s$  for all s = 1, ..., S, the stochastic model can be written as the "deterministic equivalent" [35]. This approach transforms the stochastic problem into a large linear programming problem and can be expressed as follows:

$$c^{T}x + p_{1}q^{T}y_{1}(x) + p_{2}q^{T}y_{2}(x) + \dots + p_{S}q^{T}y_{S}(x)$$
s.t.
$$Ax = b$$

$$T_{1}x + W_{1}y_{1}(x) = h_{1}$$

$$T_{2}x + W_{2}y_{2}(x) = h_{2}$$

$$\vdots \qquad \vdots \qquad \vdots$$

$$T_{S}x + W_{S}y_{S}(x) = h_{S}$$

$$x \in \mathbb{R}^{n}, y_{1}(x) \in \mathbb{R}^{m}, y_{2}(x) \in \mathbb{R}^{m}, \dots, y_{S}(x) \in \mathbb{R}^{m}$$

$$(3.4)$$

Where  $c^T x$  represents the first-stage problem and corresponds to investment costs and fixed costs in this thesis.  $p_S q^T y_S(x)$  represents the second-stage problem, weighted with specific scenario probabilities and corresponds to variable costs. The variable costs are responsible for the respective dispatch of the different, flexible DH technologies in the day-ahead and intraday electricity market. Ax = b represents the constraint of the first-stage problem with A as the coefficients and x the decision variables.  $T_S$  represents the transition matrix, which is not present in this thesis.  $W_S y_S(x)$  represents the recourse matrix  $W_S$  at each scenario and  $y_S(x)$  the second-stage decision variable.

Although the transition matrix is not present, the second stage-decision variable is indirectly dependent on the first-stage decision variable. So this means the problem is still defined by a two-stage stochastic programming model.

### 3.1.2 2-Stage Stochastic Optimization Model

An early version of the district energy optimization model by [33] serves as a basis for this work. The goal was to modify the existing infrastructure of the model to accommodate power flexible district heating technologies, enabling participation in the DA, ID and



balancing electricity market.

The following district heating technologies or generation units are part of the existing model:

- Heat Pump
- Electric Boiler
- Combined Heat and Power (gas in the original model, biomass in the new model)
- Waste Incineration (in the new model Waste to Energy)
- Tank Thermal Energy Storage
- Geothermal
- Solar Thermal
- Industrial Excess Heat
- Aquifer Thermal Energy Storage
- Deep Geothermal

Not all these technologies are interesting with regard to the DA, ID and balancing electricity market. Therefore the following technologies are addressed in this work:

Heat pumps and electric boilers. These two have the greatest potential for participating in the DA and especially the ID and balancing electricity market, due to their direct power flexibility and rapid ramping capabilities.

CHP plants, as long as they are not heat-only units. This assumption is made in this thesis, therefore this technology provides both direct and indirect power flexibility.

Tank thermal energy storage is generally considered to provide indirect power flexibility.

Waste to Energy is typically treated as an inflexible technology. In the original model it was configured to produce electricity; in this thesis, that assumption is dropped and the unit is modeled solely as a heat only plant (HOP).

Geothermal includes a heat pump to lift the temperature to the district-heating supply temperature and is therefore modeled as an electricity-driven, power-flexible technology.

The remaining four technologies are only considered peripherally in this work due to their lack of direct power flexibility. Deep geothermal energy, aquifer thermal energy storage, and industrial excess heat are excluded entirely and not further considered in this thesis. Although industrial excess heat could function as a technology with indirect power flexibility, it is not further addressed here, as it cannot be directly dispatched in DA or ID or balancing markets and is also not present in the region of the case study.

Figure 3.1 illustrates the schematic of the DH system, including the various heating and storage technologies.



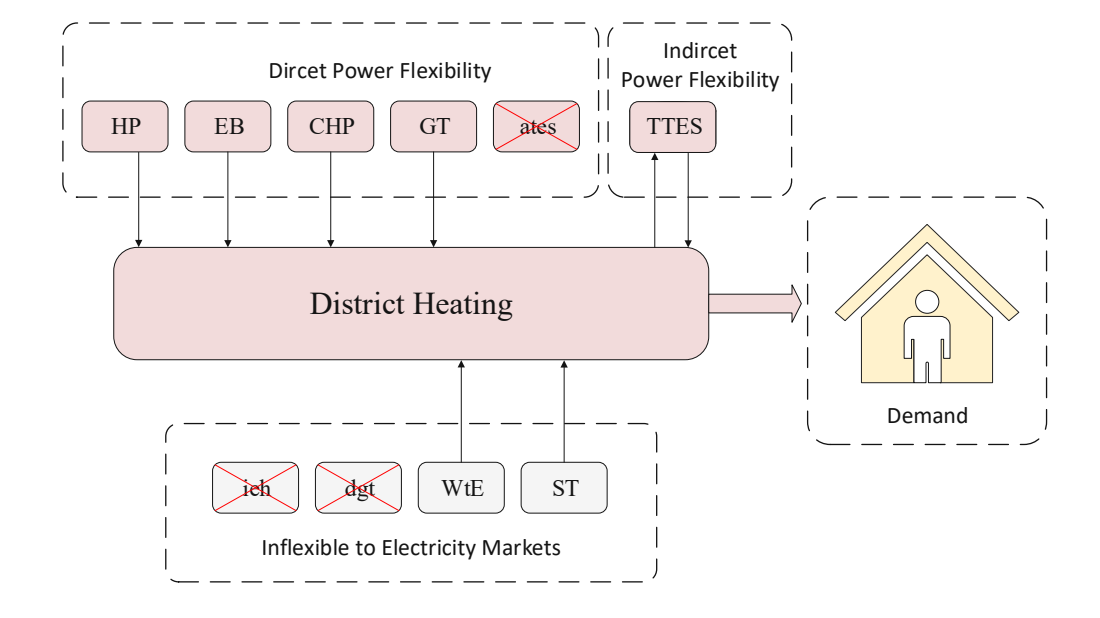


Figure 3.2: Schematic of the DH system

An overview of the heating technologies including abbreviations and descriptions is depicted in table 3.1. In the following, the abbreviation TE refers to Thermal Energy.

Technologies	Description	Input	Output
HP	Heat Pump	Electricity	TE
EB	Electric Boiler	Electricity	TE
CHP	Combined Heat and Power	Biomass	TE and Electricity
WtE	Waste to Energy	Waste	TE
TTES	Tank Thermal Energy Storage	TE	TE
GT	Geothermal	TE through Heat Pump	TE
ST	Solar Thermal	Solar Energy	TE

Table 3.1: Technologies

### 3.1.3 Objective Function

The existing LP model follows the general structure of cost minimization as the objective function, including investment costs, fixed costs, and variable costs across all technologies. In this work, the objective function was extended into a two-stage stochastic problem incorporating different DA and ID electricity price scenarios. These scenarios reflect the uncertain nature of electricity markets and their prices which are, among other factors, linked to uncertain weather data. More about that in section 4. The modified and extended objective function is given as follows:

3 Methodology

$$\min_{\mathbf{C}} \sum_{\tau \in \mathcal{T}} \sum_{y \in \mathbf{Y}} \left( C_{\tau,y}^{inv}(Q, c_{inv}) + C_{\tau,y}^{fix}(Q, c_{fix}) + \sum_{s \in \mathbf{S}} \left( p_s \sum_{t \in \mathbf{T}} C_{\tau,s,y,t}^{var}(q_{DA}, q_{ID}, DA, ID) \right) \right) + \beta \left( \tau_{risk} + \frac{1}{1 - \alpha} \sum_{s \in \mathbf{S}} p_s \delta_s \right) \tag{3.5}$$

and the respective technologies are represented through the vector  $\tau$ :

$$\mathcal{T} = \{HP, EB, CHP, WtE, TTES, GT, ST\}. \tag{3.6}$$

The model sets, variables and parameter are described in the following tables, table 3.2, table 3.3 and table 3.4 respectively:

### Pyomo Sets

$y \in \mathbf{Y} = \{2025, 2030, \dots, 2050\},  t \in \mathbb{N}$	Years with index $y$
$s \in \mathbf{S} = \{1, 2, 3, \dots, 10\},  t \in \mathbb{N}$	Electricity Price Scenarios with index $s$
$t \in \mathbf{T} = \{1, 2, 3, \dots, 8760\},  t \in \mathbb{N}$	Hours with index $t$

Table 3.2: Model setsl



Pyomo Variables	Description	Unit
$C_{ au,y}^{inv}$	Investment costs of the respective technology with index $\tau$ and index $y$ over years	€
$C_{ au,y}^{fix}$	Fixed costs of the respective technology with index $\tau$ and index $y$ over years	€
$C^{var}_{ au,s,y,t}$	Variable costs of the respective technology with index $\tau$ , index $s$ over scenarios, index $y$ over years and index $t$ over hours	€
Q	New installed generation or storage output of the respective technology per year with index $y$	MW
$q_{DA}$	Dispatch of the respective technology with index $\tau$ in the DA electricity market, index $s$ over scenarios, index $y$ over years and index $t$ over hours	MWh
$q_{ID}$	Dispatch of the respective technology with index $\tau$ in the ID electricity market, index $s$ over scenarios, index $y$ over years and index $t$ over hours	MWh

Table 3.3: Model variables

Pyomo Parameters	Description	Unit
$c_{inv}$	Specific investment costs of the respective technology with index $\tau$ and index $y$ over years	€/MWh
$c_{fix}$	Specific fixed costs of the respective technology with index $\tau$ and index $y$ over years	€/MWh
$p_s$	Probability of the respective scenario with index $s$	$\mathbb{N}$
DA	DA electricity price of the respective scenario with index $\tau$ , index $y$ over years and index $t$ over hours	€
ID	ID electricity price of the respective scenario with index $\tau$ , index $y$ over years and index $t$ over hours	€

Table 3.4: Model parameters



## 3.1.4 Conditional Value at Risk (CVaR)

To account for the inherent uncertainty and volatility in electricity prices—particularly in the ID market—this work incorporates a risk-averse optimization approach using CVaR. Although average electricity prices in the ID market are often lower compared to the DA market, they are also subject to significantly higher short-term fluctuations. If the optimization model were to minimize expected costs alone, it might over-utilize the ID market based solely on its lower average prices, neglecting the potential for extreme cost outcomes under unfavorable scenarios. To mitigate this risk, a CVaR-based penalty term is integrated into the objective function.

The CVaR term is expressed in monetary units (Euro) and penalizes scenarios within the upper tail of the cost distribution—specifically, the most expensive 10\% of scenarios when using a confidence level of  $\alpha = 0.90$ . This effectively discourages the model from dispatching excessive amounts of EB or HP output via the ID market if such a strategy results in high-cost outcomes under certain price scenarios.

Formally, the CVaR component added to the objective function is:

$$\beta \left( \tau_{risk} + \frac{1}{1 - \alpha} \sum_{s \in \mathbf{S}} p_s \delta_s \right) \tag{3.7}$$

where:

- $\tau$  is a decision variable representing the Value-at-Risk (VaR) threshold, i.e., the  $\alpha$ -quantile of scenario-dependent costs,
- $\delta_s$  is a non-negative slack variable representing the amount by which the cost in scenario s exceeds  $\tau$ ,
- $p_s$  is the probability weight of scenario s,
- $\bullet$   $\beta$  is a risk-weighting factor determining the influence of CVaR in the objective function,
- **S** is the set of all price scenarios.

The model enforces that at most  $(1-\alpha)$  of the total probability mass exceeds the threshold  $\tau$ , thus implementing a probabilistic upper-bound on high-cost realizations. The variables  $\delta_s$  allow the model to quantify the excess cost in such cases, and these excesses are then penalized proportionally.

This mechanism introduces a risk-sensitive behavior in the optimization. Rather than relying purely on expected value minimization, the model explicitly accounts for tail risks

in the cost distribution of ID electricity procurement. As a result, dispatch decisions for HP and EB are made more conservatively when relying on volatile ID prices. The model thereby strikes a balance between exploiting the typically lower mean prices of the ID market and avoiding excessive exposure to unfavorable pricing scenarios.

This formulation is aligned with methods presented in recent literature, particularly those using CVaR to control the cost risks of CHP and heat pump operation under electricity market uncertainty. It provides a theoretically sound and practically relevant extension for optimizing flexible technologies under stochastic market conditions.

# 3.1.5 Constraints

Several constraints in this model are based on the deterministic district energy optimization framework developed by [33], which was taken over at an early development stage. These constraints have been substantially adapted or extended in the course of this thesis. In particular, additional formulations were introduced to reflect the explicit participation in both the DA and ID electricity markets.

## **Demand Balance Constraint**

To ensure that the thermal demand is met at every point in time, the following constraint defines the hourly heat balance for all scenarios and years. The sum of thermal energy supplied by all generation technologies, including the discharge from the thermal energy storage, must equal the respective hourly heat demand. In contrast to the original formulation in [33], the thermal storage in this model is exclusively charged by electricitybased technologies, allowing for flexible operation based on electricity market price signals.

$$q_{s,y,t}^{\text{HP}} + q_{s,y,t}^{\text{EB}} + q_{s,y,t}^{\text{CHP}} + q_{s,y,t}^{\text{WtE}} + q_{s,y,t}^{\text{GT}} + q_{s,y,t}^{\text{ST}} + q_{s,y,t}^{\text{TTES,out}} - q_{s,y,t}^{\text{TTES,in}} = q_{s,y,t}^{\text{D}} : \forall s \in \mathbf{S}, \ y \in \mathbf{Y}, \ t \in \mathbf{T}$$
(3.8)

Table 3.5 provides an overview of the model variables involved in the demand balance constraint, including their functional meaning and corresponding unit of measurement:

32



Pyomo Variables	Description	Unit
$q_{s,y,t}^{ m HP}$	Thermal energy supplied by the heat pump in scenario $s$ , year $y$ , and hour $t$	MWh
$q_{s,y,t}^{\mathrm{EB}}$	Thermal energy supplied by the electric boiler in scenario $s, \ {\rm year} \ y, \ {\rm and \ hour} \ t$	MWh
$q_{s,y,t}^{\text{CHP}}$	Thermal energy supplied by the combined heat and power plant in scenario $s$ , year $y$ , and hour $t$	MWh
$q_{s,y,t}^{ m WtE}$	Thermal energy supplied by the waste-to-energy plant in scenario $s,$ year $y,$ and hour $t$	MWh
$q_{s,y,t}^{\mathrm{GT}}$	Thermal energy supplied by the geothermal source in scenario $s$ , year $y$ , and hour $t$	MWh
$q_{s,y,t}^{\mathrm{ST}}$	Thermal energy supplied by the solar thermal plant in scenario $s$ , year $y$ , and hour $t$	MWh
$q_{s,y,t}^{\mathrm{TTES,out}}$	Thermal energy discharged from TTES to the district heating network	MWh
$q_{s,y,t}^{\mathrm{TTES,in}}$	Thermal energy charged into the TTES from generation units	MWh
$q_{s,y,t}^{\mathrm{D}}$	Thermal heat demand to be met by the system in scenario $s,$ year $y,$ and hour $t$	MWh

Table 3.5: Model variables used in the demand balance constraint

# **Heat Pump Constraints**

The heat pump's variable operating cost accounts for DA and ID electricity procurement, variable O&M and grid energy charges, and a credit from mFRR-down capacity reservation (no activation energy is modeled):

$$c_{s,y,t}^{\text{HP,var}} = q_{s,y,t}^{\text{HP,el,DA}} \cdot p_{s,y,t}^{\text{DA}} + q_{s,y,t}^{\text{HP,el,ID}} \cdot p_{s,y,t}^{\text{ID}} - q_{s,y,t}^{\text{HP,mFRR}\downarrow} \cdot p_{s,y,t}^{\text{mFRR}\downarrow}, \quad : \forall s \in \mathbf{S}, \ y \in \mathbf{Y}, \ t \in \mathbf{T}.$$

$$(3.9)$$

Consistency with the device's electrical headroom is enforced by limiting reserved mFRRdown capacity to the unused electrical input at each hour:

$$q_{s,y,t}^{\text{HP,mFRR}\downarrow} \leq \frac{Q_{s,y}^{\text{HP,max}}}{\text{COP}_{s,y,t}} - \left(q_{s,y,t}^{\text{HP,el,DA}} + q_{s,y,t}^{\text{HP,el,ID}}\right), \quad : \forall s \in \mathbf{S}, \ y \in \mathbf{Y}, \ t \in \mathbf{T}. \tag{3.10}$$

Symbol	Description	Unit
$c_{s,y,t}^{\mathrm{HP,var}}$	Variable operating cost of HP in $(s, y, t)$ , incl. DA/ID purchases, O&M, grid charge, and mFRR-down credit (capacity only)	€
$q_{s,u,t}^{\mathrm{HP,el,DA}}$	Electrical consumption bought on DA market	MWh
$q_{s,y,t}^{\text{IP,el,ID}}$ $q_{s,y,t}^{\text{HP,el,ID}}$	Electrical consumption bought on ID market	MWh
$q_{s,y,t}^{ ext{HP,mFRR}\downarrow}$	Reserved mFRR-down electrical capacity (no activation)	MWh
$p_{s,u,t}^{\mathrm{DA}}, p_{s,u,t}^{\mathrm{ID}}$	DA / ID electricity price	€/MWh
$p_{s,y,t}^{ ext{mFRR}\downarrow}$	mFRR-down capacity price	€/MWh

Table 3.6: Heat pump variables/parameters used in (3.9)–(3.10).

The investment cost constraint for the heat pump links the newly installed capacity to its specific investment cost. This constraint ensures that investment costs are only incurred for additional capacity built in a given year and scenario:

$$c_{s,y}^{\mathrm{HP,inv}} = Q_{s,y}^{\mathrm{HP,inv}} \cdot c_{s,y}^{\mathrm{HP,unit}} : \forall s \in \mathbf{S}, \ y \in \mathbf{Y}$$
 (3.11)

Variable / Parameter	Description	Unit
$c_{s,y}^{\mathrm{HP,inv}}$	Investment cost of the heat pump in scenario $s$ and year $y$	€
$Q_{s,y}^{ m HP,inv}$	Newly installed heat pump capacity	MW
$c_{s,y}^{\mathrm{HP,unit}}$	Specific investment cost of the heat pump	€/MW

Table 3.7: Heat pump investment variables

In addition to investment costs, annual fixed O&M costs are accounted for in a separate constraint. These are assumed to be 0.21% of the specific investment costs, as detailed in Section 2.2.2.

To ensure consistent accounting of heat flows, the following constraint enforces the internal heat balance of the heat pump. The total heat output must equal the sum of the heat directly fed into the district heating network and the heat directed to the thermal energy storage:



$$q_{s,y,t}^{\mathrm{HP}} = q_{s,y,t}^{\mathrm{HP} \to \mathrm{TTES}} + q_{s,y,t}^{\mathrm{HP} \to \mathrm{DHN}} \quad : \forall s \in \mathbf{S}, \ y \in \mathbf{Y}, \ t \in \mathbf{T}$$
 (3.12)

Variable / Parameter	Description	Unit
$q_{s,y,t}^{ m HP}$	Total thermal output of the heat pump	MWh
$q_{s,y,t}^{\mathrm{HP}  o \mathrm{TTES}}$	Heat from HP directed to the tank thermal energy storage	MWh
$q_{s,y,t}^{\mathrm{HP} \to \mathrm{DHN}}$	Heat from HP directly fed into the district heating network	MWh

Table 3.8: Heat pump internal heat flow variables

The following constraint links the electricity consumption from both the day-ahead and intraday markets to the thermal output of the heat pump. The total heat generated comprising the amount directly supplied to the district heating network and the portion injected into TTES must equal the sum of electricity consumed in both markets multiplied by the respective COP:

$$q_{s,y,t}^{\text{HP}\to\text{TTES}} + q_{s,y,t}^{\text{HP}\to\text{DHN}} = \left(q_{s,y,t}^{\text{HP,el,DA}} + q_{s,y,t}^{\text{HP,el,ID}}\right) \cdot \text{COP}_{s,y,t}^{\text{HP}} \quad : \forall s \in \mathbf{S}, \ y \in \mathbf{Y}, \ t \in \mathbf{T}$$
(3.13)

Variable / Parameter	Description	Unit
$\mathrm{COP}^{\mathrm{HP}}_{s,y,t}$	Coefficient of performance of the heat pump at hour $t$	_

Table 3.9: Heat pump thermal-electric coupling variables

To ensure that the heat pump does not exceed its installed thermal capacity, the following constraint sets an upper bound on the total hourly heat feed-in:

$$q_{s,y,t}^{\mathrm{HP}} \le Q_{s,y}^{\mathrm{HP,max}} \quad : \forall s \in \mathbf{S}, \ y \in \mathbf{Y}, \ t \in \mathbf{T}$$
 (3.14)



Variable / Parameter	Description	Unit
$Q_{s,y}^{\mathrm{HP,max}}$	Installed thermal capacity of the heat pump in scenario $s$ and year $y$ , defining the maximum hourly heat feed-in	MW

Table 3.10: Heat pump capacity constraint parameter

# **Electric Boiler Constraints**

The electric boiler's variable operating cost accounts for DA and ID electricity procurement and a credit from mFRR-down capacity reservation (no activation energy is modeled):

$$c_{s,y,t}^{\text{EB,var}} = q_{s,y,t}^{\text{EB,el,DA}} \cdot p_{s,y,t}^{\text{DA}} + q_{s,y,t}^{\text{EB,el,ID}} \cdot p_{s,y,t}^{\text{ID}} - q_{s,y,t}^{\text{EB,mFRR}\downarrow} \cdot p_{s,y,t}^{\text{mFRR}\downarrow}, \quad : \forall s \in \mathbf{S}, \ y \in \mathbf{Y}, \ t \in \mathbf{T}.$$

$$(3.15)$$

Consistency with the device's electrical headroom is enforced by limiting reserved mFRRdown capacity to the unused electrical input at each hour:

$$q_{s,y,t}^{\text{EB,mFRR}\downarrow} \leq \frac{Q_{s,y}^{\text{EB,max}} - q_{s,y,t}^{\text{EB,th}}}{\eta_{s,y}^{\text{EB}}}, : \forall s \in \mathbf{S}, y \in \mathbf{Y}, t \in \mathbf{T}.$$
 (3.16)

Symbol	Description	Unit
$c_{s,y,t}^{\mathrm{EB,var}}$	Variable operating cost of EB in $(s, y, t)$ , incl. DA/ID purchases and mFRR-down credit (capacity only)	€
$q_{s,y,t}^{\mathrm{EB,el,DA}}$	Electrical consumption bought on DA market	MWh
$q_{s,y,t}^{ ext{EB,el,ID}}$	Electrical consumption bought on ID market	MWh
$q_{s,y,t}^{\mathrm{EB,mFRR}\downarrow}$	Reserved mFRR-down electrical capacity (no activation)	MWh
$q_{s,y,t}^{ ext{EB,th}}$	Thermal output dispatched by EB	MWh
$Q_{s,y}^{ m \widetilde{E}\dot{B}, max}$	Installed thermal capacity of EB	MW
$\eta_{s,y}^{ ext{EB}}$	EB efficiency (th/el)	_

Table 3.11: Electric boiler variables/parameters used in (3.15)–(3.16).

The investment cost constraint for the electric boiler links the newly installed capacity to its specific investment cost. This ensures that capital expenditures are only incurred for additional capacity built in a given year and scenario:

$$c_{s,y}^{\mathrm{EB,inv}} = Q_{s,y}^{\mathrm{EB,inv}} \cdot c_{s,y}^{\mathrm{EB,unit}} : \forall s \in \mathbf{S}, \ y \in \mathbf{Y}$$
 (3.17)

In addition to investment costs, annual fixed O&M costs are accounted for in a separate constraint. These are assumed to be 0.21% of the specific investment costs, as detailed in Section 2.2.2.

To ensure consistent accounting of heat flows, the following constraint enforces the internal heat balance of the electric boiler. The total thermal output must equal the sum of the heat directly fed into the district heating network and the heat directed to the thermal energy storage:

$$q_{s,y,t}^{\text{EB}} = q_{s,y,t}^{\text{EB} \to \text{TTES}} + q_{s,y,t}^{\text{EB} \to \text{DHN}} : \forall s \in \mathbf{S}, \ y \in \mathbf{Y}, \ t \in \mathbf{T}$$
 (3.18)

Variable / Parameter	Description	Unit
$q_{s,y,t}^{ m EB}$	Total thermal output of the electric boiler	MWh
$q_{s,y,t}^{\mathrm{EB}  o \mathrm{TTES}}$	Heat from EB directed to the tank thermal energy storage	MWh
$q_{s,y,t}^{\mathrm{EB}  o \mathrm{DHN}}$	Heat from EB directly fed into the district heating network	MWh

Table 3.12: Electric boiler internal heat flow variables

The following constraint ensures consistency between electricity consumption and thermal output. The total heat generated, both directly supplied to the district heating network and injected into the thermal storage, must equal the electricity consumption (from both markets) multiplied by the electric boiler's efficiency:

$$q_{s,y,t}^{\text{EB}\to\text{TTES}} + q_{s,y,t}^{\text{EB}\to\text{DHN}} = \left(q_{s,y,t}^{\text{EB,el,DA}} + q_{s,y,t}^{\text{EB,el,ID}}\right) \cdot \eta_{s,y}^{\text{EB}} \quad : \forall s \in \mathbf{S}, \ y \in \mathbf{Y}, \ t \in \mathbf{T} \quad (3.19)$$

To ensure that the electric boiler does not exceed its installed thermal capacity, the following constraint sets an upper bound on the total hourly heat feed-in:

$$q_{s,y,t}^{\text{EB}} \le Q_{s,y}^{\text{EB,max}} : \forall s \in \mathbf{S}, \ y \in \mathbf{Y}, \ t \in \mathbf{T}$$
 (3.20)



## **Combined Heat and Power Constraints**

The variable operating costs of the CHP unit are derived from fuel input and market interactions. Biomass consumption is multiplied by the biomass price, while electricity consumed from the DA and ID markets is credited against the total cost, reflecting the CHP's co-generation structure and potential electricity recovery:

$$c_{s,y,t}^{\text{CHP,var}} = q_{s,y,t}^{\text{CHP,bio}} \cdot p_{s,y,t}^{\text{bio}} - \left(q_{s,y,t}^{\text{CHP,el,DA}} \cdot p_{s,y,t}^{\text{DA}} + q_{s,y,t}^{\text{CHP,el,ID}} \cdot p_{s,y,t}^{\text{ID}}\right) \quad : \forall s \in \mathbf{S}, \ y \in \mathbf{Y}, \ t \in \mathbf{T}$$

$$(3.21)$$

Variable / Parameter	Description	Unit
$c_{s,y,t}^{\mathrm{CHP,var}}$	Variable cost of heat pump operation	€
$q_{s,y,t}^{ m CHP,bio}$	Biomass input to the CHP plant	MWh
$p_{s,y,t}^{ m bio}$	Biomass price in scenario $s$ , year $y$ and hour $t$	€/MWh
$q_{s,y,t}^{\mathrm{CHP,el,DA}}$	Electricity consumption of heat pump from DA market	MWh
$q_{s,y,t}^{\mathrm{CHP,el,ID}}$	Electricity consumption of heat pump from ID market	MWh

Table 3.13: Combined Heat and Power cost-related variables

The investment cost constraint for the combined heat and power unit links the newly installed electrical capacity to its specific investment cost. This ensures that capital expenditures are only incurred for additional capacity built in a given year and scenario:

$$c_{s,y}^{\text{CHP,inv}} = Q_{s,y}^{\text{CHP,el,inv}} \cdot c_{s,y}^{\text{CHP,unit}} : \forall s \in \mathbf{S}, \ y \in \mathbf{Y}$$
 (3.22)

Variable / Parameter	Description	Unit
$c_{s,y}^{\mathrm{CHP,inv}}$	Investment cost of the CHP unit	€
$Q_{s,y}^{ m CHP,inv}$	Newly installed electrical capacity of CHP unit	MW
$c_{s,y}^{\mathrm{CHP,unit}}$	Specific investment cost of CHP unit	$\in$ /MW

Table 3.14: CHP investment variables

In addition to investment costs, annual fixed O&M costs are accounted for in a separate constraint. These are assumed to be 4.3% of the specific investment costs, as detailed in Section 2.2.2.

To ensure consistent energy accounting and technical feasibility of CHP operation, the following constraints define the relationship between fuel input, thermal and electrical output, and the maximum combined feed-in capacity of the CHP unit:

$$q_{s,y,t}^{\text{CHP}} + q_{s,y,t}^{\text{CHP,el}} \le Q_{s,y}^{\text{CHP,mix,max}} : \forall s \in \mathbf{S}, \ y \in \mathbf{Y}, \ t \in \mathbf{T}$$
 (3.23)

$$q_{s,y,t}^{\text{CHP}} = q_{s,y,t}^{\text{CHP,bio}} \cdot \eta_{s,y}^{\text{CHP}} \cdot \alpha_{s,y}^{\text{CHP,heat}} \quad : \forall s \in \mathbf{S}, \ y \in \mathbf{Y}, \ t \in \mathbf{T}$$
 (3.24)

$$q_{s,y,t}^{\text{CHP,el}} = q_{s,y,t}^{\text{CHP,bio}} \cdot \eta_{s,y}^{\text{CHP}} \cdot \alpha_{s,y}^{\text{CHP,el}} \quad : \forall s \in \mathbf{S}, \ y \in \mathbf{Y}, \ t \in \mathbf{T}$$
 (3.25)

$$q_{s,y,t}^{\text{CHP,el}} = q_{s,y,t}^{\text{CHP,el,DA}} + q_{s,y,t}^{\text{CHP,el,ID}} : \forall s \in \mathbf{S}, \ y \in \mathbf{Y}, \ t \in \mathbf{T}$$
 (3.26)

Variable / Parameter	Description	Unit
$q_{s,y,t}^{ m CHP}$	Thermal output of the CHP unit	MWh
$q_{s,y,t}^{\mathrm{CHP,el}}$	Electrical output of the CHP unit	MWh
$Q_{s,y}^{ m CHP,mix,max}$	Maximum combined thermal and electrical feed-in capacity	MW
$\eta_{s,y}^{ ext{CHP}}$	Overall efficiency of the CHP unit	_
$lpha_{s,y}^{ ext{CHP,heat}}$	Heat share of the useful output	_
$lpha_{s,y}^{ ext{CHP,el}}$	Electricity share of the useful output	_

Table 3.15: CHP heat and electricity balance variables

# Waste to Energy Constraints

The variable operating costs of the WtE unit are calculated based on the amount of waste processed and emissions produced. A gate fee is credited, while costs are incurred for the carbon content of the waste stream according to the CO<sub>2</sub> certificate price (see Section 2.2.2).

$$c_{s,y,t}^{\text{WtE,var}} = \left(\frac{q_{s,y,t}^{\text{WtE}}}{h_{s,y}^{\text{WtE}}}\right) \cdot \left(-c_{s,y}^{\text{waste}}\right) + \left(\frac{q_{s,y,t}^{\text{WtE}}}{h_{s,y}^{\text{WtE}}}\right) \cdot \gamma_{s,y}^{\text{WtE,CO2}} \cdot p_{s,y,t}^{\text{CO2}} \quad : \forall s \in \mathbf{S}, \ y \in \mathbf{Y}, \ t \in \mathbf{T}$$

$$(3.27)$$

Variable / Parameter	Description	Unit
$c_{s,y,t}^{ ext{WtE,var}}$	Variable cost of WtE operation	€
$q_{s,y,t}^{ m WtE}$	Thermal output from WtE plant	MWh
$h_{s,y}^{ m WtE}$	Specific heat content of waste	MWh/ton
$c_{s,y}^{ m waste}$	Gate fee for waste disposal	€/ton
$\gamma_{s,y}^{ ext{WtE,CO2}}$	CO <sub>2</sub> emission factor of waste	$t\mathrm{CO}_2/\mathrm{ton}$
$p_{s,y,t}^{\mathrm{CO2}}$	CO <sub>2</sub> certificate price	$\in$ /tCO <sub>2</sub>

Table 3.16: WtE variable cost-related parameters

The investment cost of the WtE unit is defined by the specific investment cost and the additional installed capacity:

$$c_{s,y}^{\text{WtE,inv}} = Q_{s,y}^{\text{WtE,inv}} \cdot c_{s,y}^{\text{WtE,unit}} \quad : \forall s \in \mathbf{S}, \ y \in \mathbf{Y}$$
 (3.28)

Variable / Parameter	Description	Unit
$c_{s,y}^{ ext{WtE,inv}}$	Investment cost of the WtE unit	€
$Q_{s,y}^{ m WtE,inv}$	Newly installed thermal capacity of WtE unit	MW
$c_{s,y}^{ m WtE,unit}$	Specific investment cost of WtE unit	€/MW

Table 3.17: WtE investment parameters

In addition to investment costs, annual fixed O&M costs are accounted for in a separate constraint. These are assumed to be 4.5% of the specific investment costs, as detailed in Section 2.2.2.

The thermal output of the WtE unit is determined by the amount of waste input, its heat content, and the efficiency of the process:

$$q_{s,y,t}^{\text{WtE}} = q_{s,y,t}^{\text{waste}} \cdot \eta_{s,y}^{\text{WtE}} \cdot h_{s,y}^{\text{WtE}} \quad : \forall s \in \mathbf{S}, \ y \in \mathbf{Y}, \ t \in \mathbf{T}$$
(3.29)

The following constraint limits the maximum thermal output of the WtE unit:

$$q_{s,y,t}^{\text{WtE}} \le Q_{s,y}^{\text{WtE,max}} : \forall s \in \mathbf{S}, \ y \in \mathbf{Y}, \ t \in \mathbf{T}$$
 (3.30)

Variable / Parameter	Description	Unit
$q_{s,y,t}^{\mathrm{waste}}$	Waste input to the WtE unit	ton
$\eta_{s,y}^{ ext{WtE}}$	Thermal efficiency of WtE unit	_
$Q_{s,y}^{ m WtE,max}$	Maximum thermal output capacity of WtE unit	MW

Table 3.18: WtE balance and capacity variables

## **Geothermal Constraints**

The geothermal heat pump unit converts electricity from the DA and ID markets into heat with a fixed COP. Variable operating costs include both electricity procurement and additional electricity-related O&M costs of 5.7 EUR/MWh, which are added per unit of electricity consumed. For reasons of readability, these O&M costs are incorporated directly into the electricity price terms and are not shown separately in the equation.

$$c_{s,y,t}^{\text{GT,var}} = q_{s,y,t}^{\text{GT,el,DA}} \cdot \left(p_{s,y,t}^{\text{DA}}\right) + q_{s,y,t}^{\text{GT,el,ID}} \cdot \left(p_{s,y,t}^{\text{ID}}\right) \quad : \forall s \in \mathbf{S}, \ y \in \mathbf{Y}, \ t \in \mathbf{T}$$
 (3.31)

Variable / Parameter	Description	Unit
$c_{s,y,t}^{\mathrm{GT,var}}$	Variable cost of geothermal operation	€
$q_{s,y,t}^{ m GT,el,DA}$	Electricity input from DA market	MWh
$q_{s,y,t}^{ m GT,el,ID}$	Electricity input from ID market	MWh

Table 3.19: Geothermal variable cost components

Geothermal heat output is directly derived from the sum of DA and ID electricity input multiplied by the geothermal COP:

$$q_{s,y,t}^{\mathrm{GT}} = \left(q_{s,y,t}^{\mathrm{GT,el,DA}} + q_{s,y,t}^{\mathrm{GT,el,ID}}\right) \cdot \mathrm{COP}_{s,y}^{\mathrm{GT}} \quad : \forall s \in \mathbf{S}, \ y \in \mathbf{Y}, \ t \in \mathbf{T}$$
 (3.32)

The geothermal feed-in is technically limited by the installed thermal capacity:

$$q_{s,y,t}^{\text{GT}} \le Q_{s,y}^{\text{GT,max}} : \forall s \in \mathbf{S}, \ y \in \mathbf{Y}, \ t \in \mathbf{T}$$
 (3.33)

Investment costs are incurred only when new thermal capacity is installed:

$$c_{s,y}^{\text{GT,inv}} = Q_{s,y}^{\text{GT,inv}} \cdot c_{s,y}^{\text{GT,unit}} : \forall s \in \mathbf{S}, \ y \in \mathbf{Y}$$
 (3.34)

Variable / Parameter	Description	Unit
$q_{s,y,t}^{\mathrm{GT}}$	Thermal output of geothermal unit	MWh
$Q_{s,y}^{\mathrm{GT,max}}$	Maximum thermal feed-in capacity	MW
$\mathrm{COP}_{s,y}^{\mathrm{GT}}$	Coefficient of performance of the geothermal system	_
$Q_{s,y}^{ m GT,inv}$	Newly installed thermal capacity	MW
$c_{s,y}^{\mathrm{GT,inv}}$	Investment cost for geothermal unit	€
$c_{s,y}^{\mathrm{GT,unit}}$	Specific investment cost	€/MW

Table 3.20: Geothermal capacity and investment parameters



In addition to investment costs, annual fixed O&M costs are accounted for in a separate constraint. These are assumed to be 0.83\% of the specific investment costs, as detailed in Section 2.2.2.

# Solar Thermal Constraints

The ST module models a collector field coupled with an absorption heat pump. The total thermal output consists of the collected solar heat and the effect of the heat pump, defined by a thermal COP. No electricity consumption is considered for the absorption unit, so variable costs are set constant.

$$c_{s,y,t}^{\text{ST,var}} = 1.4 \quad : \forall s \in \mathbf{S}, \ y \in \mathbf{Y}, \ t \in \mathbf{T}$$
 (3.35)

Variable / Parameter	Description	Unit
$c_{s,y,t}^{\mathrm{ST,var}}$	Variable cost of solar thermal operation including land lease	€

Table 3.21: Solar thermal cost-related variables

The investment cost constraint for the solar thermal system distinguishes between the installed thermal collector capacity and the absorption heat pump component. It also accounts for land lease costs proportional to collector surface:

$$c_{s,y}^{\mathrm{ST,inv}} = Q_{s,y}^{\mathrm{ST,thermal}} \cdot c_{s,y}^{\mathrm{ST,unit}} + Q_{s,y}^{\mathrm{ST,HP}} \cdot c_{s,y}^{\mathrm{HP,unit}} \quad : \forall s \in \mathbf{S}, \ y \in \mathbf{Y}$$
 (3.36)

Variable / Parameter	Description	Unit
$c_{s,y}^{\mathrm{ST,inv}}$	Investment cost of the ST system	€
$Q_{s,y}^{\mathrm{ST,thermal}}$	Installed thermal collector output	MW
$Q_{s,y}^{ m ST,HP}$	Installed absorption heat pump capacity	MW
$c_{s,y}^{ m ST,unit}$	Specific investment cost of ST field	$\in$ /MW
$c_{s,y}^{ m HP,unit}$	Specific investment cost of absorption HP	€/MW

Table 3.22: ST investment variables

In addition to investment costs, annual fixed O&M costs are accounted for in a separate constraint. These are assumed to be 0.28% of the specific investment costs, as detailed in Section 2.2.2. Additionally, land lease costs based on collector area are included.

The total thermal output from the solar thermal system in any hour must not exceed the installed thermal capacity:

$$q_{s,y,t}^{\text{ST}} \le Q_{s,y}^{\text{ST,max}} : \forall s \in \mathbf{S}, \ y \in \mathbf{Y}, \ t \in \mathbf{T}$$
 (3.37)

Variable / Parameter	Description	Unit
$q_{s,y,t}^{\mathrm{ST}}$	Total thermal output of solar thermal system	MW
$Q_{s,y}^{ m ST,max}$	Installed thermal capacity of the ST system	MW

Table 3.23: Solar thermal feed-in constraint variables

The absorbed solar energy is calculated based on the solar irradiance, collector area, and efficiency:

$$q_{s,y,t}^{\text{ST,source}} = \frac{p_{s,y,t}^{\text{ST,irr}} \cdot p_{s,y}^{\text{ST,area}}}{1.000.000} \cdot \eta_{s,y}^{\text{ST}} \quad : \forall s \in \mathbf{S}, \ y \in \mathbf{Y}, \ t \in \mathbf{T}$$
 (3.38)

Variable / Parameter	Description	Unit
$q_{s,y,t}^{\text{ST,source}}$	Thermal energy directly from solar radiation	MW
$p_{s,y,t}^{ m ST,irr}$	Solar irradiance in scenario $s$ , year $y$ , hour $t$	$\mathrm{W/m^2}$
$p_{s,y}^{\mathrm{ST,area}}$	Installed collector area	$m^2$
$\eta_{s,y}^{ ext{ST}}$	Solar thermal efficiency	_

Table 3.24: Solar radiation utilization variables

To capture the performance of the integrated absorption heat pump, the following constraint ensures that the total thermal output of the solar thermal system corresponds to the solar collector output multiplied by the thermal COP:

$$q_{s,y,t}^{\text{ST}} = q_{s,y,t}^{\text{ST,source}} \cdot \text{COP}_{s,y}^{\text{ST}} : \forall s \in \mathbf{S}, \ y \in \mathbf{Y}, \ t \in \mathbf{T}$$
 (3.39)

3 Methodology

Variable / Parameter	Description	Unit
$\mathrm{COP}^{\mathrm{ST}}_{s,y}$	Thermal coefficient of performance of absorption HP	_

Table 3.25: Solar thermal absorption heat pump coupling

# Tank Thermal Energy Storage Constraints

To ensure that the thermal energy input and output of the TTES system does not exceed the allowable maximum charge and discharge rates, the following constraints are implemented:

$$q_{s,y,t}^{\text{TTES,in}} \le R_{s,y}^{\text{TTES}} : \forall s \in \mathbf{S}, \ y \in \mathbf{Y}, \ t \in \mathbf{T}$$
 (3.40)

$$q_{s,y,t}^{\text{TTES,out}} \le R_{s,y}^{\text{TTES}} : \forall s \in \mathbf{S}, \ y \in \mathbf{Y}, \ t \in \mathbf{T}$$
 (3.41)

Variable / Parameter	Description	Unit
$q_{s,y,t}^{\mathrm{TTES,in}}$	Thermal energy discharged from TTES into the DH network	MWh
$q_{s,y,t}^{\mathrm{TTES,out}}$	Thermal energy stored in TTES as output from the DH network (EB, HP)	MWh
$R_{s,y}^{\mathrm{TTES}}$	Maximum charge and discharge rate	MW

Table 3.26: TTES power flow constraints

The state of charge (SOC) of the TTES is governed by the following dynamic constraint. It accounts for thermal losses and round-trip efficiency:

$$k_{s,y,t}^{\text{TTES}} = \begin{cases} k_{s,y-5,8759}^{\text{TTES}} \cdot \lambda_{s,y} + \eta_{s,y}^{\text{TTES}} \cdot q_{s,y,0}^{\text{TTES},\text{out}} - \frac{q_{s,y,0}^{\text{TTES},\text{in}}}{\eta_{s,y}^{\text{TTES}}}, & \text{if } t = 0, y > 2025 \\ 0, & \text{if } t = 0, y = 2025 \end{cases}$$

$$k_{s,y,t-1}^{\text{TTES}} \cdot \lambda_{s,y} + \eta_{s,y}^{\text{TTES}} \cdot q_{s,y,t}^{\text{TTES},\text{out}} - \frac{q_{s,y,t}^{\text{TTES},\text{in}}}{\eta_{s,y}^{\text{TTES}}}, & \text{otherwise} \end{cases}$$

Variable / Parameter	Description	Unit
$k_{s,y,t}^{\mathrm{TTES}}$	Thermal energy content (state of charge)	MWh
$k_{s,y}^{\mathrm{TTES,max}}$	Maximum storage capacity	MWh
$\lambda_{s,y}$	Thermal loss factor	_
$\eta_{s,y}^{ ext{TTES}}$	Round-trip efficiency	_

Table 3.27: TTES energy balance parameters

The total energy stored must not exceed the maximum capacity:

$$k_{s,y,t}^{\text{TTES}} \le k_{s,y}^{\text{TTES,max}} : \forall s \in \mathbf{S}, \ y \in \mathbf{Y}, \ t \in \mathbf{T}$$
 (3.43)

To ensure a smooth year-to-year transition, the final SOC at the end of the planning horizon is constrained to a minimum value:

$$k_{s,y,8759}^{\text{TTES}} = 0 \quad : \forall s \in \mathbf{S}, \ y \in \mathbf{Y}$$
 (3.44)

Investment costs are calculated based on newly installed capacity:

$$c_{s,y}^{\text{TTES,inv}} = k_{s,y}^{\text{TTES,inv}} \cdot c_{s,y}^{\text{TTES,unit}} \quad : \forall s \in \mathbf{S}, \ y \in \mathbf{Y}$$
 (3.45)

Annual fixed costs are modeled as 1% of the corresponding investment costs and are only incurred in years with newly installed capacity.

The variable operating costs of the TTES depend on the total energy charged and discharged. A fixed surcharge of 0.1 EUR/MWh is applied but not shown explicitly:

$$c_{s,y,t}^{\text{TTES,var}} = \left(q_{s,y,t}^{\text{TTES,in}} + q_{s,y,t}^{\text{TTES,out}}\right) \cdot c_{s,y}^{\text{TTES,ch/dis}} \quad : \forall s \in \mathbf{S}, \ y \in \mathbf{Y}, \ t \in \mathbf{T}$$
 (3.46)

Variable / Parameter	Description	Unit
$c_{s,y}^{\rm TTES, charge/discharge}$	Specific charge/discharge cost of the TTES	€/MWh

Table 3.28: TTES charge/discharge cost parameter



# 3.2 Electricity Price Simulation

# 3.2.1 AR-X Forecasting Model

This subsection follows the open, reproducible EPF setup introduced by [32] and uses it as a reference point for modeling choices. In that framework, the LEAR model is a parameter-rich AR-X specification (multivariate 24-hour formulation) estimated via LASSO; it combines recent price lags, day-ahead exogenous forecasts, and weekday dummies, typically after a variance-stabilizing transformation, and is re-estimated on rolling windows. The study also codifies best practices (year-long test sets, rigorous baselines, standardized evaluation) and provides the EPFtoolbox for reproducibility [36].

# LEAR (reference model per Lago et al.)

Let  $p_{d,h}$  denote the day-ahead price for delivery day d, hour h, and let  $X_{d,h}$  denote the exogenous feature vector composed of the 24-hour blocks of exogenous inputs for days d, d-1, and d-7. The LEAR reference model has the following structure:

$$p_{d,h} = f(\mathbf{p}_{d-1}, \mathbf{p}_{d-2}, \mathbf{p}_{d-3}, \mathbf{p}_{d-7}, \mathbf{x}_{d}^{i}, \mathbf{x}_{d}^{i}, \mathbf{x}_{d-1}^{i}, \mathbf{x}_{d-1}^{i}, \mathbf{x}_{d-7}^{i}, \mathbf{x}_{d-7}^{i}, \boldsymbol{\theta}_{h}) + \varepsilon_{d,h}$$

$$= \sum_{i=1}^{24} \theta_{h,i} \cdot p_{d-1,i} + \sum_{i=1}^{24} \theta_{h,24+i} \cdot p_{d-2,i} + \sum_{i=1}^{24} \theta_{h,48+i} \cdot p_{d-3,i} + \sum_{i=1}^{24} \theta_{h,72+i} \cdot p_{d-7,i}$$

$$+ \sum_{i=1}^{24} \theta_{h,96+i} \cdot \mathbf{x}_{d,i}^{1} + \sum_{i=1}^{24} \theta_{h,120+i} \cdot \mathbf{x}_{d,i}^{2} + \sum_{i=1}^{24} \theta_{h,144+i} \cdot \mathbf{x}_{d-1,i}^{1} + \sum_{i=1}^{24} \theta_{h,168+i} \cdot \mathbf{x}_{d-1,i}^{2}$$

$$+ \sum_{i=1}^{24} \theta_{h,192+i} \cdot \mathbf{x}_{d-7,i}^{1} + \sum_{i=1}^{24} \theta_{h,216+i} \cdot \mathbf{x}_{d-7,i}^{2} + \sum_{i=1}^{7} \theta_{h,240+i} \cdot \mathbf{z}_{d,i} + \varepsilon_{d,h}.$$

$$(3.47)$$

Here,  $\theta_h = [\theta_{h,1}, \dots, \theta_{h,247}]^{\top}$  collects the 247 coefficients of the LEAR specification for hour h (96 price-lag terms + 144 exogenous terms + 7 weekday dummies). In the original benchmark of [32], estimating this specification with LASSO shrinks many of these coefficients exactly to zero.

Variance-stabilizing transforms (e.g., asinh on median/MAD-standardized prices) and daily rolling recalibration are recommended and shown to improve robustness [32].

## Modified model used in this thesis (pure X-model with ridge)

For scenario generation rather than minimum-MAE (Mean Absolute Error) forecasting, the autoregressive part is intentionally removed and the estimation switched from LASSO to ridge. Implementation follows the EPF toolbox documentation [36] (LEAR/feature handling), with adaptations for pure X-model ridge estimation.

Let  $p_{d,h}$  denote the day-ahead price for delivery day d and hour h. Let  $x_{d,i}^1$  and  $x_{d,i}^2$ be the exogenous forecasts for wind and PV available on d-1 for delivery day d, hour  $i=1,\ldots,24$ . Let  $z_{d,k}$  be weekday dummies  $(k=1,\ldots,7)$ . For each hour h, the X-model drops all price lags and uses only the current-day 24-hour blocks of exogenous inputs (hourly wind and PV forecasts available on d-1) plus weekday effects:

$$p_{d,h} = \theta_{h,0} + \sum_{i=1}^{24} \theta_{h,i} \cdot x_{d,i}^{1} + \sum_{i=1}^{24} \theta_{h,24+i} \cdot x_{d,i}^{2} + \sum_{k=1}^{7} \theta_{h,48+k} \cdot z_{d,k} + \varepsilon_{d,h}.$$
 (3.48)

The coefficient vector for hour h is  $\boldsymbol{\theta}_h = [\theta_{h,1}, \dots, \theta_{h,55}]^{\top}$  (24 wind + 24 PV + 7 weekday dummies), with intercept  $\theta_{h,0}$ .

Parameters are estimated hour-by-hour via ridge regression on a rolling window, with standardized targets and features (intercept unpenalized). This design deliberately removes autoregressive price terms to avoid persistence-driven fits and to preserve a transparent mapping from fundamentals to prices, which is preferable for scenario generation; LEAR remains a strong forecasting benchmark with high accuracy reported in the literature.

# Training-testing setup and recalibration

- Day-Ahead (DA): rolling daily re-estimation with a two-year calibration window; the test period is one full year, during which price paths are produced day by day from the re-estimated hourly models. This aligns with the recommendation to evaluate over year-long spans [32].
- Intraday (ID): only the year 2019 of ID3 is available; to maintain the rolling protocol, the 2019 series is duplicated to construct a one-year training segment (weekday-aligned) preceding the one-year test segment. Models are then re-estimated daily on a one-year window and used to generate hourly ID paths.

## Scenario generation mechanism

For each scenario family (e.g., low ... high), the exogenous drivers are scaled according to literature-based factors (separately for wind and PV). The calibrated hourly ridge models are then evaluated on these counterfactual inputs to produce five distinct price paths per market (DA and ID), with the full procedure repeated over the test year as described in the next subsection 4. The result is a set of structurally different, reproducible trajectories that reflect sensitivity to renewable conditions rather than optimized point accuracy [32].

# 3.2.2 Scenario Generation

In this section, the methodology for generating electricity price scenarios for the optimization of the district heating system is presented. The focus lies on the generation

48



of DA and ID price scenarios, their correlation with renewable electricity generation (photovoltaic and wind), and the construction of representative scenario paths to be used in the two-stage stochastic optimization model as presented in 3.1.2.

# 3.2.3 DA Price Simulation Methodology

As shown in section 3.2.1, the Day-Ahead price scenarios are generated using a modified AR-X framework, where the autoregressive (AR) component is intentionally omitted. This results in a pure exogenous (X) model driven solely by external inputs, specifically forecasted photovoltaic (PV) and wind power generation. The goal is not to accurately predict prices but to explore a plausible range of future electricity price developments under varying renewable generation conditions. A high MAE is deliberately accepted to ensure scenario diversity.

The exogenous inputs are based on real forecast data up to 04.05.2025. For the period beyond that date, data from 2024 are reused in a weekday-aligned fashion (e.g., 06.05.2024) was a Monday, so it is reused for 05.05.2025, also a Monday). This ensures realistic intraday and seasonal patterns while maintaining internal consistency.

For each market (DA and later ID), five scenario paths are generated based on different assumptions regarding renewable generation as described in sector 4. These paths are labeled as follows:

• High: Extremely high PV and wind generation (upper bound of literature-based forecast range)

• **Higher**: Moderately high renewable generation

• Base: Median level

• Lower: Moderately low renewable generation

Low: Very low PV and wind generation (historical reference level, e.g., 2023/2024)

Each scenario is simulated using the same price generation model, with the only difference being the input levels of PV and wind generation.

## Correlation Between DA Prices and Renewables

The inverse relationship between electricity prices and renewable generation is a welldocumented phenomenon, primarily driven by the merit-order effect. To validate this within the scenario framework, historical and simulated data are analyzed.

# Scatterplot Analysis

The following scatterplots show the relationship between DA prices and PV (left) and wind generation (right):

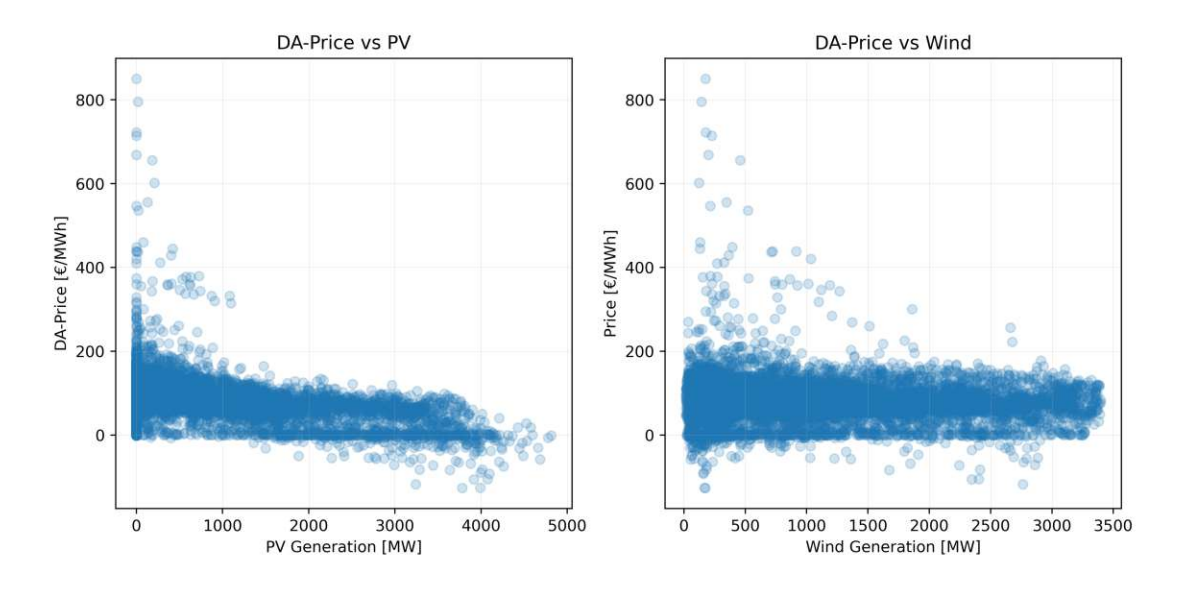


Figure 3.3: Scatterplot correlation between DA prices and pv / wind generation forecast

It is evident that both PV and wind generation exhibit a negative correlation with DA prices. High renewable infeed tends to lower the marginal cost of electricity generation, thus suppressing market prices. This behavior is reflected in the structure of the price simulation model.

## **Time-Series Visualization**

To further illustrate this dynamic over time, a representative week in summer 2024 (calendar week 30) is shown in figure 3.4.

Here, we observe that price minima often coincide with PV or wind generation peaks. Conversely, during periods of low renewable availability, price spikes become more frequent. This temporal behavior confirms that the price simulation model appropriately maps renewable infeed to expected price signals.

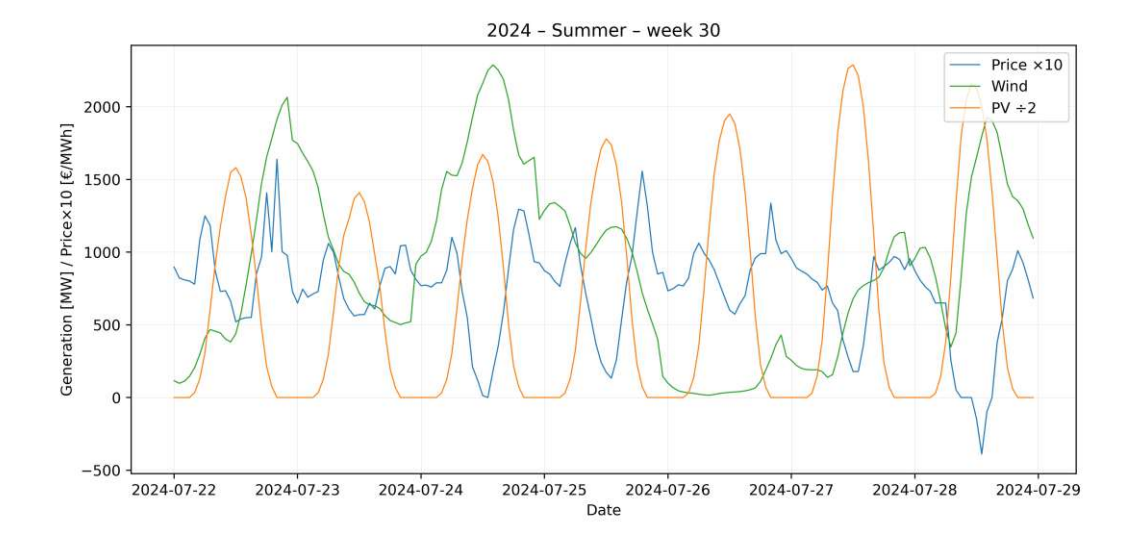


Figure 3.4: Relationship between pv, wind and DA price in summer 2024 (week 30)

# **Validation of Price Simulation**

The simulated prices are compared against real DA prices to assess whether the magnitude and structure of price variation is realistic, without aiming for high forecast precision. The figure below compares the daily mean values of original DA prices with a high renewable scenario simulation for the year 2035:



Figure 3.5: Daily average DA prices in 2025/2024 with simulated high RES DA price path in 2035



It is visible that the simulation captures the general seasonal price trend and realistic variability. Deviations are expected and desired, as the purpose is to span a representative uncertainty range for the stochastic optimization.

Additionally, the simulated price path for the high scenario in 2035 is shown below for the two-week period from 01.07.2024 to 14.07.2024:

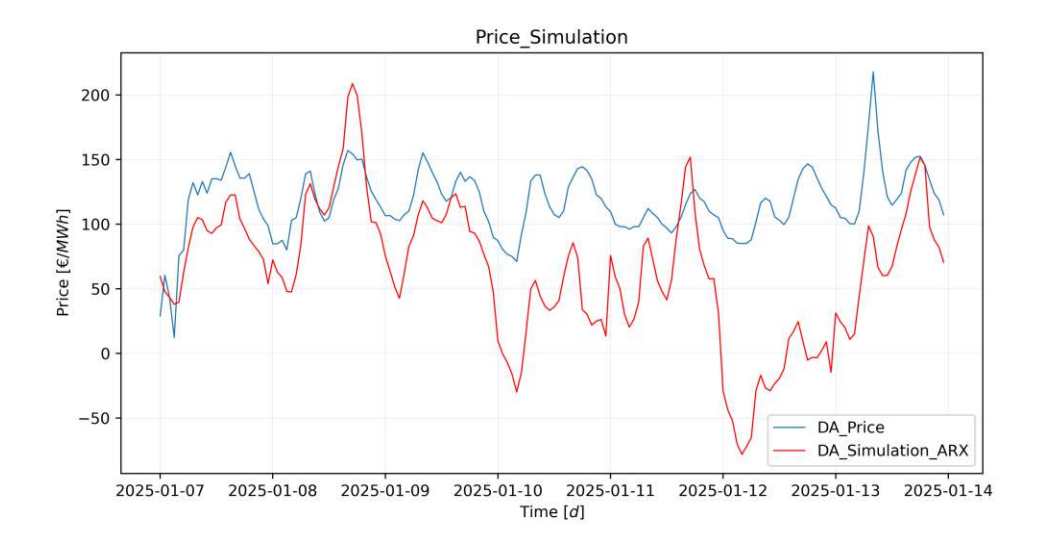


Figure 3.6: 2 week comparision of DA price 2024 with siumlated high RES DA price 2035

The variation over time reflects expected shifts due to renewable generation patterns, as well as occasional spikes due to modeled volatility in market dynamics. The spread of simulated values forms the basis for defining the five DA scenario paths.

# 3.2.4 ID Price Simulation Methodology

Unlike for the Day-Ahead market, no full dataset of ID prices is available for future years. The only historical data accessible covers the year 2019. Therefore, a spread-based methodology is applied to derive ID price scenarios.

# **Historical Spread Calculation**

The historical spread is defined as the difference between DA and ID prices at each hourly time step t:

$$Spread_{2019}(t) = DA_{2019}(t) - ID_{2019}(t)$$
(3.49)

This spread reflects the systematic difference between both markets and exhibits distinct temporal patterns due to trading dynamics, renewable forecast errors, and market liquidity.

To ensure temporal consistency between DA and ID price spreads, the 2019 spread values are matched by weekday and hour to the simulation horizon. For example, all Mondays at 13:00 in the simulated DA price series are assigned spread values from Mondays at 13:00 in 2019. This alignment preserves typical weekly patterns in the DA-ID price differences and avoids distortions caused by mismatched calendar structures.

# Statistical Characterization of the Spread

The spread is analyzed over the course of the year to identify recurring structures. Key statistical indicators such as mean and standard deviation are computed. A plot of the annual spread time series is included to visualize typical patterns.

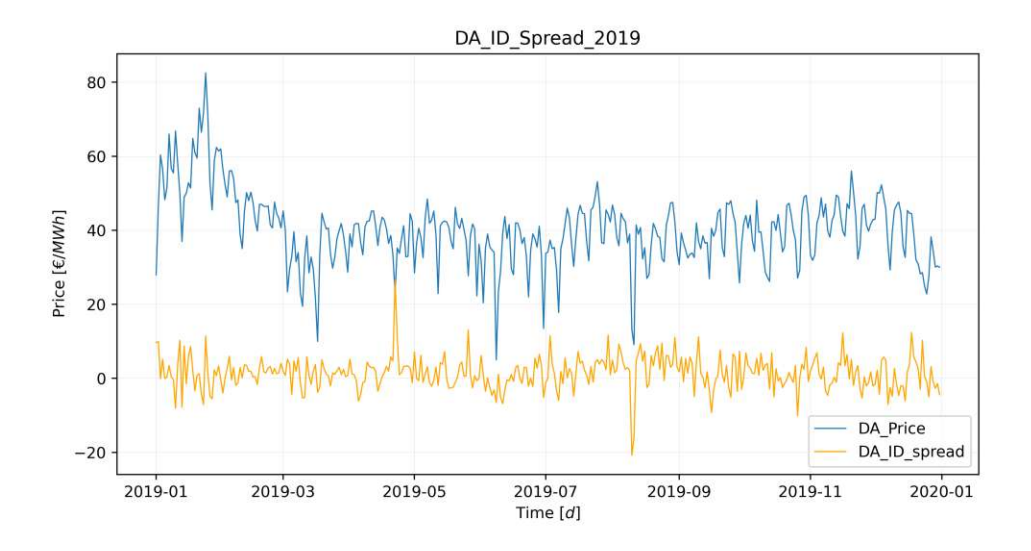


Figure 3.7: Daily average DA prices in 2019 with corresponding DA-ID spread

The analysis shows that the average spread in 2019 was  $+ 1.44 \in /MWh$ , indicating that intraday prices were, on average, lower than day-ahead prices. This observation reflects



the typical behavior of an electricity market, where late adjustments in generation or demand are often made at lower marginal costs.

Additionally, the standard deviation of the spread was found to be  $8.30 \in MWh$ . This considerable variability highlights the necessity of modeling multiple spread paths instead of relying on a single deterministic correction. The spread's volatility reflects the complex dynamics of short-term market behavior and justifies the use of five distinct spread scenarios in the stochastic optimization model.

# Forecast Errors and Economic Interpretation

To improve the explanatory quality and realism of spread modeling, an X-model approach is applied using renewable forecast errors as exogenous variables. The underlying economic rationale is as follows:

- Positive Forecast Error (FE): The forecast overestimates actual generation, i.e., . This leads to a shortage of renewables in real time, requiring expensive balancing measures. The ID price rises, hence the spread decreases.
- Negative Forecast Error (FE): The forecast underestimates actual generation, i.e., . More renewables are available in real time than expected, leading to oversupply. The ID price drops, and the spread increases.

Formally, the forecast error is defined as:

$$FE_{PV}(t) = PV_{\text{forecast}}(t) - PV_{\text{actual}}(t) \quad \text{and}$$

$$FE_{Wind}(t) = Wind_{\text{forecast}}(t) - Wind_{\text{actual}}(t).$$
(3.50)

Expectation Fall A:

$$FE_{PV,Wind} > 0 \Rightarrow ID \text{ price } \uparrow \Rightarrow Spread \downarrow$$
 (3.51)

**Expectation Fall B:** 

$$FE_{PV\ Wind} < 0 \Rightarrow ID\ price \downarrow \Rightarrow Spread \uparrow$$
 (3.52)

This leads to a **negative correlation** between forecast error and the DA-ID spread. This hypothesis is tested empirically in the dataset.

However, data inspection revealed significant limitations in the PV forecast data. Starting from February 2019, the PV forecasts and actual generation values became nearly identical, resulting in almost zero variability in the PV forecast error. This can be clearly seen in the corresponding scatterplot, where all values concentrate around zero.



# TU **Bibliothek**, Die approbierte gedruckte Originalversion dieser Diplomarbeit ist an der TU Wien Bibliothek verfügbar wien knowledge hub. The approved original version of this thesis is available in print at TU Wien Bibliothek.

# 3 Methodology

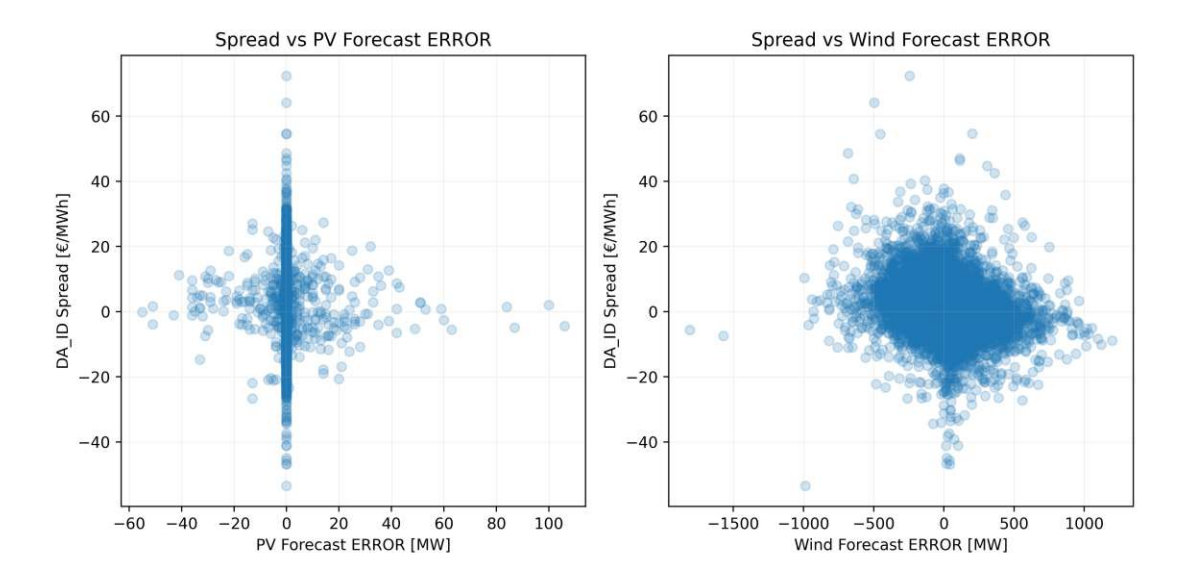


Figure 3.8: Scatterplot correlation between spread and pv / wind forecast errors

# Therefore, PV forecast errors were excluded from the X-model.

Wind forecast errors, by contrast, remained variable throughout the year. Their distribution ranges from approximately -1500 MW to +1000 MW, and they exhibit a weak to moderate negative correlation with the spread ( $\rho = -0.225$ ). This confirms their explanatory power for modeling the spread.

# Scenario Generation and Application

Using the same X-model approach as for the DA prices, spread scenarios are generated based on five predefined wind forecast error trajectories. These correspond to: High, Higher, Base, Lower, and Low forecast deviation paths.

The final intraday price scenarios are then computed using the following relation:

$$ID(t) = DA(t) - Spread(t)$$
(3.53)

This method ensures internal consistency between DA and ID prices and avoids implausible market dynamics such as negative prices or unrealistic divergences. It also captures the structural effect of wind forecast uncertainty on the spread. To preserve coherence across scenarios, each DA price path—generated based on varying renewable generation forecasts—is paired with a corresponding spread path derived from different levels of forecast error. Table 3.29 provides an overview of the selected pairings and their rationale.



Forecast Trajectory	DA Price	Spread	Rationale
High PV/Wind	Very low	Low Error	Excellent forecast quality; ID prices significantly lower than DA.
Higher PV/Wind	Low	Lower Error	Good forecast; ID market still yields cheaper prices than DA.
Base	Medium	Base Error	Mid-level generation with average forecast reliability.
Lower PV/Wind	High	Higher Error	Reduced generation and decreasing forecast quality.
Low PV/Wind (2025)	Very high	High Error	Unchanged 2025 forecast trajectory; high forecast error, ID remains high

Table 3.29: Scenario pairing of DA price paths and spread price paths

# Scenario Tree Construction

The five DA scenario paths are later combined with five corresponding ID paths (generated via spread modeling, see section 4.1) to form a total of 25 scenario combinations. Each combination is assigned a joint probability based on literature-based assumptions about PV and wind forecast accuracy.

This probabilistic scenario tree is then used as input for the two-stage stochastic optimization problem, enabling the model to optimally invest in and dispatch flexible heat generation technologies under uncertainty in electricity market prices.

To simulate plausible electricity price trajectories until 2035, this thesis integrates scenariobased variations in renewable electricity generation from photovoltaic (PV) and wind. These variations are guided by three major Austrian scenario sources, which provide quantitative long-term outlooks on technology-specific development paths as described in Chapter 4.2.

# 4.1 Scenario Tree

The respective projections serve as reference points for defining five stylized expansion trajectories per technology: low, lower, base, higher, and high. These trajectories are used as exogenous inputs to the electricity price simulation model described in Chapter 3.2.1. In line with fundamental energy market logic, a high expansion trajectory for renewables typically results in a low electricity price scenario, and vice versa, as shown in the following figure, which presents the resulting scenario tree:

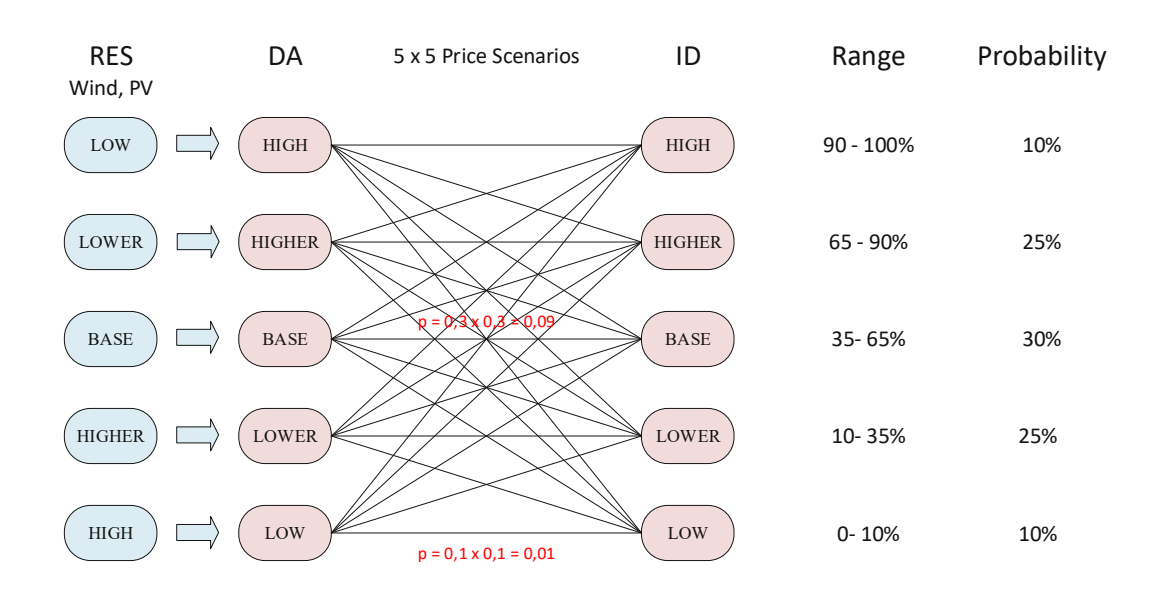


Figure 4.1: Scenario tree of electricity price scenarios

Each of the five renewable expansion paths results in five corresponding electricity price trajectories in both the DA and Intraday ID markets. Combining these DA and ID trajectories yields 25 unique scenario combinations, reflecting the full range of possible market outcomes.

To represent uncertainty in a structured way, each trajectory is assigned a heuristic probability range. The bounds of these ranges are not strictly determined by the scenario studies themselves; rather, the three Austrian scenarios are used as orientation, and the upper and lower bounds for each trajectory are extended beyond the scenario corridor to capture a broader spectrum of uncertainty. These probability intervals are not derived from empirical data, but reflect plausibility-based likelihood bands for each expansion level:

• High: 90–100% Higher: 65–90% • Base: 30–65% Lower: 10–30% • Low: 0–10%

The joint probability of each DA-ID scenario is calculated as the product of the respective DA and ID trajectory probabilities. For example, if both the DA and ID "base" trajectories are assigned a probability of 30%, the resulting combined scenario has a joint probability of:

$$p = 0.3 \times 0.3 = 0.09 \tag{4.1}$$

The resulting electricity price paths serve as stochastic inputs to the two-stage stochastic optimization model, as described in Chapter 3.1.2.

# 4.2 DA Forecast Trajectories

The first source is the EU project SUSPLAN[37], whose Austrian analysis foresees that installed capacities could rise to approximately 18 GW of photovoltaics and 4 GW of wind by 2050. TU Wien's "Green" and "Red" scenario variants illustrate divergent trajectories. More specifically, between 2030 and 2040, the "Green" pathway projects a approximately 430% rise in PV (corresponding to an average annual growth rate—Compound Annual Growth Rate, CAGR—of 15%) and 38% in wind (3.5% CAGR).

The second scenario framework used in this work is the national "Stromstrategie 2040" developed by Austrian authorities. According to the baseline scenario, photovoltaic electricity generation is projected to increase from 6.93 TWh in 2024 to 32.6 TWh by



2040 (CAGR 10.2%). In the more ambitious "ÖNIP" trajectory, PV output is expected to rise to 40.5 TWh over the same period, implying an annual growth rate of 11.7%. Wind generation increases from 10.8 TWh in 2024 to 39.9 TWh in 2040 (CAGR 8.5%).

The following figure presents the "Stromstrategie 2040" scenario projection:

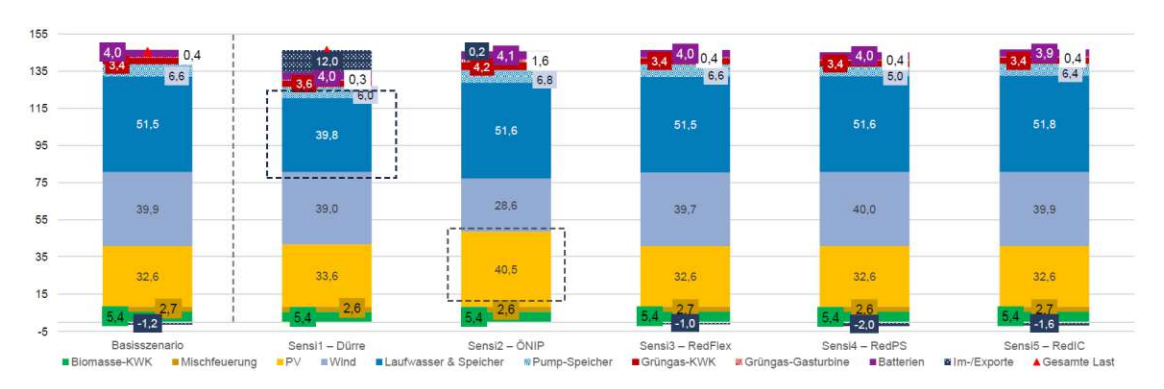


Figure 4.2: Electricity generation scenarios in "Stromstrategie 2040"; Source: [38]

Finally, the third source used to frame the scenario corridor is an analytical projection from e.venture. It estimates Austria's installed PV capacity to grow from 8 GW in 2024 to 13 GW by 2030 (CAGR 8.4%) and to 19 GW by 2035 (CAGR 7.9%). Wind capacity is projected to rise from 4 GW to 7 GW by 2030 (9.8% per year), and further to 10 GW by 2035 (7.4% CAGR).

Taken together, these three scenario sources provide a robust and differentiated basis for the stylized trajectories used in this thesis. The derived scenario corridor reflects varying levels of ambition in renewable expansion and directly informs the stochastic input to the electricity price model.

To ensure transparency and reproducibility, Table 4.1 summarizes the quantitative assumptions for all five stylized expansion trajectories (low, lower, base, higher, high) for each technology (PV and wind). For each trajectory, the table provides the initial value of installed capacity for 2025, the compound annual growth rate (CAGR) for the periods 2025–2030 and 2030–2035, as well as the resulting capacities for 2030 and 2035. These values serve as exogenous scenario inputs for the electricity price model described above.



Trajectory	2025	CAGR 2030	2030	CAGR 2035	2035
	[GW]	[%]	[GW]	[%]	[GW]
PV					
low	8.25	1.00	8.25	1.00	8.25
lower	8.25	1.075	11.84	1.0675	16.42
base	8.25	1.10	13.29	1.09	20.44
higher	8.25	1.1125	14.06	1.1025	22.90
high	8.25	1.15	16.59	1.14	31.95
Wind					
low	4.04	1.00	4.04	1.00	4.04
lower	4.04	1.0713	5.70	1.06	7.63
base	4.04	1.095	6.36	1.08	9.34
higher	4.04	1.1013	6.54	1.09	10.06
high	4.04	1.12	7.12	1.10	11.47

Table 4.1: Definition of renewable capacity expansion trajectories for PV and wind for scenario analysis

The quantitative scenario definitions for photovoltaic (PV) and wind are not only presented in Table 4.1, but also visualized in the following figures. Each plot illustrates the full set of stylized development paths ("trajectories") from 2025 to 2035, providing an intuitive comparison of the possible expansion corridors for each technology.

Figure 4.3 shows the five PV trajectories, highlighting both conservative and ambitious growth assumptions.

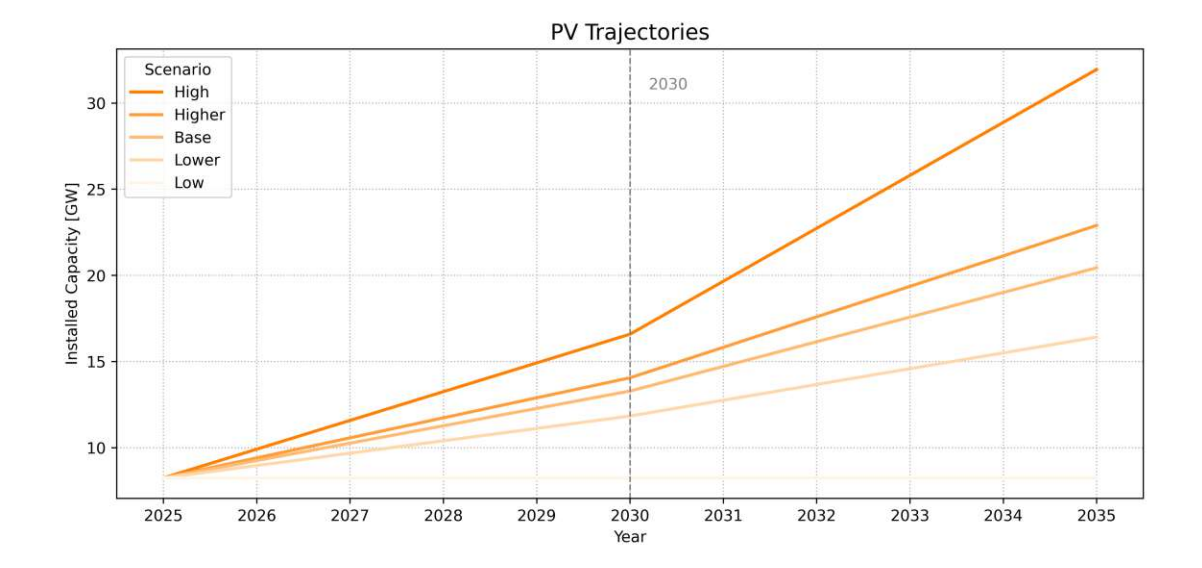


Figure 4.3: PV Trajectories

The corresponding scenario set for wind installed capacity is depicted in Figure 4.4. The spread between the "low" and "high" scenarios illustrates the breadth of possible wind power expansion in Austria.

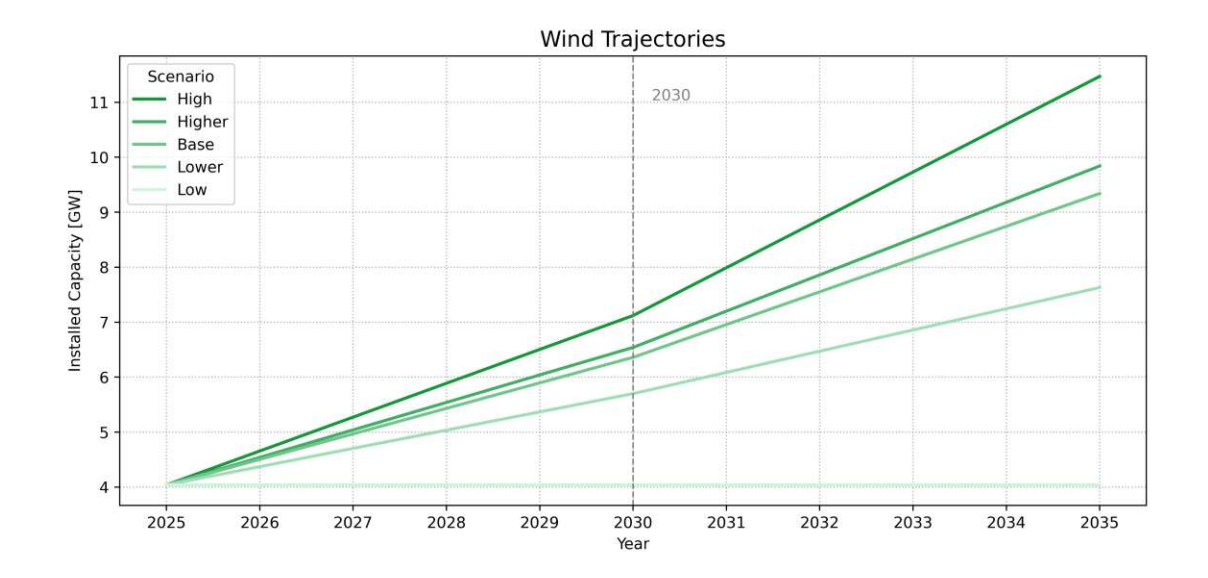


Figure 4.4: Wind Trajectories

# 4.3 Spread Forecast Error Trajectories

To account for the uncertainty in forecast accuracy, five wind forecast error scenarios are defined for each future year  $(y \in \{2030, 2035\})$ . These are implemented by scaling the historical 2019 wind forecast error time series with scenario-specific factors  $\alpha_y^{\text{scen}}$ .

The scaling factors are based on findings from [39], which demonstrate a measurable improvement in day-ahead wind forecast accuracy between 2013 and 2020 in several European countries. The reported MAE reductions of 20-30% support the plausibility of improved accuracy scenarios.

Table 4.2: Wind forecast error scaling factors for scenario generation

Scenario	Description	$\alpha_{2030}^{\mathrm{scen}}$	$\alpha_{2035}^{\rm scen}$
Low	Highly accurate forecasts	0.6	0.5
Lower	Improved forecasts with better models	0.8	0.7
Base	Reference level: current forecast quality	1.0	1.0
Higher	Slightly degraded forecasts (volatility)	1.2	1.1
High	Extreme uncertainty (e.g., due to climate change)	1.5	1.4

Each scenario is applied by multiplying the original 2019 forecast error time series with the respective  $\alpha_y^{\text{scen}}$ . This method provides a consistent and data-driven way to represent varying levels of future uncertainty in forecast accuracy.

In this chapter, the results of the developed district heating optimization models are presented and compared. Two model configurations are analyzed to evaluate the impact of electricity market integration and uncertainty on optimal investment and dispatch decisions.

The first model represents a conventional deterministic optimization approach, in which a single trajectory of DA electricity prices is used without scenario-based uncertainty or participation in additional electricity markets.

The second model extends this formulation by incorporating uncertainty in both DA and ID electricity prices through a scenario-based stochastic framework. Furthermore, it includes the possibility to participate in the balancing market via mFRR down reserve provision. This configuration is designed to answer the research questions posed in this thesis by demonstrating how flexible electricity market participation affects the operation and structure of district heating systems.

The following sections present the results of each model individually and conclude with a comparative analysis highlighting the key differences in costs, technology deployment, and market interactions.

# 5.1 Deterministic Model Results

This section discusses the outcomes of the deterministic optimization where a single DA electricity price trajectory determines both investment and dispatch decisions. The model co-optimizes technology capacities for heat supply (EB, HP, ST, WtE, GT, CHP) as well as TTES, and schedules hourly operation over the representative model years 2025, 2030 and 2035. Unless noted otherwise, reported costs aggregate investment, incremental fixed costs (i.e., the yearly increase in fixed cost relative to the previous model year), and variable costs over the hours of the respective model year.

## 5.1.1 Load curve and load duration curve

The chronological load curve for 2025 demonstrates how the portfolio meets the hourly district heating demand while using the storage to shift heat across hours. WtE provides a high, near-baseload contribution for most hours; the HP operates intermittently at or close to its capacity in clusters when electricity prices and temperatures are favorable;



EB is largely unused in 2025; TTES both discharges (positive) and charges (negative), visible as areas above and below the zero line. The demand trajectory sits above the stacked supply, confirming that the operational constraints balance in every hour.

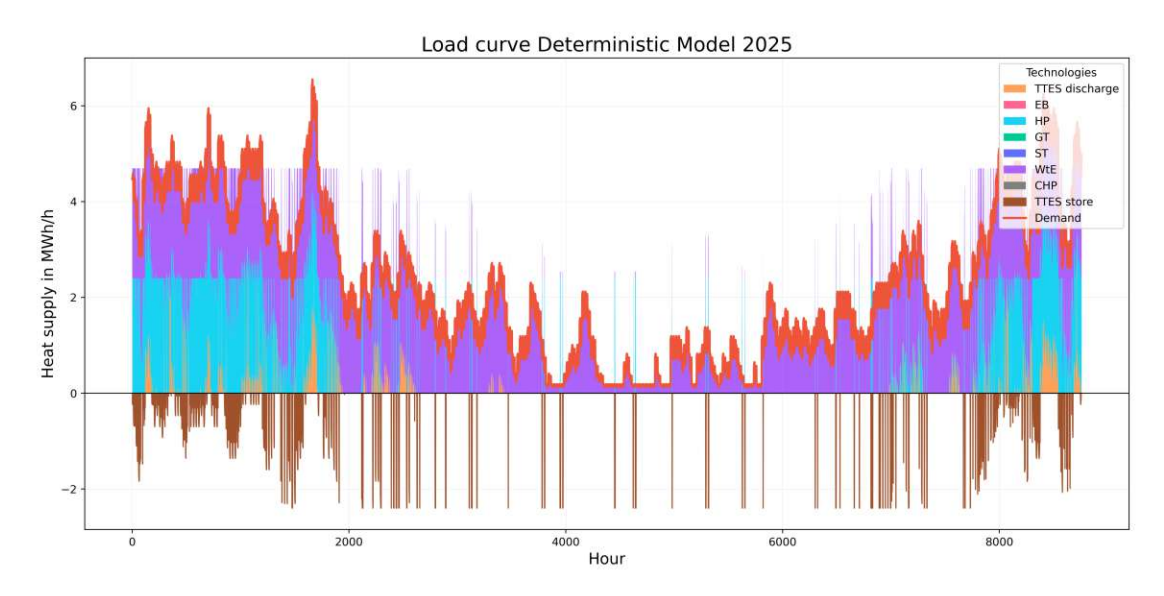


Figure 5.1: Load curve in 2025 deterministic model.

The load duration curve (LDC) for 2025 obtained by sorting hours by descending demand highlights roles more clearly. WtE spans a large share of the ranked hours and thus acts as the system's backbone. HP is concentrated toward higher-load hours, i.e., it is dispatched strategically to shave peaks together with TTES discharge. Charging of TTES spreads over a wide range of lower-load hours (negative area), indicating systematic arbitrage between moderate-demand periods and peak periods. The absence of CHP, ST and GT in the LDC is consistent with their non-investment in this scenario.

Two single-technology load curves further explain operating patterns: the HP runs in bursts around its nameplate output, with long stretches of zero—typical for an asset driven by electricity price and temperature; WtE, by contrast, is near constant with limited turndown, reflecting a baseload unit with low (sometimes even negative) marginal cost.

## Annual dispatch by technology (2025-2035)

Annual heat dispatch evolves over time as capacities change. In 2025, WtE dominates the supply mix and TTES performs meaningful charge-discharge cycles. By 2030, HP's annual output increases markedly; by 2035, HP becomes the second strong pillar next to WtE, while EB appears as a peak-shaving and residual balancing unit. ST, CHP and GT

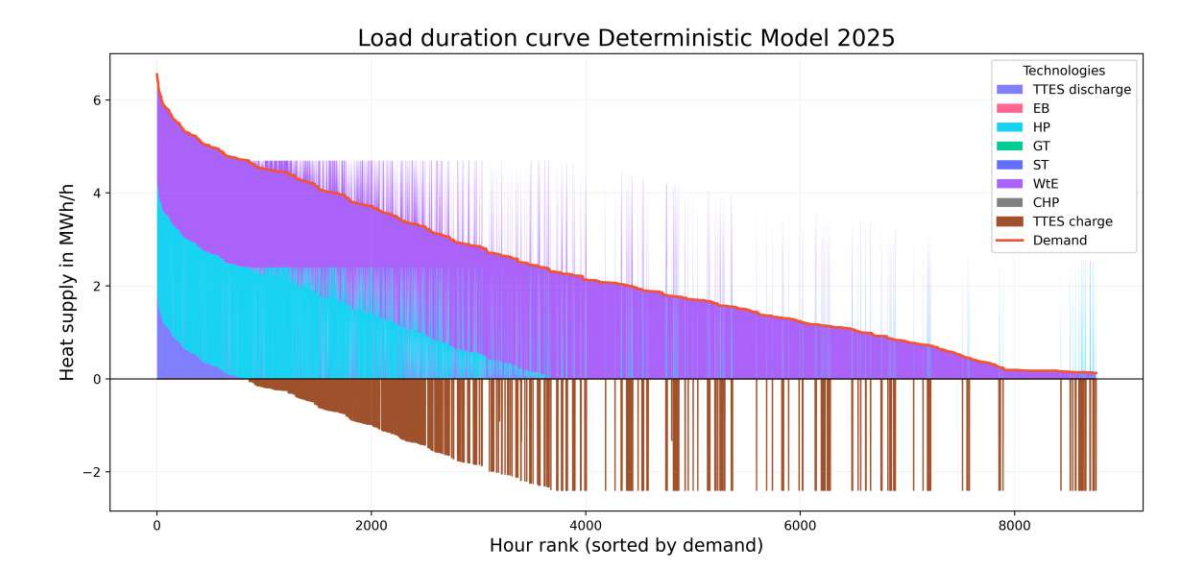


Figure 5.2: Load duration curve in 2025 deterministic model

remain unused.

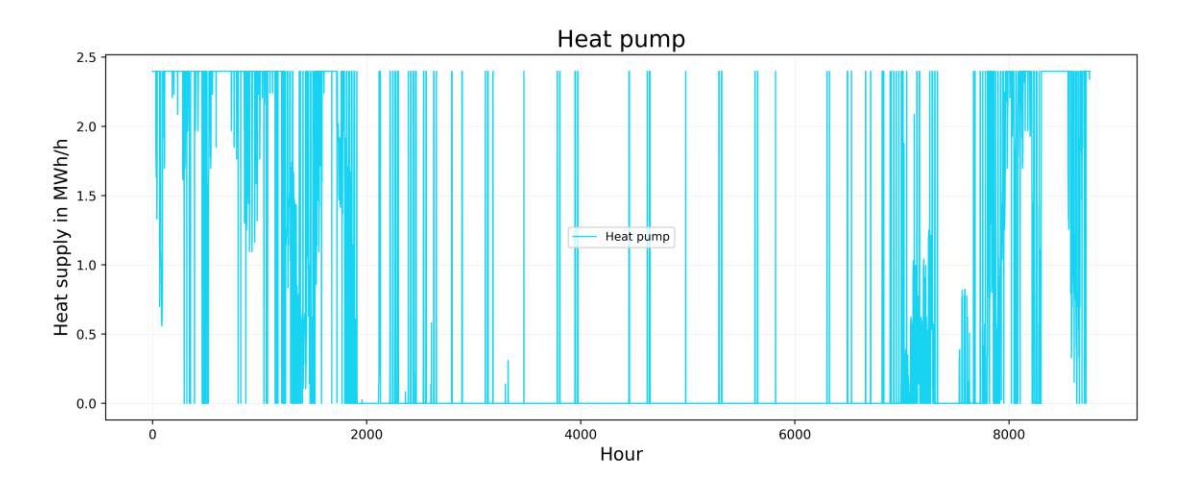


Figure 5.3: Hourly heat supply of the Heat Pump in 2025.

Policy note (WtE CO<sub>2</sub>): Starting in 2030, the deterministic setting includes  $CO_2$ prices for WtE to reflect potential policy changes under uncertain legislation. This shifts WtE's effective marginal cost upward compared to 2025, mildly reducing its dispatch share where economically justified and reinforcing the role of HP and TTES in covering higher-load hours.

This evolution indicates a strategy of baseload + flexible electrification: commit to a stable WtE block, then grow electrified heat with HP (and later EB) to follow residual demand, and use TTES to time-shift between electricity price/demand conditions.

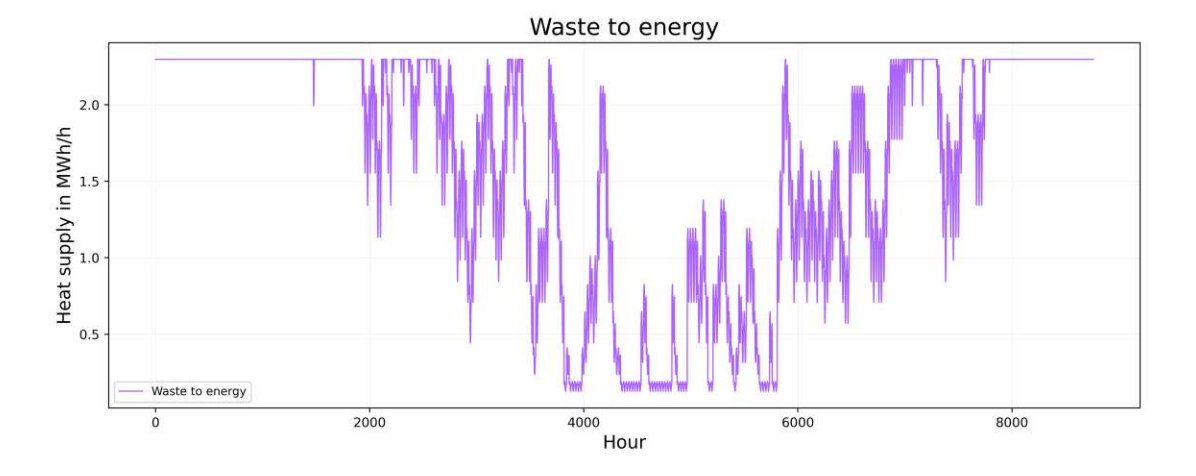


Figure 5.4: Hourly heat supply of Waste-to-Energy in 2025.

# New installed capacities

The capacity expansion schedule confirms this narrative. The model installs a large block of HP and substantial WtE together with a sizeable TTES in 2025. In 2030, the system adds another tranche of HP and a small amount of storage. In 2035, it introduces EB capacity, while other technologies remain unchanged.

## Interpreting this path:

- Front-loading HP and WtE in 2025 leverages immediate cost and emissions benefits: WtE as a steady, low-marginal-cost provider; HP as a high-efficiency, priceresponsive source.
- Additional HP in 2030 expands the flexible share as electricity prices and demand patterns make electrification increasingly attractive.
- EB in 2035 acts as a low-CAPEX, high-marginal-cost peaker to cover short residual peaks that would be expensive for HP to size for, and to provide operational resilience.
- TTES is built early to enable shifting from moderate-price hours to peak hours; a small top-up in 2030 fine-tunes the balance between HP sizing and storage depth.
- ST, CHP, GT: the model finds no investment case under the assumed cost and price trajectories.

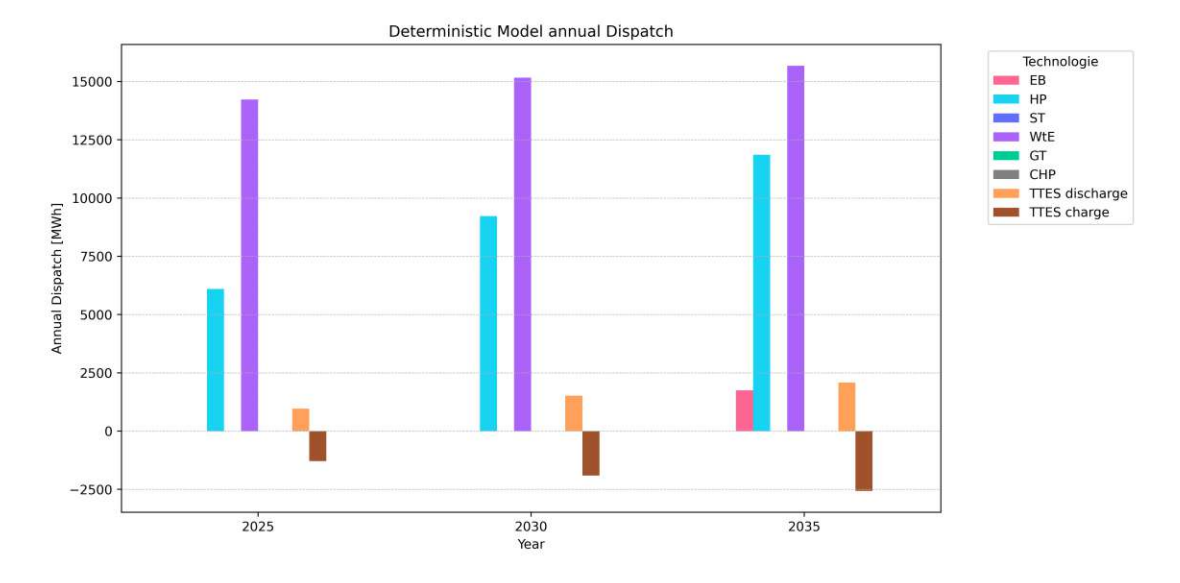


Figure 5.5: Annual heat dispatch by technology (2025/2030/2035).

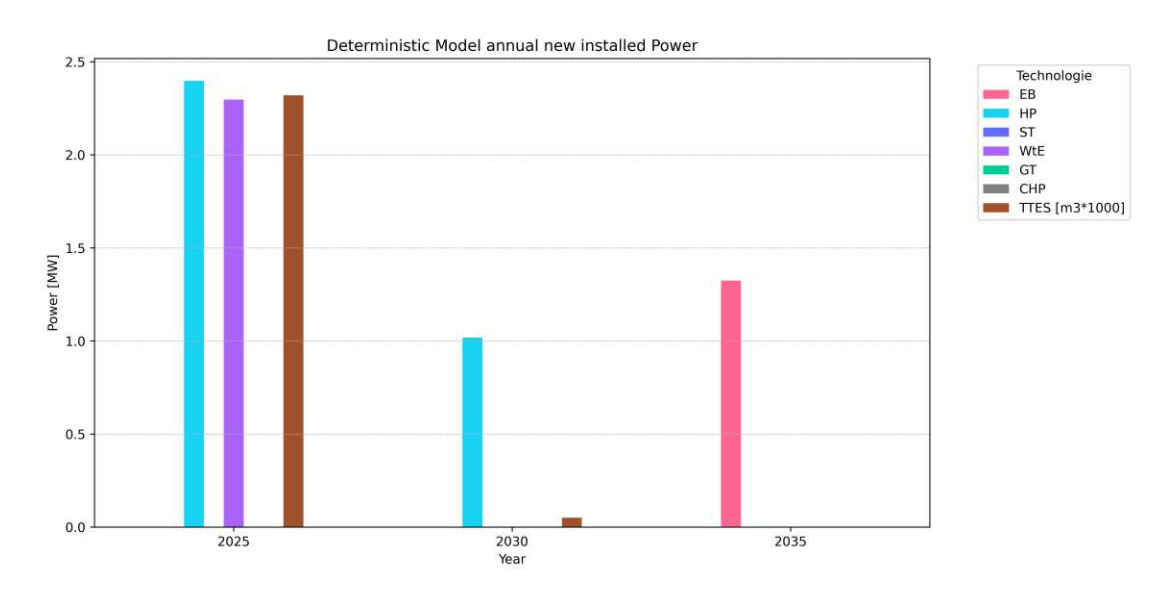


Figure 5.6: New installed capacity by model year (TTES in  $10^3 \,\mathrm{m}^3$ ).

# Cost breakdown by technology

Figure 5.7 reports total annual cost per technology for 2025 (CAPEX for 2025, the increment in fixed cost versus 2020/previous model year, and the sum of hourly variable

cost). WtE and HP form the largest cost blocks, consistent with their output shares and investments. TTES contributes a distinct but much smaller cost component driven by investment and fixed charges (variable cost is minor). ST is negligible; EB has no noticeable cost in 2025 because capacity is not yet installed.

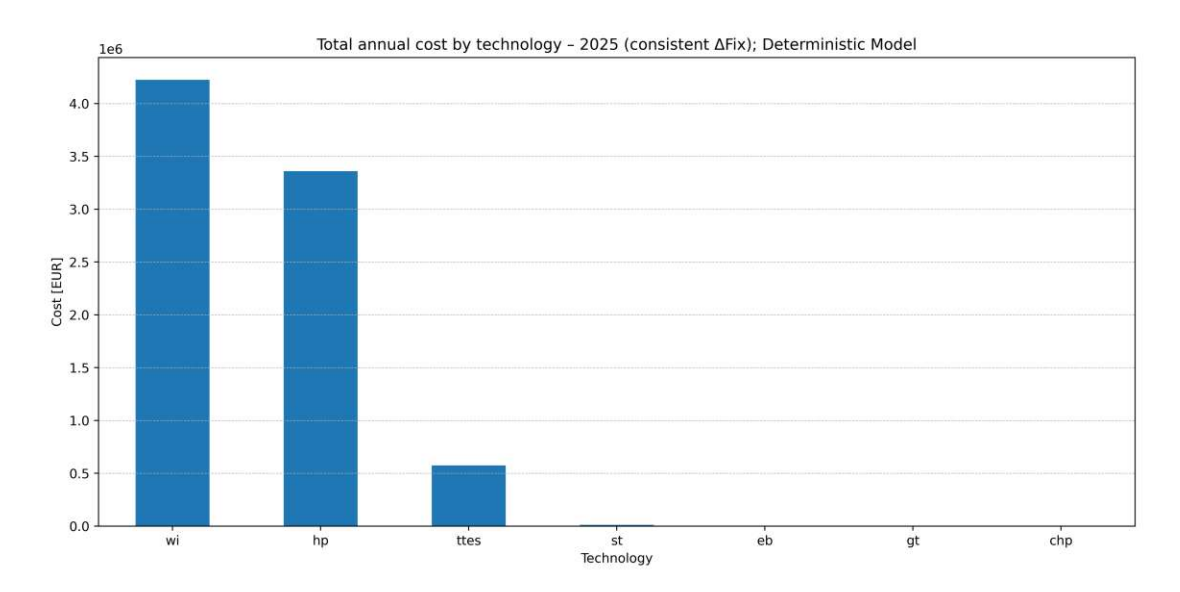


Figure 5.7: Total annual cost by technology in 2025 (CAPEX +  $\Delta$ Fix + Var).

Summing over the horizon 2025–2035 (as the sum of the three annual blocks—i.e., CAPEX in each model year + that year's  $\Delta$ Fix + that year's Var, without any extra weighting because the weighting is already embedded in the constraints), HP becomes the highest-cost technology across the period. WtE ranks second, TTES third, EB fourth, with ST, CHP, and GT negligible.

### A few remarks are important for interpretation:

- The model's WtE variable cost can be negative in some hours/years (e.g., gate fees offsetting operating cost). Even so, total annual WtE cost can be positive once CAPEX and fixed charges are included; in other years with little new investment and strong gate-fee effects, the net annual WtE cost may turn small or negative.
- HP costs are dominated by investment and fixed charges (capacity-driven) plus electricity purchase (variable). The pronounced 2025 and 2030 investments explain the high contribution in those years and the overall horizon total.
- EB appears only in 2035. Its modest horizon total signals a classic peaker role: low CAPEX installed late, modest operating hours, but valuable for covering residual peaks.



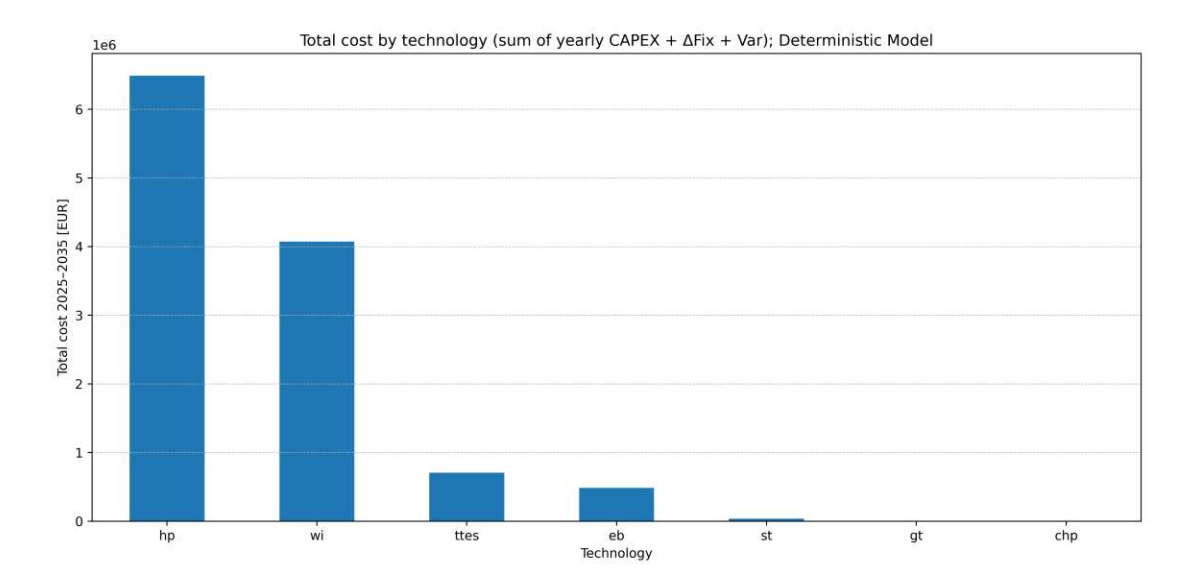


Figure 5.8: Total cost by technology over 2025-2035, computed as the sum of yearly (CAPEX +  $\Delta$ Fix + Var).

• TTES costs consist primarily of CAPEX and fixed charges. The benefits are visible indirectly through reduced peak capacity needs and shifted HP/EB operation rather than through the TTES bar itself.

## 5.2 2-Stage Stochastic Model Results

Model set-up. The two-stage stochastic model optimizes first-stage investments and second-stage operations across multiple price and demand scenarios. All reported costs are scenario-probability expected values and are defined consistently year by year as: CAPEX in the respective model year + Delta Fix (incremental fixed charge) + hourly variable costs. Hourly costs are already weighted inside the model via year\_expansion\_range; no additional weighting is applied in the plots.

Dispatch structure over time (expected value). Figure 5.9 separates DA, ID, and mFRR-down reserve for EB/HP and shows thermal feed-in for all technologies. HP delivers the bulk of flexible heat; electrical input is procured via both DA and ID and shifts as electrification grows. EB becomes more active in 2035 and provides a large amount of mFRR-down reserve, which reduces net operating costs through capacity payments. WtE remains the thermal baseload; from 2030 onward, CO<sub>2</sub> pricing is applied to WtE in the model (reflecting regulatory uncertainty), which slightly increases its variable term. TTES shifts energy from lower-price to higher-price hours.

Figure 5.10 complements this view with the chronological load curve and the load-duration

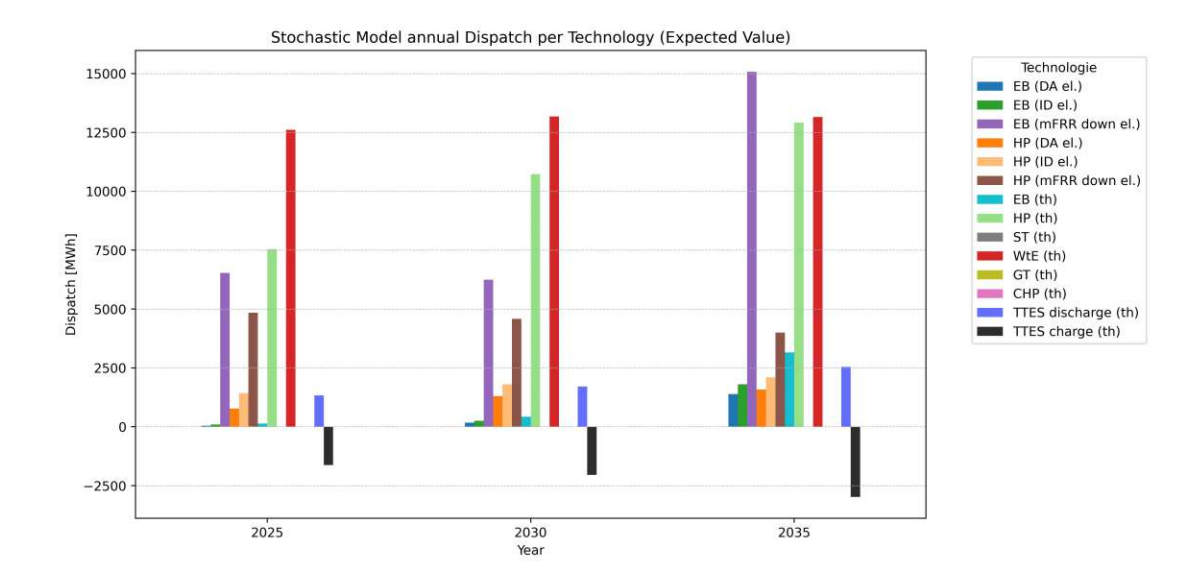


Figure 5.9: Stochastic model: annual dispatch per technology and market channel (expected value).

curve for 2035: HP and WtE cover broad bands; EB fills short residual peaks; TTES charges in low-load/low-price hours and discharges near peaks.

Investments (expected value). The expected new capacity per model year (Figure 5.11) broadly follows the deterministic pattern: early HP and TTES in 2025, a small HP top-up in 2030, and a noticeable EB addition in 2035. In expectation, a minor EB share appears already in 2025, reflecting that some scenarios install EB earlier.

Costs by technology in 2035. The side-by-side comparison to the deterministic model for 2035 (Figure 5.12) shows lower stochastic costs for EB and HP due to price-adaptive DA/ID procurement and EB's mFRR-down provision. WtE remains stable but slightly higher once  $CO_2$  charges apply.

Costs over the full horizon (2025–2035). Aggregating the three model years as a sum of annual blocks (CAPEX + Delta Fix + Var per year; no extra weighting), the stochastic model achieves lower totals (Figure 5.13). HP remains the largest cost contributor, but is slightly lower than in the deterministic case. WtE decreases overall despite CO<sub>2</sub> pricing due to interactions with HP/TTES. EB acts as a late peaker with modest horizon cost. TTES is mainly CAPEX/fixed-charge driven; its benefit appears indirectly via reduced capacity needs and avoided price spikes.

System total. Figure 5.14 summarizes the total system cost: the stochastic solution is cheaper than the deterministic reference.

Remark on balancing services. In the model, mFRR-down is represented as reserve

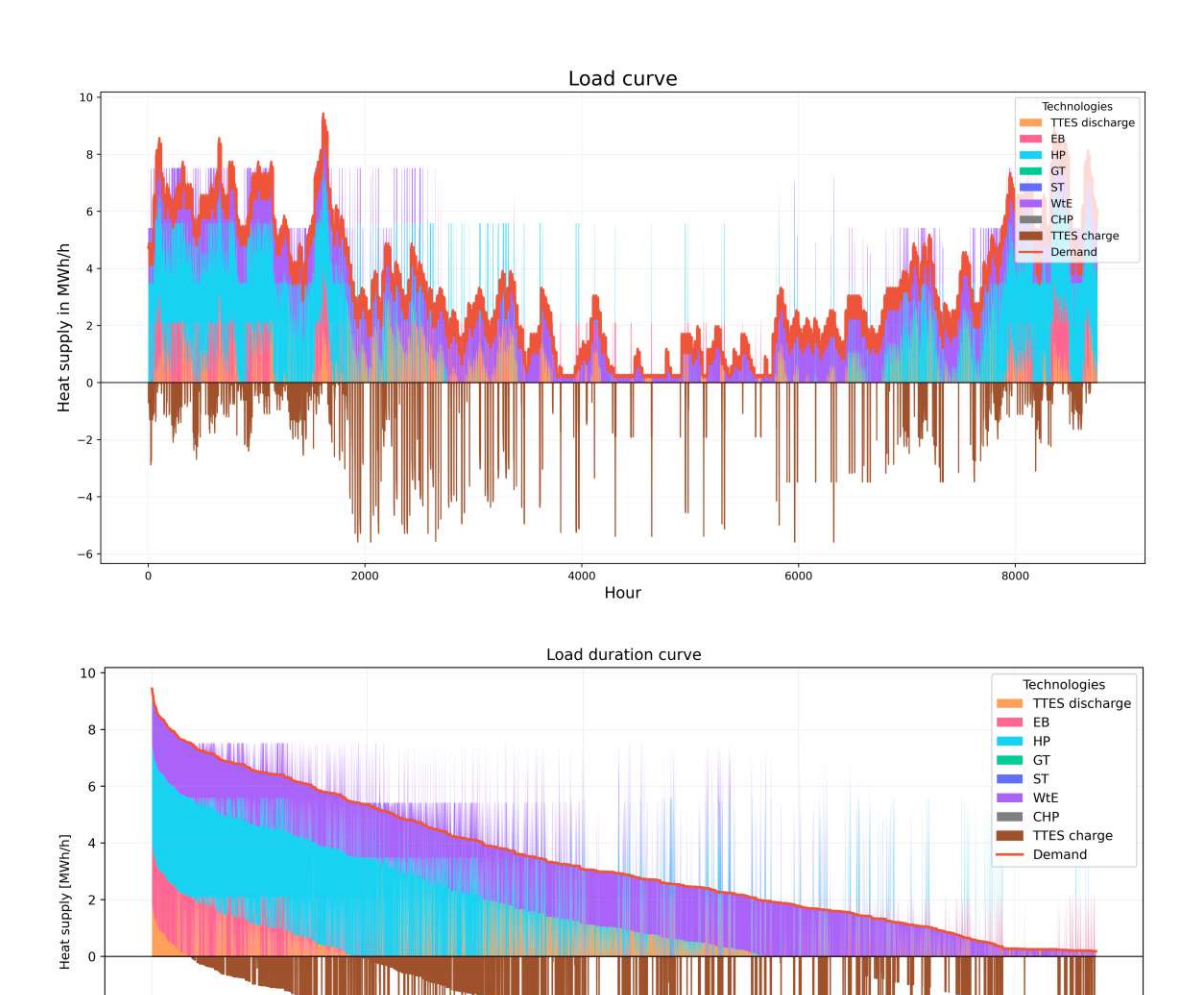


Figure 5.10: Stochastic model: chronological load curve (top) and load-duration curve (bottom) for 2035.

2000

4000 Hour rank (sorted by demand)

6000

8000

availability (capacity provision). The physical activation of balancing energy and its settlement is neglected. Including activation revenues would likely further improve the economics of flexible assets (EB/HP), so the reported stochastic costs should be seen as conservative.



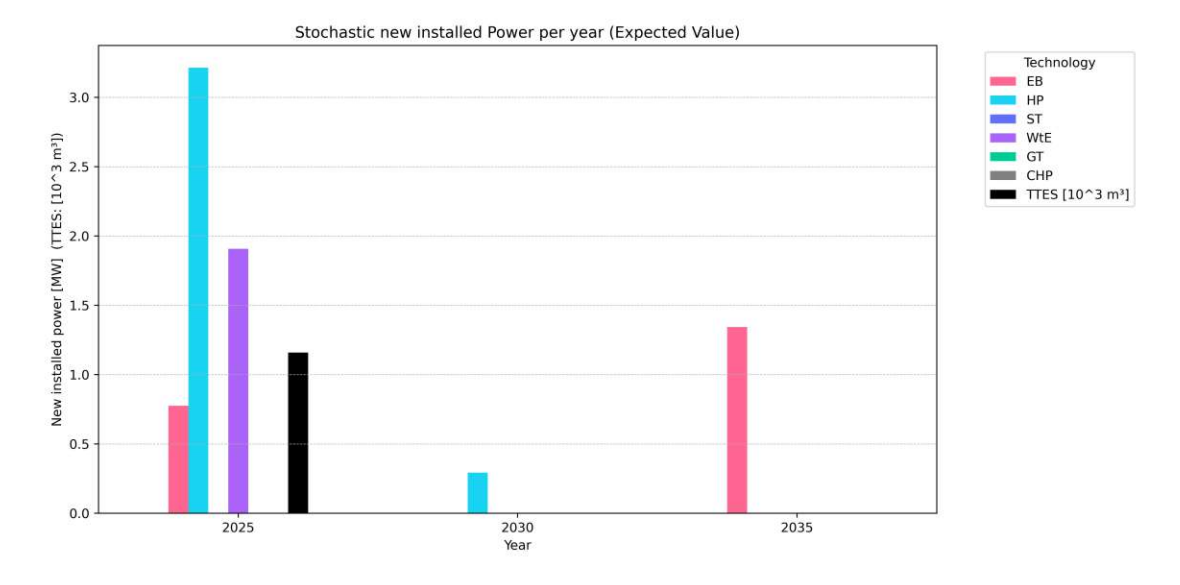


Figure 5.11: Stochastic model: expected new installed power per year.

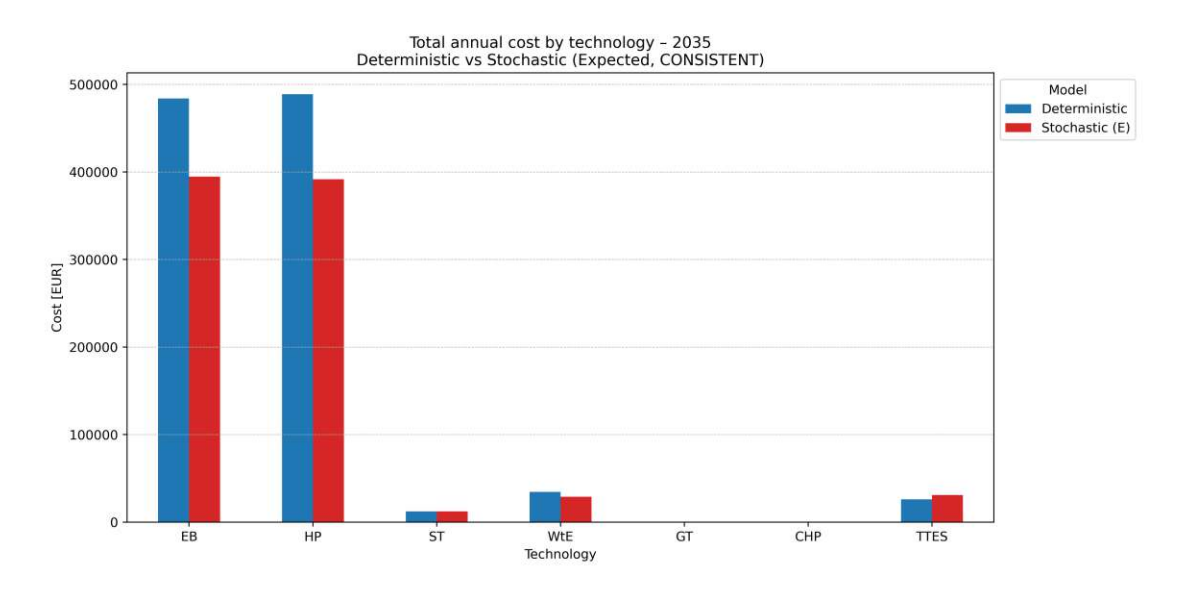


Figure 5.12: Costs by technology in 2035: deterministic vs stochastic (expected, consistent definition).

## 5.3 Comparison of the 2 Models

Market participation under uncertainty. Compared to the deterministic case, the stochastic framework explicitly values DA/ID procurement options and mFRR-down



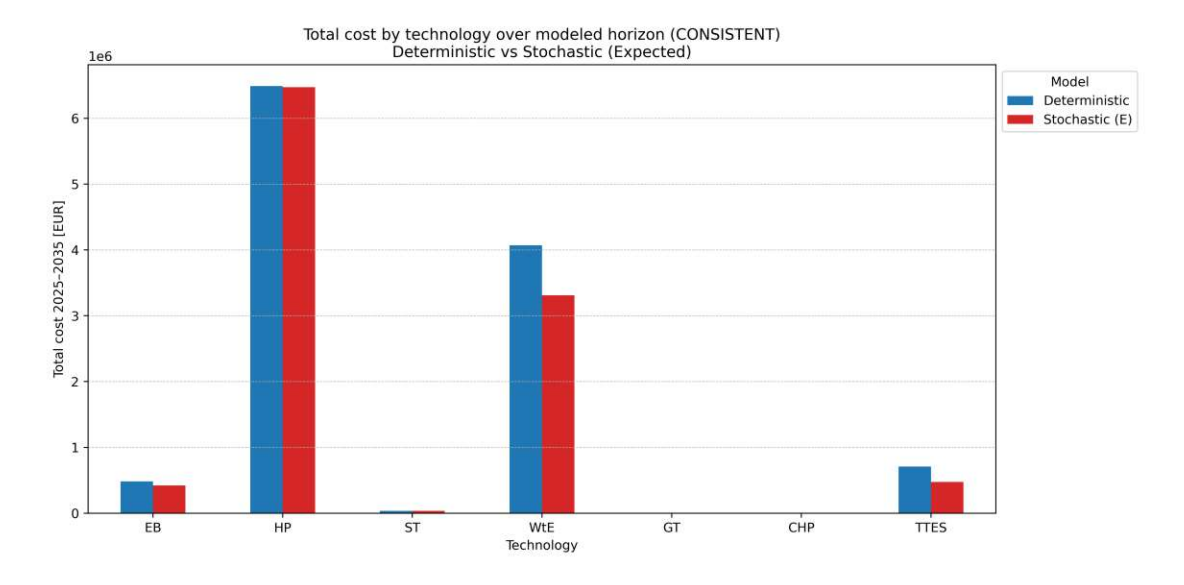


Figure 5.13: Total cost by technology over 2025–2035 (sum of annual CAPEX + Delta Fix + Var): deterministic vs stochastic.

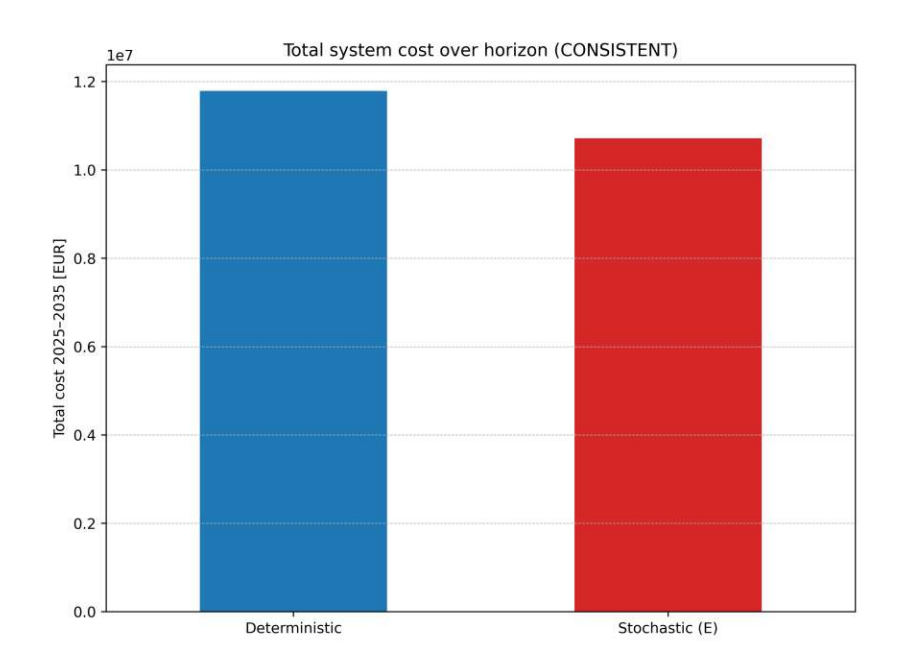


Figure 5.14: Total system cost over 2025–2035: deterministic vs stochastic (expected).

reserve provision. It shifts HP operation more opportunistically into low-price hours and



monetizes EB's reserve capability in 2035, while TTES is used more effectively against price spreads.

**Investment timing.** Both models electrify early (HP and TTES in 2025). In the stochastic expected solution, a small EB share already appears in 2025 (reflecting a subset of scenarios), but the qualitative pattern remains "HP/WTES first, EB later."

Cost impact. Across years and over the full horizon, the stochastic model reduces total costs, in particular for EB and HP in 2035, while WtE remains dependable but carries CO<sub>2</sub> charges after 2030. WtE contributes less cost in the stochastic run because more hours are shifted to HP and EB whenever expected DA/ID prices make electrification cheaper (including  $CO_2$ ), and TTES reinforces this shift by arbitraging between price levels. Numerically, total system cost over 2025–2035 amounts to about 11.79 million€ in the deterministic model and 10.70 million € in the stochastic expected solution; the stochastic design is therefore cheaper by roughly 1.09 million €, i.e. about 9.2%.

System architecture. Both solutions converge to a robust two-block portfolio: baseload (WtE) plus flexible electrified heat (HP + EB), coordinated by TTES. The stochastic solution fine-tunes dispatch and (slightly) investment shares where expected marginal value is highest.

Limitations and implication. Because balancing-energy activation is not modeled, the stochastic cost advantage is likely understated. Extending the model with activation settlement would probably increase the economic value of EB/HP further.

## Conclusion and Outlook

While the Day-ahead (DA) electricity market is already considered in optimization models, the Intraday (ID) market and balancing services are often neglected. In response to Research Question 1, this work develops a modeling framework that integrates DA, ID, and mFRR-down into a two-stage stochastic optimization for district-heating portfolios. Building on a deterministic portfolio model, the formulation is independently extended to a two-stage setting with DA/ID price scenario paths and a CVaR term to manage downside risk. The framework is calibrated to an existing physical district heating network in Salzburg (stylized representation) and focuses on electricity-driven heat supply alongside Waste to Energy (WtE), Combined Heat and Power (CHP), Solar Thermal (ST), Geothermal (GT), and Tank Thermal Energy Storage (TTES).

Regarding the integration itself (Research Question 1), three building blocks were essential. First, electricity procurement for heat pumps (HP) and electric boilers (EB) is split explicitly between DA and ID; participation in mFRR-down is modeled as capacity reservation only (no activation energy settlement). Second, the case-study technology set was tailored to the Salzburg context: no natural-gas technologies; WtE modeled as heat-only plant (HOP); biomass-fired CHP (instead of gas); deep geothermal and aquifer TES omitted; no industrial excess heat. Third, several transparent simplifications keep the problem tractable and focused on market-driven flexibility: ID represented via ID3; reserve prices applied as daily averages (hourly series difficult to source at scale); network hydraulics not modeled; TTES is modeled with constant charging and discharging efficiencies (implying a fixed round-trip efficiency) and with hourly standing losses.

Concerning knowledge gain (Research Question 2), three robust differences emerge when comparing the Salzburg-calibrated stochastic framework with the rebuilt deterministic DA-only baseline (same techno-economic parameters and demand). (i) Dispatch becomes more price-responsive: HP operation systematically shifts into low-price hours, and EB headroom is monetized through reserve Provision. (ii) The resulting portfolio exhibits a persistent two-block pattern: WtE supplies dependable baseload, while HP/EB coordinated by TTES provide the flexible, arbitrage-oriented share across DA/ID. (iii) Total system costs decline materially in the case study (by  $\approx 9\%$ ), showing that explicit ID participation can change both operational schedules and investment timing in economically meaningful ways.

Implications are twofold. Where ID access and balancing products are available—or

### 6 Conclusion and Outlook

electricity price volatility is material, the proposed two-stage stochastic framework is preferable to DA-only deterministic models, because it captures both the value and the risk of short-notice flexibility and better informs HP/EB sizing and Timing. For early-stage screening, or in contexts without ID access and negligible reserve options, a simpler DA-only formulation remains adequate. Looking ahead, a combined pathway is promising: retain the market-integration layer developed here when power-to-heat is central, and complement it with broader scenario families (weather extremes, fuel and CO<sub>2</sub> price trajectories, regulatory shifts) when such uncertainties are decision-relevant for the region under study. Where access to mFRR-down exists, the case-study results indicate that capacity reservation can provide a meaningful cost contribution; the full economics of activation are left for future work.

Outlook. Several targeted extensions would strengthen the analysis:

- Add balancing-energy activation: endogenize random activation volumes, energy remuneration, and baseline interactions to capture full reserve economics and the dispatch trade-off between DA/ID schedules and expected activation.
- Use higher-resolution reserve prices: move from daily averages to hourly series (via automated data collection or from synthetic hourly shapes calibrated to daily aggregates) to sharpen price-spread signals for TTES and EB.
- Broaden uncertainty beyond electricity prices: introduce stochastic biomass and CO<sub>2</sub> price paths; a compact design with a small set of cross-cutting scenarios (low/base/high levels and slopes) keeps problem size tractable (with scenario reduction if needed).
- Evolving market design: test sensitivities where ID/real-time trading becomes dominant or DA liquidity changes; in such regimes, short-notice flexibility (HP/EB with TTES) gains value and the stochastic treatment becomes even more important.
- Network-tariff reform for power-to-heat: evaluate reduced/exempt capacity and energy charges; such policies directly lower HP/EB operating costs and can shift optimal sizing and timing toward earlier/larger electrification.

Treating market uncertainty endogenously rather than optimizing to a single expected trajectory, changes both operations and structure in economically meaningful ways. Embedding activation mechanics, richer stochastic drivers (including fuels and CO<sub>2</sub>), higher-resolution reserve prices, and prospective tariff/market reforms is a natural next step and is expected to further strengthen the business case for flexible, electrified heat portfolios coordinated by modest thermal storage.



- Muhammad Bilal Siddique, Dogan Keles, Fabian Scheller, and Per Sieverts Nielsen. "Dispatch strategies for large-scale heat pump based district heating under high renewable share and risk-aversion: A multistage stochastic optimization approach." In: Energy Economics 136 (2024), p. 107764. ISSN: 0140-9883. DOI: https://doi. org/10.1016/j.eneco.2024.107764. URL: https://www.sciencedirect.com/ science/article/pii/S0140988324004729.
- Susanne Radke and Georgia Pletzer. Umsetzungskonzept KEM Oberpinzgau Energiereich. Report. Mittersill, Austria: Regionalverband Oberpinzgau; Nationalpark Hohe Tauern, 2015. URL: https://www.klimaundenergiemodellregionen.at/ assets/Uploads/bilder/doku/B370022\_konzept.pdf (visited on 08/25/2025).
- Biowärme Mittersill GmbH. Biowärme Mittersill GmbH Das Nachhaltige Heizen! [3] https://www.bwm.co.at/. abgerufen am 7. August 2025. 2025.
- Simon Pezzutto, Stefano Zambotti, Silvia Croce, Pietro Zambelli, Giulia Garegnani, Chiara Scaramuzzino, Ramón Pascual Pascuas, Alyona Zubaryeva, Franziska Haas, Dagmar Exner, Andreas Müller, Michael Hartner, Tobias Fleiter, Anna-Lena Klingler, Matthias Kühnbach, Pia Manz, Simon Marwitz, Matthias Rehfeldt, Jan Steinbach, and Eftim Popovski. Hotmaps Project, D2.3 WP2 Report - Open Data Set for the EU28. https://gitlab.com/hotmaps/load\_profile/load\_profile\_ residential\_heating\_yearlong\_2010. Reviewed by Lukas Kranzl, Sara Fritz (TU Wien). Funded by Horizon 2020, Grant Agreement No. 723677. Licensed under CC BY 4.0. 2018.
- 4DH Research Centre. District Heating Technology Evolution 4th Generation District Heating (4GDH). 2020. URL: https://www.4dh.eu/about-4dh/4gdhdefinition.html (visited on 05/08/2025).
- Joana Neves and Brian Vad Mathiesen. Heat Roadmap Europe: Potentials for Large-Scale Heat Pumps in District Heating. Copenhagen: Allborg University, Department of Planning, Dec. 2018. URL: https://heatpumpingtechnologies.org/annex47/ wp-content/uploads/sites/54/2019/07/heat-roadmap-europe.pdf (visited on 08/23/2025).



- Paardekooper, Susana and Lund, Rasmus Søgaard and Mathiesen, Brian Vad and Chang, Miguel and Petersen, Uni Reinert and Grundahl, Lars and David, Andrei and Dahlbæk, Jonas and Kapetanakis, Ioannis Aristeidis and Lund, Henrik and Bertelsen, Nis and Hansen, Kenneth and Drysdale, David William and Persson, Urban. Heat Roadmap Europe 4: Quantifying the Impact of Low-Carbon Heating and Cooling Roadmaps. Deliverable D6.4 of the Horizon 2020 project Heat Roadmap Europe (HRE4). 2018. URL: https://vbn.aau.dk/en/publications/1b572149-8a69-4f8a-8388-5ceb64161c8b (visited on 05/08/2025).
- E-Control. Strom- und Gaskennzeichnungsbericht 2024: Berichtsjahr 2023. Wien: E-Control, 2024. URL: https://www.e-control.at/documents/1785851/1811582/ E-Control-Strom-und-Gaskennzeichnungsbericht-2024.pdf/291cbae9-5a73-68d9-a905-623529e0af90?t=1730104254587 (visited on 08/23/2025).
- European Energy Exchange (EEX). Market Data Hub Environmentals Spot. Accessed CO<sub>2</sub> spot market prices. 2025. URL: https://www.eex.com/en/marketdata/market-data-hub/environmentals/spot (visited on 05/09/2025).
- Pahle, Michael and Sitarz, Joanna and Osorio, Sebastian and Görlach, Benjamin. The EU-ETS price through 2030 and beyond: A closer look at drivers, models and assumptions - Input material and takeaways from a workshop in Brussels. Kopernikus-Projekt Ariadne, Potsdam-Institut für Klimafolgenforschung. 2022. URL: https://ariadneprojekt.de/media/2023/01/Ariadne-Documentation\_ ETSWorkshopBruessel\_December2022.pdf (visited on 05/19/2025).
- Danish Energy Agency and Energinet. Technology Data Energy Plants for Electricity and District Heating Generation. Version 0009. First published 2016-08; amendments through 2020-04. Copenhagen: Danish Energy Agency and Energinet, Apr. 2020. URL: https://ens.dk/sites/ens.dk/files/Statistik/technology\_ data\_catalogue\_for\_el\_and\_dh\_-\_0009.pdf (visited on 08/23/2025).
- Biowärme Mittersill GmbH. Wärmelieferungsvertrag (WLV) Allgemeine Be-[12]dingungen (Vorlage ab 2020). Version GWa 13.03.2019. Mittersill, Mar. 13, 2019. URL: https://www.bwm.co.at/wp-content/uploads/2019/03/WLV-Vorlageab-2020-GWa-13.03.19.pdf (visited on 08/23/2025).
- Klima- und Energiefonds. Faktencheck Wärmepumpe Antworten auf die 8 wichtigsten Fragen zu Wärmepumpen. In Zusammenarbeit mit AIT Austrian Institute of Technology und klimaaktiv. Wien: Klima- und Energiefonds, Sept. 2024. URL: https://www.klimafonds.gv.at/wp-content/uploads/2024/09/Faktencheck-Waermepumpe-2024.pdf (visited on 08/23/2025).
- Anna Billerbeck, Christiane Bernath, Pia Manz, Gerda Deac, Anne Held, Jenny Winkler, Ali Kök, and Mario Ragwitz. "Integrating district heating potentials into European energy system modelling: An assessment of cost advantages of renewable and excess heat." In: Smart Energy 15 (2024), p. 100150. ISSN: 2666-9552. DOI:



- 10.1016/j.segy.2024.100150. URL: https://doi.org/10.1016/j.segy.2024. 100150 (visited on 08/23/2025).
- [15] Agora Energiewende and Fraunhofer IEG. Roll-out von Großwärmepumpen in Deutschland: Strategien für den Markthochlauf in Wärmenetzen und Industrie. Version 1.0. Lizenz: CC BY-NC-SA 4.0. Berlin: Agora Energiewende; Fraunhofer IEG, June 2023. URL: https://www.agora-energiewende.de/publikationen/ roll-out-von-grosswaermepumpen-in-deutschland (visited on 08/23/2025).
- Jürgen Neubarth, Andreas Moser, and Enes Hamidovic. Technische und energiewirtschaftliche Bewertung von Power-to-Heat-Optionen für Biomasseheizwerke im Land Salzburg (Update 2022). 2022. URL: https://e3-consult.at/files/ 2022\_PtG-Analyse%20Biomasseheizwerke%20Salzburg%20\_update.pdf (visited on 05/11/2025).
- Ingwald Obernberger and Alfred Hammerschmid and Michaela Forstinger. Techno-[17]economic evaluation of selected decentralised CHP applications based on biomass combustion with steam turbine and ORC processes. BIOS BIOENERGIESYSTEME GmbH, Graz, prepared for IEA Bioenergy Task 32. 2015. URL: https://task32. ieabioenergy.com/wp-content/uploads/sites/2/2017/03/IEA-CHP-Q2final.pdf (visited on 05/09/2025).
- Patrícia Alves Dias, Konstantinos Kanellopoulos, Hrvoje Medarac, Zoi Kapetaki, Edesio Miranda-Barbosa, Ruth Shortall, Veronika Czako, Thomas Telsnig, Cristina Vazquez-Hernandez, Roberto Lacal Arántegui, Wouter Nijs, Iratxe Gonzalez Aparicio, Marco Trombetti, Giovanni Mandras, Estathios Peteves, and Evangelos Tzimas. EU coal regions: opportunities and challenges ahead. Luxembourg, 2018. DOI: 10.2760/064809. URL: https://data.europa.eu/doi/10.2760/064809 (visited on 05/16/2025).
- Federal Ministry of Agriculture, Forestry, Environment and Water Management (BMLFUW). Waste-to-Energy in Austria — Whitebook: Figures, Data, Facts. 3rd, extended edition. Vienna, 2015. URL: https://www.bmluk.gv.at/dam/jcr: f1f00934-8133-4644-b27d-ed455b2d1c84/Whitebook\_Waste\_to\_Energy.pdf (visited on 08/23/2025).
- [20] Umweltbundesamt GmbH. Die Bestandsaufnahme der Abfallwirtschaft in Österreich — Statusbericht 2023 für das Referenzjahr 2021. Wien: Bundesministerium für Klimaschutz, Umwelt, Energie, Mobilität, Innovation und Technologie (BMK), Aug. 4, 2023. URL: https://www.bmluk.gv.at/service/publikationen/ klima - und - umwelt / die - bestandsaufnahme - der - abfallwirtschaft - in oesterreich-statusbericht-2023-fuer-das-referenzjahr-2021.html (visited on 08/23/2025).



- European Parliament and Council. Directive (EU) 2023/959 of 10 May 2023 amending Directive 2003/87/EC establishing a system for greenhouse gas emission allowance trading within the Union. Official Journal of the European Union, L 130, 16 May 2023. 2023. URL: https://eur-lex.europa.eu/legal-content/EN/TXT/ ?uri=CELEX%3A32023L0959 (visited on 05/18/2025).
- Energieinstitut an der Johannes Kepler Universität Linz. Industrielle Nutzung von Geothermie - Endbericht. 2018. URL: https://energieinstitut-linz.at/ wp-content/uploads/2019/04/Industrielle-Nutzung-von-Geothermie\_ Endbericht\_EIJKU\_2018.pdf (visited on 05/21/2025).
- IEA SHC Task 68. Solar-District-Heating Info Package Efficient Solar Dis-[23]trict Heating Systems. Presentation PDF, accessed for project descriptions and investment cost data. 2024. URL: https://task68.iea-shc.org/ (visited on 05/14/2025).
- [24]BVES – Bundesverband Energiespeicher Systeme e.V. Saisonale Wärmespeicher für die Wärmewende. https://www.bves.de/wp-content/uploads/2023/09/ 2300824\_Saisonalspeicher\_fuer\_die\_Waermewende\_BVES.pdf. 2023. (Visited on 05/13/2025).
- Jörg Worlitschek. Saisonale Wärmespeicher: attraktiv und dennoch vernachlässigt. [25]Vortragsfolien (Slides). May 11, 2022. URL: https://speicher.aeesuisse.ch/wpcontent/uploads/sites/15/2022/05/Jo%CC%88rg-Worlitschek.pdf (visited on 08/23/2025).
- [26]Ioannis Sifnaios, Daniel Møller Sneum, Adam R. Jensen, Jianhua Fan, and Rasmus Bramstoft. "The impact of large-scale thermal energy storage in the energy system." In: Applied Energy 349 (2023), p. 121663. DOI: 10.1016/j.apenergy.2023. 121663. URL: https://doi.org/10.1016/j.apenergy.2023.121663 (visited on 05/13/2025).
- Ioannis Sifnaios, Daniel Møller Sneum, Adam R. Jensen, Jianhua Fan, and Rasmus Bramstoft. "The impact of large-scale thermal energy storage in the energy system." In: Applied Energy 349 (2023), p. 121663. DOI: 10.1016/j.apenergy.2023. 121663. URL: https://doi.org/10.1016/j.apenergy.2023.121663 (visited on 05/19/2025).
- Ville Sihvonen, Iisa Ollila, Jasmin Jaanto, Aki Grönman, Samuli Honkapuro, Juhani Riikonen, and Alisdair Price. "Role of power-to-heat and thermal energy storage in decarbonization of district heating." In: Energy 305 (2024), p. 132372. ISSN: 0360-5442. DOI: 10.1016/j.energy.2024.132372. URL: https://doi.org/10. 1016/j.energy.2024.132372 (visited on 08/23/2025).



- International Renewable Energy Agency (IRENA). Innovation Outlook: Thermal Energy Storage. 2020. URL: https://www.irena.org/publications/2020/Nov/ Innovation-Outlook-Thermal-Energy-Storage (visited on 05/19/2025).
- Dogan Keles, Massimo Genoese, Dominik Möst, and Wolf Fichtner. "Comparison of extended mean-reversion and time series models for electricity spot price simulation considering negative prices." In: Energy Economics 34.4 (2012), pp. 1012–1032. ISSN: 0140-9883. DOI: 10.1016/j.eneco.2011.08.012. URL: https://www. sciencedirect.com/science/article/pii/S0140988311001721 (visited on 08/11/2025).
- Michał Narajewski and Florian Ziel. "Econometric modelling and forecasting of [31]intraday electricity prices." In: Journal of Commodity Markets 19 (2020), p. 100107. ISSN: 2405-8513. DOI: 10.1016/j.jcomm.2019.100107. URL: https://www. sciencedirect.com/science/article/pii/S2405851319300728 (visited on 08/11/2025).
- [32]Jesus Lago, Grzegorz Marcjasz, Bart De Schutter, and Rafał Weron. "Forecasting day-ahead electricity prices: A review of state-of-the-art algorithms, best practices and an open-access benchmark." In: Applied Energy 293 (2021), p. 116983. ISSN: 0306-2619. DOI: 10.1016/j.apenergy.2021.116983. URL: https://www. sciencedirect.com/science/article/pii/S0306261921004529 (visited on 08/11/2025).
- Simon Jordan. "Two-stage stochastic optimization of district energy systems: a case study from the United States." Master's Thesis. Vienna, Austria: Technische Universität Wien, 2025. URL: https://repositum.tuwien.at/bitstream/ 20.500.12708/213803/1/Jordan%20Simon%20-%202025%20-%20Two-stage% 20stochastic%20optimization%20of%20district%20energy...pdf (visited on 07/11/2025).
- Hans Auer, Sebastian Zwickl-Bernhard, Antonia Golab, Theresia Perger, and An-[34]dreas Fleischhacker. Energiemodelle und Analysen. Skriptum zur Lehrveranstaltung 373.011, Technische Universität Wien, Institut für Energiesysteme und Elektrische Antriebe, Energy Economics Group (EEG). 2023.
- Martha Loewe. Deterministic Equivalent (DE) GAMS Solver Manual. DE is a solver for stochastic programs modeled with GAMS Extended Mathematical Programming (EMP SP), capable of solving multi-stage LP, MIP, QCP, NLP and MINLP stochastic programming models. GAMS Development Corporation. 2025. URL: https://www.gams.com/50/docs/S\_DE.html.
- Jesus Lago, Grzegorz Marcjasz, Bart De Schutter, and Rafał Weron. epftoolbox: [36]Electricity Price Forecasting Toolbox. Python library. See paper for benchmark details. 2021. URL: https://epftoolbox.readthedocs.io/en/latest/.



- Umweltbundesamt GmbH and Austrian Power Grid AG (APG) and TU Wien and TU Graz and Greenpeace and WWF and GLOBAL 2000. Stromszenario 2050 -Abschlussbericht der Diskussionsplattform e-Trend Forum. Wien, 2011. URL: https: //www.umweltbundesamt.at/fileadmin/site/publikationen/REP0335.pdf (visited on 06/15/2025).
- [38]Compass Lexecon. Modellierung der Stromstrategie 2040 — Endbericht. Wien: Österreichs Energie, Aug. 2, 2024. URL: https://oesterreichsenergie.at/ fileadmin/user\_upload/Oesterreichs\_Energie/Publikationsdatenbank/ Studien/2024/Modellierung\_Stromstrategie\_2040.pdf (visited on 08/23/2025).
- Henrik Zsiborács, Gábor Pintér, András Vincze, and Nóra Hegedűsné Baranyai. "Wind Power Generation Scheduling Accuracy in Europe: An Overview of ENTSO-E Countries." In: Sustainability 14.24 (Dec. 2022), p. 16446. ISSN: 2071-1050. DOI: 10.3390/su142416446. URL: http://dx.doi.org/10.3390/su142416446.

## **Statutory Declaration**

I declare that I have authored this thesis independently, that I have not used other than the declared sources/resources, and that I have explicitly marked all material which has been quoted either literally or by content from the used sources.

Wien,			
	D		C:
	Date		Signature